THE EFFECTS OF DIETARY IRON ON HEPATIC GLUCOSE METABOLISM AND CIRCADIAN RHYTHM

by

Judith Anne Simcox

A dissertation submitted to the faculty of
The University of Utah
in partial fulfillment of the requirements for the degree of

Doctor of Philosophy

Department of Biochemistry

The University of Utah

May 2014

The University of Utah Graduate School

STATEMENT OF THESIS APPROVAL

The following faculty members served as the supervisory committee chair and members for the thesis of Judith Anne Simcox.

Dates at right indicate the members' approval of the thesis.

Donald McClain, Chair	7/15/2013 Date Approved
Janet Lindsley, Member	7/16/2013 Date Approved
Dennis Winge, Member	7/29/2013 Date Approved
Jared Rutter, Member	7/17/2013 Date Approved
Diane Ward, Member	7/22/2013 Date Approved

The thesis has also been approved by Wesley I Sundquist

Chair of the Department/School/College of Biochemistry

and by David B Kieda, Dean of The Graduate School

ABSTRACT

Iron is a micronutrient important in energy homeostasis. Due to its oxidative capacity, it serves as the active site for many redox enzymes both as a component of iron sulfur clusters and heme, and iron-containing proteins are found in biochemical pathways important in energy utilization such as the citric acid cycle and the electron transport chain. The oxidative properties of iron can also be toxic since reduced iron is able to undergo Fenton chemistry to catalyze the formation of reactive oxygen species (ROS). At normal levels, ROS serves a signaling function important for a diverse array of processes, including cellular differentiation, metabolic adaptation, and innate immunity. Excess ROS can produce oxidative stress that affects those pathways and can also oxidize lipids, proteins, and nucleic acids.

Herein we explored the role of dietary iron in glucose metabolism both as it affects adenosine monophosphate-activated protein kinase (AMPK) and the circadian factor Rev-Erbα. In the study of both of these proteins, we found that moderate increases in dietary iron are able to create a shift in the oxidative potential of the cell as measured by increased levels of protein carbonylation, and decreased levels glutathione (GSH), and a decreased ratio of reduced to oxidized nicotinamide adenine dinucleotide phosphate (NADPH/NADP+). Through changes in cellular oxidation, iron is able to alter Sirtuin 1 (Sirt1) activity to deacetylate serine threonine kinase B1(LKB1), which is known to cause a shift from nuclear to cytosolic localization to then increase activation of AMPK.

Iron's effects on oxidation also increase transcription of Peroxisome proliferator-activated receptor gamma coactivator 1-alpha (PGC-1α), which promotes transcription of the rate-limiting enzyme in heme synthesis, Aminolevulinate synthase 1 (ALAS-1). Increases in heme levels increase the nuclear receptor subfamily 1, group D, member 2 (Rev-Erbα) and nuclear receptor corepressor (NCOR) complex formation. The increased activity of AMPK and Rev-Erbα with increased dietary iron altered changes in whole body glucose metabolism by decreasing gluconeogenesis to improve glucose tolerance. These results indicate that dietary iron is able to modulate multiple pathways to alter glucose homeostasis, and suggest that more work is needed to gain a full understanding of the optimal levels of iron and how they impact physiology.

This thesis is dedicated to my grandparents, Josè and Anunciación Javier, and Burnette and Olga Pickens, who worked tirelessly to build a better life for their families

TABLE OF CONTENTS

LIST OF FIGURES

Figure

ACKNOWLEDGMENTS

I would like to thank members of the McClain lab, past and present, for their technical assistance and their help in experimental protocols. I would like to especially thank Deborah Jones, Robert Cooksey, and Soh-hyun Lee for their help with *in vivo* experiments, including circadian harvests, hepatic perfusions, and other various physiological measurements of glucose parameters. I could not have completed this work without their expertise. Also, Yan Gao, Scott Gabrielsen, Bai Luo, Creighton Mitchell, and Jingyu Huang were especially helpful in experimental design and lending their expertise in the metabolic field. Finally, many undergraduate students dedicated their time to help me in completion of these experiments, including Daniel King, Steven Just, Scott Anjewierden, David Thorup, Chris Hanson, Brett Baggett, Amy Shen Wegesser, and David Gabrielsen.

Members of the metals interest group, seminars in metabolism, and the biochemistry department were pivotal in my growth as a scientist and helped provide critical feedback in my project. I would particularly like to thank James Cox, who ran all of the metabolomics analysis, and Hyung Kim, who provided assistance with heme and iron measurements.

I would also like to thank the members of my committee, Jared Rutter, Diane Ward, Dennis Winge, and Janet Lindsley, for their contribution to the development of this project and for my development as a researcher. Most importantly, I would like to

thank my thesis advisor, Don McClain, whose support and guidance were the most important factor in the completion of my degree. He is an exceptional researcher and mentor, as well as the truest epistemophiliac I've ever met.

Finally, I would like to thank my family and friends for their support through graduate school. My parents, Andrew and Jocelyn Pickens, have always been devoted to my education, and supporting me in my various passions. My husband Jeffery was particularly wonderful and proved himself to be my greatest support by always providing a critical ear, bringing me late night dinners to lab, and bringing me more joy than I deserve. I have failed many times but it was their constant support that allowed me to move forward and strive for better.

CHAPTER 1

INTRODUCTION

Diabetes mellitus affects 347million people worldwide, and according to the American Diabetes Association costs 245 billion annually in the US alone (Danaei *et al.*, 2011). This group of metabolic diseases are defined by hyperglycemia but are also characterized by multiple abnormalities in lipid and protein metabolism. The principal forms of diabetes are type 1, type 2, and gestational. Type 1 diabetes is caused by the loss of pancreatic beta cells, usually from an autoimmune basis, and the central treatment strategy is insulin replacement. Type 2 diabetes (T2D) is a disease of peripheral tissue insulin resistance. Initially, beta cells of the pancreas increase insulin production to overcome that resistance, but as insulin resistance worsens, insulin production fails to maintain glycemia. This excessive production eventually leads to oxidative stress and beta cell death, which worsens glucose control. Gestational diabetes is similar to T2Ds and is triggered by the increased metabolic stress of pregnancy.

Of the three forms, T2D is the most prevalent, accounting for 90% of all cases worldwide. Although obesity is the strongest single risk factor for T2D, a complete understanding of the factors that lead to its development is lacking (WHO, 1999). Many environmental and genetic factors contribute to diabetes risk (Colditz *et al.*, 1995; Kahn *et al.*, 2006). Among these are specific dietary components and the timing of sleep and

feeding (Huang *et al.,* 2011; Gonnissen *et al.*, 2013). The micronutrient iron has been shown to be connected to both irregular glucose metabolism and with maintenance of diurnal rhythms, although the mechanisms underlying this relationship are unknown. The aim of this dissertation is to explore various mechanisms through which dietary iron is able to modulate cellular metabolism and contribute to circadian rhythms.

In this introduction, I will discuss studies that show a correlation between abnormal circadian rhythms and hyperglycemia. I will then explain the molecular components that regulate clock function, and the interplay of these transcriptional regulators with metabolism. Finally, I will explain the relationship between iron and circadian rhythms, and briefly review my findings that dietary iron functions to regulate clock components.

Circadian rhythms and glucose metabolism

The connection between circadian rhythms and glucose homeostasis were first observed in case studies of shift workers. Numerous large cohort studies have shown increased risk of T2D in individuals who perform shift work for long periods of time (Spiegel *et al.,* 2009; Pan *et al*., 2011). Moreover, chronic abnormal sleep patterns of either long (9 hours or more) or short (5 hours or less) duration are both associated with increased rates of T2D, hypertension, and high cholesterol (Ayas *et al.*, 2003). These results are confounded by the fact that altered sleep patterns and shift work are also associated with higher body mass index (BMI) and adjustment for BMI in most studies removes the statistical significance for the association. These results suggest that the association of aberrant sleep patterns with diabetes could be connected to multiple

factors, including changes in the molecular clock, altered stress, social disruption, or other lifestyle factors.

Changes in glucose homeostasis are also observed in short-term clinical studies of sleep deprivation. This was first shown by Spiegel *et al.* (1999) who restricted the sleep of 11 healthy male volunteers, aged 18 to 27 years, to 4 hours for 6 consecutive nights. During the sleep deprivation, the subjects had a 40% increase in area under the glucose curve and insulin resistance when challenged with intravenous glucose administration, compared to a controlled rested state where the individuals were allowed to sleep for 12 hours. These studies were later repeated with a single night of sleep deprivation (4 hours of sleep within a 24-hour day) with insulin sensitivity measured by hyperinsulinemic euglycemic clamp with infusion of [6,6-$^2H_2$]D-glucose (Donga *et al.*, 2010). The results of this clinical study found that a single night of restricted sleep led to a significant decreased glucose infusion, decreased glucose disposal, and increased endogenous glucose production.

Other studies linking circadian rhythms with T2D include genome wide association studies (GWAS) and targeted haplotype analysis. Associations of T2D, metabolic syndrome, and hypertension have been noted with polymorphisms of circadian transcription factors Cry2, Clock, Per2, and a two-marker haplotypes of the Bmal1 promoter (Woon *et al.*, 2007; Dupuis *et al.*, 2010). Another GWAS study showed an association between T2D and polymorphisms in a modulator of whole body synchrony, the melatonin receptor 1B. These melatonin receptor 1B polymorphisms were functional: When expressed in Hek293 cells, the receptor exhibited lower affinity for melatonin (Bonnefond *et al.*, 2012).

Causal relationships between glucose homeostasis and circadian rhythms have been established in animal models. Mice expressing a whole body mutation of the circadian transcription factor Clock in which exon 19 is missing due to a transversion ($Clock^{\Delta 19/\Delta 19}$) have increased body weight, higher *ad libitum* glucose levels, lower *ad libitum* insulin levels, and worsened glucose tolerance (Turek *et al.*, 2005; Marcheva *et al.*, 2010). Moreover, targeted knock out models of the circadian transcription factor Bmal1 using either the albumin-cre to target the liver or Pdx-cre to target the beta cell are characterized by hypoglycemia or hyperglycemia, respectively (Lamia *et al.*, 2008; Marcheva *et al.*, 2010).

Central and peripheral clocks

A circadian rhythm is a 24-hour cycle of behavioral, and biochemical processes that are maintained by a system of transcription factor feedback loops. Circadian rhythms in behavior are regulated by light/dark cycles. Light excites the photopigment melanopsin, which is present in intrinsically photoreceptive retinal ganglion cells; when these cells depolarize, the impulse travels along the retinohypothalamic tract, to the suprachiasmatic nucleus (SCN) in the hypothalamus. The SCN is thought of as the central clock regulating circadian feeding, thermoregulation, and sleep/wake cycles. Lesion studies of the hypothalamus showed an ablation of circadian drinking behavior and activity (Mohawk *et al.*, 2012; Steven and Zucker, 1972). Furthermore, the SCN maintains synchrony between the various clocks in peripheral tissues, and is thought to perform this function through controlling body temperature in mammals (Buhr *et al.*, 2010).

Circadian rhythms in peripheral tissues were only discovered recently (Yamazaki *et al.*, 2000; Yoo *et al*., 2004). Initially these peripheral clocks were thought to be regulated solely by the SCN; however, subsequent studies showed that timing in peripheral clocks could be shifted by other external signals called zeitgebers (time setters). One such study involved restricting the feeding of rats to an 8-hour period during the daytime, a shift from their normal crepuscular feeding patterns in the evening and early morning. In these rats, a luciferase reporter under the control of a Per1 promoter was used as a real-time measure of circadian rhythms. When these rats were restricted to daytime feeding, the peak expression of luciferase in the liver shifted by 12 hours, while the peak expression in the SCN was unchanged (Stokkan *et al.*, 2001). These results suggested not only that food is a zeitgeber for the liver clock, but also that peripheral tissues can become dyssynchronous from the central clock. Dyssynchrony between the SCN and peripheral tissues is the leading hypothesis as to why night shift workers have such a high incidence of metabolic disease and type 2 diabetes.

Molecular components of circadian rhythm

Much of the genome exhibits circadian expression with estimations from microarray studies showing that 10 to 50% of all genes exhibit rhythmic fluctuations; although the proportion of these directly affected by the core molecular clock is unknown, cycling in these transcripts may be largely due to factors downstream of the clock or due to behavioral rhythms (Panda *et al.*, 2002; Yan *et al.*, 2008). The core molecular clock is composed of both a positive and negative arm of transcriptional regulation. In mammals, the positive arm consists of the transcription factor brain and muscle aryl-hydrocarbon receptor nuclear translocator-like 1 (Bmal1), and the histone

acetyl-transferase circadian locomotor output cycles kaput (Clock or its paralogue NPAS2), which heterodimerize and bind to an Ebox sequence in the promoter of clock controlled genes (CCGs) (Konopka and Benzer, 1971; Huang *et al.*, 2011) (Figure 1.1).

Some of the transcription factors that are positively regulated by the Clock/Bmal1 complex include the negative branch of circadian factors, including nuclear receptor subfamily 1, group D, member 1 (Rev-Erbα), Period (Per1, Per2), and Cryptochrome (Cry1, Cry2, Cry3). The nuclear receptor Rev-Erbα competes with the transcriptionally activating retinoic acid–related orphan receptor α (RORα) to bind to the ROR response element (RORE) in the Bmal1 promoter to repress its transcription in a complex with nuclear receptor co-repressor 1 (NCOR1). More recently, an RORE has also been described in the Clock promoter (Crumbley and Burris, 2011). The second negative arm of circadian rhythms is comprised of period and cryptochrome proteins that heterodimerize in the cytosol and then are shuttled back into the nucleus to directly inhibit the function of the Clock/Bmal1 complex (Shearman *et al.*, 2000; Lee *et al.*, 2001; Sato *et al.*, 2006).

There are several posttranslational mechanisms that control this circadian feedback system, including phosphorylation, ubiquitination, O-linked glycosylation, and acetylation. The nuclear abundance of period and cryptochrome is regulated by a phosphorylation by casein kinase 1ε (CK1ε) or AMPK, respectively, which tags them for polyubiquitylation by the E3 ubiquitin ligase complex β-transducin repeat containing protein (β-TrCP1), and F-box and leucine-rich repeat protein 3 (FBXL3), which leads to their subsequent degradation by the 26S proteasome (Akashi *et al.*, 2002; Eide *et al.,* 2005; Godhino *et al,* 2007; Spieka *et al.*, 2007). Ck1ε also plays an important role in

nuclear translocation of the Per/Cry complex, and may be important in some of the inhibitory properties (Meng *et al.*, 2010). Degradation of Per2, Clock and Bmal1 is countered by O-linked glycosylation to regulate circadian timing (Kim *et al.*, 2012; Kaasik *et al.*, 2013; Li *et al.*, 2013). Finally, acetylation of Bmal1 facilitates cryptochrome interaction with this complex to affect its repression (Hirayama *et al.*, 2007; Asher *et al.*, 2008).

Recently, this canonical control of circadian rhythms by transcriptional regulation has been challenged by the discovery of a circadian rhythm in anucleated red blood cells. Red blood cells maintain a circadian rhythm in the oxidative state of certain proteins peroxiredoxin and haemoglobin (O'Neil and Reddy, 2012). Other cell types also have redox cycles; however, they are thought to function downstream of the transcriptional regulators, as seen in the SCN where redox signals function to regulate the excitability of neurons (Wang *et al.*, 2012).

Cross-regulation between circadian rhythms and metabolism

The leading hypothesis as to why circadian rhythms are evolutionarily advantageous is that they synchronized energy utilization and energy availability. Much of the rationale behind this hypothesis is found by assessing known circadian controlled pathways including genes important in cell division, and the biochemical pathways that produce cellular components such as glucose and lipid homeostasis necessary for nucleotide, amino acid, and phospholipid synthesis (Matsuo *et al.*, 2003). Members of the core molecular clock directly control metabolism, including Rev-Erbα, which is known to regulate gluconeogenesis, adipogenesis, and lipogenesis (Lau *et al.*, 2004; Canaple *et al.*, 2006). Moreover, the Clock/Bmal1 heterodimer regulates peroxisome proliferator-

activated receptor (PPAR) family members α and γ that regulate lipid utilization and storage, respectively (Duez and Staels, 2008).

Metabolic pathways also regulate circadian rhythms, and indeed the interaction between the two pathways was first described with the observation that a lower NAD/NADH ratio enhanced Clock/Bmal1 heterodimerization as well as DNA binding (Rutter *et al.*, 2001). Also, the metabolic master regulator AMPK directly phosphorylates Cry1 to cause its degradation, and regulates nicotinamide phosphoribosyltransferase (NAMPT) the rate-limiting enzyme in NAD+ biosynthesis pathway (Cantó *et al.*, 2009; Lamia *et al.*, 2009). The biosynthesis of NAD+ feeds into circadian rhythms through the deacetylase Sirtuin 1 (Sirt1), which utilizes NAD energy stores for deacetylation. Sirt1 is thought to complex with Clock and Bmal1 to alter Per2 acetylation to promote its degradation as well as to regulate histone mobility (Asher *et al.*, 2008).

Circadian rhythms and iron

There is evidence that iron is both regulated by and regulates circadian rhythms. Systemic iron levels fluctuate in a circadian manner as do iron-bound proteins and proteins important in iron metabolism (Rubio *et al.*, 2003; Unger *et al.*, 2009). Moreover, in microarray studies attempting to elucidate the downstream targets of the molecular clock of the SCN by performing a 15-minute light-pulse on mice in the middle of the dark phase, 10% of the genes that were changed were associated with iron and heme metabolism (Ben-Shlomo *et al.*, 2005).

There is also evidence that iron may be necessary for maintenance of circadian rhythms of the SCN that regulates behavioral rhythms. In humans, low iron stores and aberrant brain iron levels have been shown to be causally related to restless leg syndrome

(RLS), a circadian disorder characterized by the uncontrollable urge for leg movement (Earley *et al.*, 2005). In rats fed an iron deficient diet for 28 days, there was a decrease in motility and a shift of the diurnal peak in body temperature (Youdim *et al.*, 1980). These results could be due to irons effects on the dopaminergic response, or due to iron's effects on other central clock outputs such as its control of the cellular localization of melatonin (Pablos *et al.*, 1996). Finally, drosophila with knockdown of the light chain of ferritin were unable to maintain circadian movement in dark conditions and rhythm in circadian transcripts *clock, period,* and *timeless* was disrupted in the heads of these flies (Mandilaras and Missirlis, 2012). Recently, it has been suggested that iron may also play a more direct role in circadian rhythms when it was shown to control period length in *Arabidopsis thalia,* and iron deficiency altered the cycling of molecular clock components (Chen *et al.*, 2013).

Iron also has the ability to affect the concentration of heme, a cofactor reported to bind in a regulatory manner to several circadian components, including Rev-Erbα, NPAS2, and Per2 (Yin *et al.*, 2007; Kitinashi *et al.*, 2008). In erythrocytes, iron activates an iron regulator protein that will bind to an iron-responsive element in the 5' untranslated region of ALAS2, the erythroid-specific rate-limiting enzyme in heme synthesis (Ajioka *et al.*, 2006). An ubiquitously expressed isoform of this heme synthesis-regulating enzyme, ALAS1, does not have an iron-response element but does have circadian oscillations of its transcripts that are regulated by PGC-1α (Estall *et al.*, 2009).

Summary of findings

In this introduction, I have provided evidence that circadian rhythms regulate glucose homeostasis, and that iron affects circadian rhythms and we will further expand upon the relationship that iron itself has in whole body glucose homeostasis, as well as introduce its regulation of AMPK in Chapter 2. In this dissertation, we will also describe that dietary iron alters AMPK phosphorylation through oxidative regulation of Sirt, as well as explore irons regulation of cellular redox state to assess its effects upon heme synthesis and the subsequence changes on Rev-Erbα regulation of gluconeogenesis.

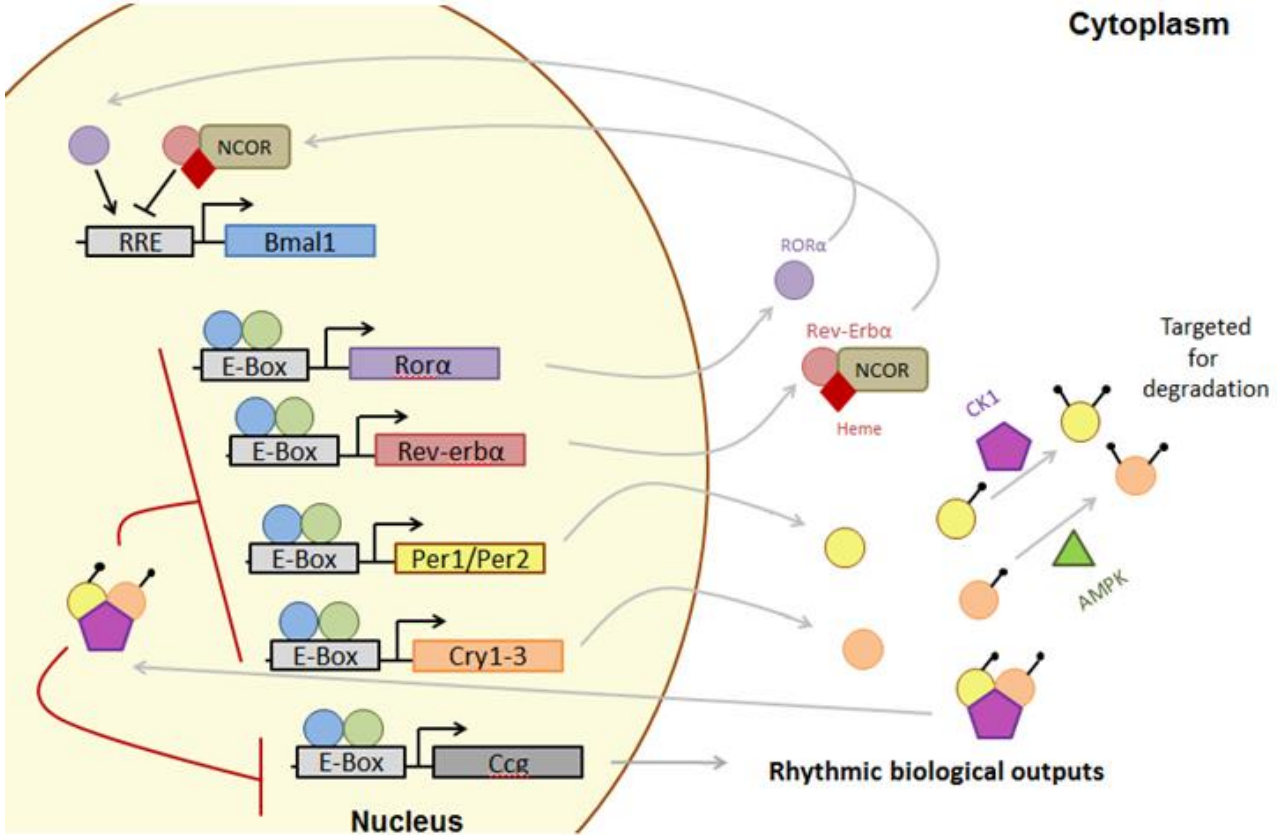

Figure 1.1 Components of the Core Molecular Clock Complex (modified from Mowhawk *et al.*, 2012)

The molecular clock consists of an autoregulatory transcriptional feedback loop involving the activators Clock and Bmal1 and their target clock controlled genes (CCG) These CCG form two negative-feedback loops, the Rev-Erbα/NCOR complex that represses Bmal1 transcription, while the Per/Cry complex inhibits the Clock/Bmal1 heterodimer.

References

Ajioka R.S., Phillips J.D., and Kushner J.P. (2006). Biosynthesis of heme in mammals. Biochim Biophys Acta. 1763(7):723-36.

Akashi M., Tsuchiya Y., Yoshino T., and Nishida E. (2002). Control of intracellular dynamics of mammalian period proteins by casein kinase I epsilon (CKIepsilon) and CKIdelta in cultured cells. MCB. 2002; 22: 1693–1703.

Asher G., Gatfield D., Stratmann M., Reinke H., Dibner C., Kreppel F., Mostoslavsky R., Alt F.W., and Schibler U. (2008). SIRT1 regulates circadian clock gene expression through PER2 deacetylation. Cell. Jul 25;134(2):317-28.

Ayas N.T., White D.P., Al-Delaimy W.K., Manson J.E., Stampfer M.J., Speizer F.E., Patel S., and Hu F.B. (2003). A prospective study of self-reported sleep duration and incident diabetes in women. Diabetes Care. 26(2):380-4.

Ben-Shlomo R., Akhtar R.A., Collins B.H., Judah D.J., Davies R., and Kyriacou C.P. (2005). Light pulse-induced heme and iron-associated transcripts in mouse brain: a microarray analysis. Chronobiol Int. 22(3):455-71.

Bonnefond A., Clement N., Fawcett K., Yengo L., Vallient E., Guillaume J.L., Dechaume M., Payne F., Roussel R., Czernichow S., *et al.* (2012). Rare MTNR1B variants impairing melatonin receptor 1B function contribute to type 2 diabetes. Nat Genet. 44(3):297-301.

Boyle J.P., Thompson T.J., Gregg E.W., Barker L.E., and Williamson D.F. (2010). Projection of the year 2050 burden of diabetes in the US adult population: dynamic modeling of incidence, mortality, and prediabetes prevalence. Population Health Metrics. 8(29) e1-12.

Buhr E.D., Yoo S.H., and Takahashi J.S. (2010). Temperature as a universal resetting cue for mammalian circadian oscillators. Science. 330(6002):379-85.

Canaple L., Rambaud J., Dkhissi-Benyahya O., Rayet B., Tan N.S., Michalik L., Dalaunay F., Wahli W., and Laudet V. (2006). Reciprocal regulation of brain and muscle Arnt-like protein 1 and peroxisome proliferator-activated receptor alpha defines a novel positive feedback loop in the rodent liver circadian clock. Mol Endocrinol. 20:1715-27.

Cantó C., Gerhart-Hines Z., Feige J.N., Lagouge M., Noriega L., Milne J.C., Elliott P.J., Puigserver P., and Auwerx J.(2009). AMPK regulates energy expenditure by modulating NAD+ metabolism and SIRT1 activity. Nature. 458(7241):1056–1060.

Chen Y.Y., Wang Y., Shin L.J., Wu J.F., Shanmugam V., Tsednee M., Lo J.C., Chen C.C., Wu S.H., and Yeh K.C. (2013). Iron is involved in the maintenance of circadian period length in Arabidopsis. Plant Physiol. 161(3):1409-20.

Colditz G.A., Willett W.C., Rotnitzky A., and Manson J.E. (1995). Weight gain as a risk factor for clinical diabetes mellitus in women. Ann Intern Med. 122, 481-486.

Crumbley C., and Burris T.P.. (2011). Direct regulation of CLOCK expression by REV-ERB. *PLoS One*. 6(3):e17290.

Danaei G., Finucane M.M., Lu Y., Singh G.M., Cowan M.J., and Paciorek C.J.(2011) National, regional, and global trends in fasting plasma glucose and diabetes prevalence since 1980: systematic analysis of health examination surveys and epidemiological studies with 370 country-years and 2.7 million participants. Lancet. 378(9785):31–40.

Definition, diagnosis and classification of diabetes mellitus and its complications. Part 1: Diagnosis and classification of diabetes mellitus. Geneva, World Health Organization, 1999 (WHO/NCD/NCS/99.2).

Donga E., van Dijk M., van Dijk J.G., Biermasz N.R., Lammers G.J., van Kralingen K.W., Corssmit E.P., and Romijn J.A. (2010). A single night of partial sleep deprivation induces insulin resistance in multiple metabolic pathways in healthy subjects. J Clin Endocrinol Metab. 95(6):2963-8.

Duez H., and Staels B. (2008) Rev-erb alpha gives a time cue to metabolism. FEBS Lett.582(1):19–25.

Dupuis J., Langenberg C., Prokopenko I., Saxena R., Soranzo N., Jackson A.U., Wheeler E., Glazer N.L., Bouatia-Naji N., Gloyn AL., *et al* . (2010).New genetic loci implicated in fasting glucose homeostasis and their impact on type 2 diabetes risk. Nat Genet. 42:105–116

Earley C.J., Connor J.R., Beard J.L., Clardy S.L., and Allen R.P. (2005). Ferritin levels in the cerebrospinal fluid and restless legs syndrome: effects of different clinical phenotypes. Sleep. 28(9):1069-75.

Eide E.J., Woolf M.F., Kang H., Woolf P., Hurst W., Camacho F., Vielhaber E.L., Giovanni A., and Virshup D.M. (2005). Control of mammalian circadian rhythm by CKIepsilon-regulated proteasome-mediated PER2 degradation. MCB. 25: 2795–2807.

Englund A., Kovanen L., Saarikoski S.T., Haukka J., Reunanen A., Aromaa A., Lönnqvist J., and Partonen T. (2009). NPAS2 and PER2 are linked to risk factors of the metabolic syndrome. J Circadian Rhythms. 26;7:5.

Estall J.L., Ruas J.L., Choi C.S., Laznik D., Badman M., Maratos-Flier E., Shulman G.I., and Spiegelman B.M. (2009). PGC-1alpha negatively regulates hepatic FGF21 expression by modulating the heme/Rev-Erb(alpha) axis. *Proc* Natl Acad Sci.106(52):22510-5.

Gonnissen H.K., Hulshof T., and Westerterp-Plantenga M.S.(2013). Chronobiology, endorcrinology, and energy- and food-reward homeostasis. Obes Rev. 14(5):405-16.

Godinho S.I., Maywood E.S., Shaw L., Tucci V., Barnard A.R., Busino L., Pagano M., Kendall R., Quwailid M.M., Romero M.R., O'Neill J., Chesham J.E., Brooker D., Lalanne Z., Hastings M.H., and Nolan P.M. (2007). The after-hours mutant reveals a role for Fbxl3 in determining mammalian circadian period. Science. 316: 897–900.

Hirayama J., Sahar S., Grimaldi B., Tamaru T., Takamatsu K., Nakahata Y., and Sassone-Corsi P.(2007) CLOCK-mediated acetylation of BMAL1 controls circadian function. Nature. Dec 13;450(7172):1086-90.

Huang W., Ramsey K.M., Marcheva B., and Bass J. (2011). Circadian rhythms, sleep, and metabolism. JCI. 121(6):2133-2141

Kaasik K., Kivimäe S., Allen J.J., Chalkley R.J., Huang Y., Baer K., Kissel H., Burlingame A.L., Shokat K.M., Ptáček L.J., and Fu Y.H. (2013). Glucose sensor O-GlcNAcylation coordinates with phosphorylation to regulate circadian clock. Cell Metab. 17(2):291-302.

Kahn S.E., Hull R.L., and Utzschneider K.M. (2006). Mechanisms linking obesity to insulin resistance and type 2 diabetes. Nature. 444, 840-846.

Kim E.Y., Jeong E.H., Park S., Jeong H.J., Edery I., and Cho J.W. (2012). A role for O-GlcNAcylation in setting circadian clock speed. Genes Dev. 26(5):490-502.

Konopka R.J., and Benzer S. (1971). Clock mutants of Drosophila melanogaster. Proc Natl Acad Sci U S A. 68(9):2112–2116.

Lamia K.A., Storch K.F., and Weitz C.J. (2008). Physiological significance of a peripheral tissue circadian clock. Proc Natl Acad Sci U S A.105(39):15172–15177.

Lamia K.A., Sachdeva U.M., DiTacchio L., Williams E.C., Alvarez J.G., Egan D.F., Vasquez D.S., Juguilon H., Panda S., Shaw R.J., Thompson C.B., and Evans R.M. (2009). AMPK regulates the circadian clock by cryptochrome phosphorylation and degradation. Science. 326(5951):437–440.

Lan F., Cacicedo J.M., Ruderman N., and Ido Y.(2008). Sirt1 modulation of the acetylation status, cytosolic localization, and activity of LKB1. JBC. 283:27628-27635.

Lau P., Nixon S.J., Parton R.G., and Muscat G.E. (2004). RORalpha regulates the expression of genes involved in lipid homeostasis in skeletal muscle cells: caveolin-3 and CPT-1 are direct targets of ROR.J Biol Chem. 279:36828-40.

Lee C., Etchegaray J.P., Cagampang F.R., Loudon A.S., and Reppert S.M. (2001). Posttranslational mechanisms regulate the mammalian circadian clock. Cell. 107: 855–867.

Li M.D., Ruan H.B., Hughes M.E., Lee J.S., Singh J.P., Jones S.P., Nitabach M.N., and Yang X. (2013). O-GlcNAc signaling entrains the circadian clock by inhibiting BMAL1/CLOCK ubiquitination. Cell Metab. 17(2):303-10.

Mandilaras K., and Missirlis F. 2012. Genes for iron metabolism influence circadian rhythms in Drosophila melanogaster. Metallomics. 24;4(9):928-36.

Marcheva B., Ramsey K.M., Buhr E.D., Kobayashi Y., Su H., Ko C.H., Ivanova G., Omura C., Mo S., Vitaterna M.H., *et al.* (2010). Disruption of the clock components CLOCK and BMAL1 leads to hypoinsulinaemia and diabetes. Nature.466(7306):627–631.

Matsuo T., Yamaguchi S., Mitsui S., Emi A., Shimoda F., and Okamura H. (2003). Control mechanism of the circadian clock for timing of cell division in vivo. Science. 302(5643):255-9.

Meng Q.J., Maywood E.S., Bechtold D.A., Lu W.Q., Li J., Gibbs J.E., Dupre S.M., Chesham J.E., Rajamohan F., Knafels J., *et al*. (2010). Entrainment of disrupted circadian behavior through inhibition of casein kinase 1 (CK1) enzymes. Proc Natl Acad Sci U S A. 107(34):15240-15245.

Mohawk J.A., Green C.B., and Takahashi J.S. (2012). Central and peripheral circadian clocks in mammals. Annu Rev Neurosci. 35:445-62.

Pablos M.I., Agapito M.T., Menéndez-Pelaez A., Acuña-Castroviejo D., Reiter R.J., and Recio J.M. (1996). Iron decreases the nuclear but not the cytosolic content of the neurohormone melatonin in several tissues in chicks. J Cell Bioch. 60(3):317-21.

Pan A., Schernhammer E.S., Sun Q., and Hu F.B..(2011). Rotating night shift work and risk of type 2 diabetes: two prospective cohort studies in women. PLoS Med. 8(12):e1001141

Panda S., M. P. Antoch , B. H. Miller, A. I. Su, A. B. Schook, M. Straume, P. G. Schultz, S. A. Kay, J. S. Takahashi, and J. B. Hogenesch. **(**2002). Coordinated transcription of key pathways in the mouse by the circadian clock. Cell 109**:**307-320.

Rutter J., Reick M., Wu L.C., and McKnight SL. (2001). Regulation of clock and NPAS2 DNA binding by the redox state of NAD cofactors. Science. 20;293(5529):510-4.

Sato T.K., Yamada R.G., Ukai H., Baggs J.E., Miraglia L.J., Kobayashi T.J., Welsh D.K., Kay S.A., Ueda H.R., and Hogenesch J.B. (2006). Feedback repression is required for mammalian circadian clock function. Nat Genet. 38: 312–319.

Scheer F.A., Hilton M.F., Mantzoros C.S., Shea S.A. (2009). Adverse metabolic and cardiovascular consequences of circadian misalignment. Proc Natl Acad Sci U S A.106(11):4453–4458.

Sena L.A., and Chandel N.S. (2012). Physiologic roles of mitochondrial reactive oxygen species. Mol Cell. 48(2):158-67.

Shearman L.P., Jin X., Lee C., Reppert S.M., and Weaver D.R. (2000). Targeted disruption of the mPer3 gene: subtle effects on circadian clock function. MCB. 20: 6269–6275.

Shearman L.P., Sriram S., Weaver D.R., Maywood E.S., Chaves I., Zheng B., Kume K., Lee C.C., van der Horst G.T., and Hastings M.H, Reppert SM. (2000). Interacting molecular loops in the mammalian circadian clock. Science. 12;288(5468):1013-9.

Siepka S.M., Yoo S.H., Park J., Song W., Kumar V., Hu Y., Lee C., and Takahashi J.S. (2007). Circadian mutant Overtime reveals F-box protein FBXL3 regulation of cryptochrome and period gene expression. Cell. 129: 1011–1023.

Spiegel K., Leproult R., and van Cauter E. (1999). Impact of sleep debt on metabolic and endocrine function. Lancet. 354, 1435–1439.

Spiegel K., Tasali E., Leproult R., and Van Cauter E. (2009). Effects of poor and short sleep on glucose metabolism and obesity risk. Nat Rev Endocrinol. 5(5):253–261.

Stephan F.K., and Zucker I. (1972). Circadian rhythms in drinking behavior and locomotor activity of rats are eliminated by hypothalamic lesions. Proc Natl Acad Sci U S A. 69(6):1583-6.

Stokkan K.A., Yamazaki S., Tei H., Sakaki Y.,and Menaker M.(2001). Entrainment of the circadian clock in the liver by feeding. Science. 291(5503):490-3.

Turek F.W., Joshu C., Kohsaka A., Lin E., Ivanova G., McDearmon E., Laposky A., Losee-Olson S., Easton A., Jensen D.R., Eckel R.H., Takahashi J.S., and Bass J. (2005). Obesity and metabolic syndrome in circadian Clock mutant mice. Science. 308(5724):1043-5.

Unger E.L., Earley C.J., and Beard J.L. (2009). Diurnal cycle influences peripheral and brain iron levels in mice. J Appl Physiol. 106(1):187-93.

Wang T.A., Yu Y.V., Govindaiah G., Ye X., Artinian L., Coleman T.P., Sweedler J.V., Cox C.L., and Gillette M.U. (2012). Circadian rhythm of redox state regulates excitability in suprachiasmatic nucleus neurons. Science.337(6096):839-42.

Woon P.Y., Kaisaki P.J., Braganaca J., Bihoreau M.T., Levy J.C., Farrall M., and Gauguier D. (2007). Aryl hydrocarbon receptor nuclear translocator-like (BMAL1) is associated with susceptibility to hypertension and type 2 diabetes. Proc Natl Acad Sci U S A. 104(36):14412–14417.

Yamazaki S., Numano R., Abe M., Hida A., Takahashi R., Ueda M., Block G.D., Sakaki Y., Menaker M., and Tei H. (2000). Resetting central and peripheral circadian oscillators in transgenic rats. Science. 288(5466):682-5.

Yan J., Wang H., Liu Y., and Shao C. (2008). Analysis of gene regulatory networks in the mammalian circadian rhythm. PLoS Comput. Biol. 4:e1000193

Yang X., Downes M., Yu R.T., Bookout A.L., He W., Straume M., Mangelsdorf D.J., and Evans R.M. (2006).Nuclear receptor expression links the circadian clock to metabolism. Cell. 126(4):801–810.

Yoo S.H., Yamazaki S., Lowrey P.L., Shimomura K., Ko C.H., Buhr E.D., Siepka S.M., Hong H.K., Oh W.J., Yoo O.J., Menaker M., and Takahashi J.S. (2004). PERIOD2::LUCIFERASE real-time reporting of circadian dynamics reveals persistent circadian oscillations in mouse peripheral tissues. Proc Natl Acad Sci U S A. 101(15):5339-5346.

Youdim M.B., Yehuda S., and Ben-Uriah Y. (1981). Iron deficiency-induced circadian rhythm reversal of dopaminergic-mediated behaviours and thermoregulation in rats.Eur J Pharmacol. 74(4):295-301.

Zhang E.E., Liu Y., Dentin R., Pongsawakul P.Y., Liu A.C., Hirota T., Nusinow D.A., Sun X., Landais S., Kodama Y., Brenner D.A., Montminy M., and Kay S.A. (2010). Cryptochrome mediates circadian regulation of cAMP signaling and hepatic gluconeogenesis. Nat Med.16(10):1152–1156.

CHAPTER 2

IRON AND DIABETES

Reprint of: JA Simcox and DA McClain. (2013). Iron and Diabetes Risk. Cell Metabolism. Reprinted with permission from Cell metabolism.

Cell Metabolism
Review

Iron and Diabetes Risk

Judith A. Simcox[1] and Donald A. McClain[1,2,*]
[1]Departments of Medicine and Biochemistry, University of Utah School of Medicine, Salt Lake City, UT 84132, USA
[2]Research Service, VA Medical Center, Salt Lake City, UT 84132, USA
*Correspondence: donald.mcclain@hsc.utah.edu
http://dx.doi.org/10.1016/j.cmet.2013.02.007

Iron overload is a risk factor for diabetes. The link between iron and diabetes was first recognized in pathologic conditions—hereditary hemochromatosis and thalassemia—but high levels of dietary iron also impart diabetes risk. Iron plays a direct and causal role in diabetes pathogenesis mediated both by β cell failure and insulin resistance. Iron also regulates metabolism in most tissues involved in fuel homeostasis, with the adipocyte in particular serving an iron-sensing role. The underlying molecular mechanisms mediating these effects are numerous and incompletely understood but include oxidant stress and modulation of adipokines and intracellular signal transduction pathways.

Type 2 diabetes is a common and ever-increasing worldwide health problem. Although well described in terms of its hallmarks of insulin resistance and β cell failure, the proximal cause(s) of type 2 diabetes and the mechanisms underlying its genetic predisposition remain largely unknown. Plausible cases have been made for the primacy of abnormalities in insulin signaling, insulin secretion, activation of stress pathways, mitochondrial dysfunction, hepatic fuel homeostasis, and central nervous system regulation (reviewed in Hotamisligil, 2003; Kahn, 1998, 2003; Lowell and Shulman, 2005). It is well accepted that the most reliable predictor for the disease is obesity; therefore, much attention has also been paid to the contribution of nutrients and nutrient-sensing pathways in situations of chronic caloric excess. Most of the interest in the role of nutrients in diabetes is centered on macronutrients, but a micronutrient, iron, is also closely associated with diabetes risk in a number of hereditary syndromes, as well as in common forms of type 2 diabetes. Iron deficiency is also associated with obesity. In this review, we will briefly summarize the control of iron homeostasis at the levels of the organism and the cell and then review the evidence that excess iron is associated with increased diabetes risk, that this relationship is causal, and that excess iron even within the "normal" range has important detrimental effects on insulin secretion, insulin sensitivity, adipokine levels, and metabolic flexibility. Finally, we will consider the molecular mechanisms for these relationships.

Iron Homeostasis

Iron plays an essential role as a cofactor for fuel oxidation and electron transport, but it also has the potential to cause oxidative damage if not carefully regulated, chaperoned, and, when in excess, sequestered. Thus, extensive mechanisms to control the uptake and fate of iron have evolved. The connections between iron and metabolism are well established, particularly in lower organisms. Iron entry into cells increases when needed for fuel oxidation, and, conversely, the metabolic fate of glucose and ethanol are dependent on the availability of iron. In *Saccharomyces cerevisiae*, both glucose exhaustion and iron limitation trigger iron uptake signaled by Snf1 kinase, the yeast ortholog of AMP-dependent kinase (AMPK) (Haurie et al., 2003). The SWI/SNF chromatin-remodeling complex also controls the induction of iron transport genes in *S. pombe* (Monahan et al., 2008). Thus, in the shift from fermentative to respiratory glucose metabolism, iron uptake is stimulated to allow metallation of the enzymes and electron carriers necessary for oxidative metabolism.

The regulation of iron metabolism has been extensively reviewed (Andrews and Schmidt, 2007; De Domenico et al., 2008; Ganz, 2011; Hentze et al., 2010) and will be briefly summarized here. This is a current summary of mechanisms and pathways that are still being explored; many details and controversies are not presented because of space constraints. Most iron in mammalian organisms is recycled at a rate of 20–25 mg/day through the erythroid pool as macrophages endocytose senescent erythrocytes. Roughly 5%–10% of that amount per day is taken up through the intestine. Mammals do not have the capacity to secrete excess iron in a regulated fashion. In equilibrium, losses through sloughing of the intestinal epithelium, death of other cells, and biliary excretion balance intestinal uptake, but when uptake exceeds loss, excess iron is sequestered intracellularly.

Because disposal of excess iron is usually a slow process in humans, uptake of iron from the intestine is highly regulated (Figure 1). In the duodenum, ferric iron (Fe^{3+}) is first reduced to ferrous iron (Fe^{2+}) by the ferrireductase duodenal cytochrome b (DCTB). Ferrous ions enter the cell through the divalent metal-ion transporter 1 (DMT1 or SLC11A2). Iron exits the enterocyte through the only known iron export channel, ferroportin (FPN or SLC40A1). The iron is oxidized to Fe^{3+} by hephaestin (HEPH), whereupon it binds to transferrin in the circulation. Transferrin-bound iron can then be taken into cells by transferrin receptors (TfRs), in most cells TfR1. A soluble form of the transferrin receptor bound to transferrin also exists, and its level in serum is a sensitive indicator of functional iron deficiency (Beguin, 2003).

TfR1 mediates iron uptake in most cells. Upon endocytosis, the endosome is acidified and ferric iron is released from transferrin, reduced by the STEAP family of ferrireductases, and enters the cytosol through DMT1, although this may not be the exclusive transporter. Non-transferrin-bound iron can also enter the cells directly through DMT1 and other transporters such as Zip14 (Liuzzi et al., 2006; Mackenzie et al., 2006). The latter mechanisms are likely to play a major role only when transferrin

Cell Metabolism
Review

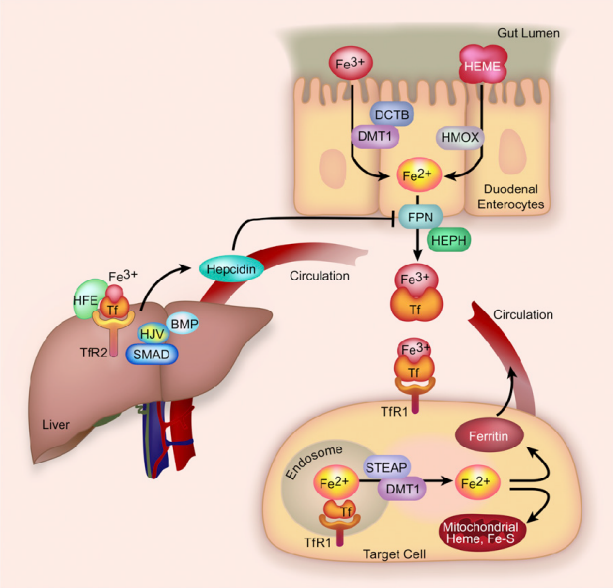

Figure 1. Overview of Iron Trafficking

Intestinal free ferric (Fe^{3+}) iron is reduced to Fe^{2+} by DCTB and enters the cell through the divalent metal-ion transporter 1 (DMT1) and possibly other carriers. Dietary heme is directly absorbed and iron is released by heme oxygenase (HMOX). Iron exits the enterocyte through the iron export channel ferroportin (FPN). After oxidization by hephaestin (HEPH), iron binds in the bloodstream to transferrin (Tf), which binds to transferrin receptors 1 and 2 (TfR1 and TfR2) on the surface of target cells. In most cells, after endocytosis of TfR1 and acidification of the endosome, iron is released, reduced by STEAP, and through DMT1 enters the cytosol, where it is used (e.g., for heme or Fe-S-cluster synthesis in the mitochondrion) or, if in excess, sequestered by ferritin. Ferritin secreted into the blood serves as a marker for tissue iron stores. In the liver, Tf binds TfR2 and the protein HFE, and, in concert with signaling via GPI-anchored protein hemojuvelin (HJV), bone morphogenic proteins (BMP) and the SMAD signal transduction pathway, production of hepcidin is signaled. Hepcidin induces internalization and degradation of FPN, thus completing a negative feedback regulatory loop.

approaches saturation, that is, in conditions of iron overload. Most of the iron is used in the mitochondrion for heme and iron-sulfur cluster synthesis, although its trafficking to the mitochondrion for such utilization is incompletely understood. Cytosolic iron levels are autoregulated through binding to iron-regulatory proteins (IRPs). Excess iron releases IRPs from the iron-responsive element (IRE) on the 3′ untranslated region (UTR) of the TFR1 messenger RNA (mRNA) and the 5′ UTR of the ferritin mRNA, as well as on the UTRs of mRNAs of several other iron-regulated proteins. This results in decreased stability of TfR mRNA, decreasing further iron uptake, and in increased translation of ferritin, sequestering iron inside the cell. Part of the increased ferritin that is translated is secreted, largely iron free, and serves as a marker of tissue iron stores.

Transferrin-bound iron also interacts with the hepatocyte TfR2 and the protein HFE on the surface of hepatocytes (D'Alessio et al., 2012). Through a signaling process that is still incompletely understood but that also requires hemojuvelin (HJV), bone morphogenic protein 6 (BMP6) (Andriopoulos et al., 2009; Meynard et al., 2009), and the SMAD (human homolog of *Drosophila* mad) pathway (Wang et al., 2005), the production of hepcidin is stimulated. The involvement of TfR2, HJV, HFE, and hepcidin in human iron homeostasis is demonstrated by human mutations in all that result in iron overload. Hepcidin, a 25 amino acid peptide, enters the systemic circulation and induces internalization and degradation of intestinal epithelial ferroportin, thus acting as a negative feedback regulator of iron absorption (Nemeth et al., 2004). Hepcidin also regulates efflux of iron from other cells that express high levels of ferroportin, including macrophages. Although iron egress from the enterocyte is the major control point for entry of iron into the body, DMT1 is also regulated by iron- and possibly hepcidin-dependent mechanisms and by the hypoxia-inducible transcription factor HIF-2α (Mastrogiannaki et al., 2009; Shah et al., 2009). Dietary heme is also directly absorbed by the enterocyte through less defined pathways (Shayeghi et al., 2005). Release of iron from heme is accomplished by heme oxygenase (HMOX).

An important fact to consider in evaluating the effects of iron on metabolism is the very wide range of "normal" serum ferritin in humans, 30–300 ng/ml in men and 15–200 ng/ml in women (Fleming et al., 2001; Nelson et al., 1978). The levels of very few human blood constituents have such a 10-fold normal variation, suggesting the possibility that "normal" may not be ideal. Despite the extensive regulation of iron uptake, it is possible with dietary iron excess to achieve levels of tissue iron higher than are necessary to maintain normal erythropoiesis and metabolic function. Commercial "normal" rodent chows vary by a factor greater than ten in iron content. More important than the absolute levels of iron is its bioavailability, but when all factors are considered, many normal chows deliver significantly higher amounts of iron than are consumed by mice living in the wild or are necessary to maintain normal breeding and blood hemoglobin concentrations. The same is true of the diets of many humans, particularly in affluent western cultures. Thus, the results to be presented below suggest that within the boundaries of tissue iron levels defined by overt iron deficiency and pathologic overload, the broad range of "normal" iron may, in fact, include levels that confer health risks of which we are currently unaware.

Iron homeostatic pathways are tightly linked to inflammatory stressors. Inflammation causes significant upregulation of

Cell Metabolism
Review

hepcidin, largely through interleukin-6 (IL-6), and also results in large increases in serum ferritin levels (reviewed in Ganz and Nemeth, 2009). The fact that inflammation results in the suppression of intestinal iron uptake has been hypothesized to be related to the beneficial effect of sequestering iron from invading microbes. It may also be important in elucidating the link of iron to diabetes that in turn is linked to inflammation (Hotamisligil, 2006). The relationships among diabetes, inflammation, and ferritin, therefore, could be complex, with ferritin reflecting excess iron stores that cause diabetes, reflecting inflammation that causes diabetes, or both. Furthermore, if iron causes diabetes, one of the mechanisms could be through its ability to cause oxidant stress that may be linked to inflammation. We will first consider the evidence that suggests that iron overload is sufficient to cause diabetes.

Diabetes Associated with Iron Overload in Pathologic States: β Cell Failure and Insulin Sensitivity

The first and clearest evidence for a relation between iron and human diabetes came from clinical observations of individuals with pathologic iron overload. These included cases of hereditary hemochromatosis (HH) (Buysschaert et al., 1997; Moirand et al., 1997), as well as transfusional iron overload (Dmochowski et al., 1993; Merkel et al., 1988). The best-studied example of the latter is beta thalassemia major, although diabetes is also a complication of other conditions requiring frequent or long-term transfusion such as bone marrow transplantation (Baker et al., 2007). Some rare causes of diabetes such as Friedreich ataxia are also associated with disturbances of iron balance and with mutations in proteins regulating iron metabolism (Radisky et al., 1999). Below we describe the phenotypes of these iron overload conditions.

Hereditary Hemochromatosis

HH is transmitted as an autosomal recessive trait and occurs in approximately five per 1,000 Caucasians of northern European descent (Pietrangelo, 2010). Most patients with hemochromatosis are homozygous for a mutation in the *HFE* gene resulting in the C282Y substitution in the HFE protein (Feder et al., 1996). Mutations in TfR2, HJV, and hepcidin are rarer causes of hemochromatosis (Pietrangelo, 2010). Normal HFE is partially required for iron stimulation of hepcidin (Nemeth et al., 2005), and in the absence of HFE, protein hepcidin expression is reduced and iron absorption is inappropriately high for a given body iron load (Nemeth et al., 2004). The high prevalence of *HFE* mutations argues that it might have served an adaptive function, preventing a restriction on iron uptake in populations evolving in locations without consistent access to dietary iron (Toomajian et al., 2003). HH was originally described as a triad of diabetes, cirrhosis, and skin pigmentation. In relatively small clinical studies not well controlled for selection bias, the prevalence of diabetes in hemochromatosis had been found to be 7%–40% (Buysschaert et al., 1997; Moirand et al., 1997). With identification of the genetic cause of HH, however, it was possible to perform more unbiased screens for diabetes prevalence. Recent studies show the prevalence of diabetes to be 13%–22% and impaired glucose tolerance 18%–30% (Hatunic et al., 2010a; McClain et al., 2006). Of note, HH is largely a disease of individuals of northern European descent, wherein the background prevalence rate of diabetes is only ~5%–10%. Other studies have not found increased diabetes prevalence in C282Y homozygotes (Beutler et al., 2002), although in that case comparing homozygotes to a control population that was of mixed racial/ethnic descent might have skewed the baseline diabetes prevalence.

The pathophysiology of diabetes associated with HH is controversial, with evidence suggesting that both insulin deficiency and insulin resistance are contributing factors (Hramiak et al., 1997; Mendler et al., 1999). Some of this work is difficult to interpret because subjects with established diabetes are studied, in which case the attendant hyperglycemia might itself have resulted in insulin resistance and insulin secretory abnormalities (Rossetti et al., 1990). In the authors' study of this question, when only HH subjects with prediabetes are considered, those subjects differ significantly from controls only in terms of insulin secretory capacity and in fact had a trend toward *increased* insulin sensitivity (McClain et al., 2006). The subjects with overt diabetes exhibit insulin resistance, but the great majority of those individuals (80%) are also obese. One interpretation of these data is that HH itself is diabetogenic mainly because of decreased insulin secretion, and diabetes usually results when insulin resistance from an independent mechanism such as obesity intervenes. Individuals with HH cannot respond with increased insulin secretion because of primary pathology in the β cells, and therefore they are highly prone to develop diabetes when insulin resistant (McClain et al., 2006). Consistent with this hypothesis, insulin secretory abnormalities but not insulin sensitivity improve when persons with HH undergo phlebotomy (Abraham et al., 2006; Hatunic et al., 2010b).

Study of mouse models of HH, namely mice with targeted deletion of *Hfe* or replacement of deleted wild-type *Hfe* with a gene encoding the C282Y mutant, have contributed to our understanding of the mechanisms involved in diabetes associated with HH (Cooksey et al., 2004). $Hfe^{-/-}$ mice exhibit decreased insulin secretory capacity secondary to oxidative stress, decreased glucose-stimulated insulin secretion, and increased β cell apoptosis. These mice have increased insulin sensitivity, however, and do not develop diabetes, supporting the hypothesis that insulin resistance is a causal but secondary factor in HH diabetes. Study of these mice has provided further mechanistic insights. For example, the observed oxidative stress in islets and other tissues is not only caused directly by the generation of free radicals from iron reacting with hydrogen peroxide (Fenton chemistry). In addition, iron interferes with the trafficking of other transition metals. Mitochondrial uptake of manganese (Mn^{2+}) is inhibited, resulting in decreased metallation and activity of superoxide dismutase 2 (SOD2), and much of the oxidant damage can be ameliorated by Mn supplementation (Jouihan et al., 2008). Thus, the effect of excess iron on the levels and trafficking of other metals is an important but understudied area.

Beta Thalassemia Major and Transfusional Iron Overload

Thalassemia is a group of disorders characterized by deficient production of the β globin subunit of hemoglobin (Weatherall, 1998). Patients with thalassemia become iron overloaded because of the numerous transfusions required to maintain adequate erythrocyte levels as well as from increased iron absorption (Weatherall, 1998). A single unit of blood contains

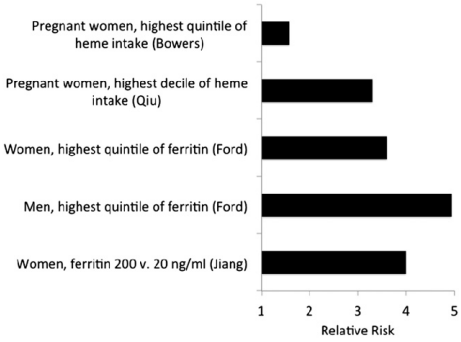

Figure 2. Relative Risk of Diabetes as a Function of Ferritin or Dietary Iron Intake in Four Studies

Plotted are the relative risks from four studies (Bowers et al., 2011; Qiu et al., 2011; Ford and Cogswell, 1999; Jiang et al., 2004), with the comparator groups listed on the y axis.

up to 100 times the amount of iron that enters the circulation daily through the gut. The prevalence of diabetes in patients with thalassemia is 6%–14% (Borgna-Pignatti et al., 2004; Vogiatzi et al., 2009). Several studies have shown that insulin resistance and insulin deficiency mark both the prediabetic state and diabetes in thalassemia (Dmochowski et al., 1993; Merkel et al., 1988; Messina et al., 2002). Insulin secretory defects, however, may appear earlier than insulin resistance (Jaruratanasirikul et al., 2008). The existence of insulin sensitivity in HH but insulin resistance in transfusional iron overload is probably explained by the different tissues in which the excess iron accumulates in situations of low hepcidin (HH) compared to high hepcidin (thalassemia patients with iron overload). The causal role of iron in the pathogenesis of diabetes is suggested by the declining rates of diabetes since the more aggressive and widespread use of iron chelation therapy (Borgna-Pignatti et al., 1998; Gamberini et al., 2008).

Transfusions for other conditions are also associated with increased diabetes risk. A relatively young cohort of survivors of pediatric bone marrow transplantation, for example, had a 5% prevalence of type 2 diabetes (Hoffmeister et al., 2004). Another study revealed a prevalence of diabetes three times that of sibling controls (Baker et al., 2007). Interpretation of these studies is complicated, however, by the additional effects of chemotherapeutic agents such as glucocorticoids and asparaginase on insulin production and action.

Effects of Iron in Nonpathologic States: Diabetes and Dietary Iron

Increased iron stores are also associated with the development of typical type 2 diabetes (reviewed in Fernández-Real et al., 2002a). For example, in 9,486 adults in the United States studied as part of the National Health and Nutrition Education Survey (NHANES), the odds ratios for newly diagnosed diabetes in those with elevated serum ferritin levels are 4.94 for men and 3.61 for women (Ford and Cogswell, 1999). This iron-associated risk approaches the relative risk engendered by obesity (Kriska et al., 2003). Similar relationships between iron and diabetes risk, insulin resistance, or both have emerged from studies of other populations, including Europeans and African Americans (Jiang et al., 2004; Tuomainen et al., 1997; Wilson et al., 2003), and from other conditions, including gestational diabetes (Afkhami-Ardekani and Rashidi, 2009) and prediabetes (Sharifi et al., 2008). The strong relationship between ferritin and diabetes risk, across sexes and in different types of diabetes (type 2 and gestational), even across the normal range of ferritin, is evident in Figure 2 (Jiang et al., 2004). Recent data from the NHANES population also demonstrate that high ferritin approximately doubles the risk for metabolic syndrome after accounting for age, race, alcohol, smoking, and inflammatory state as assessed by C-reactive protein (CRP) levels (Jehn et al., 2004). High ferritin is also positively correlated with central adiposity (Gillum, 2001; Iwasaki et al., 2005), hepatic steatohepatitis (Dongiovanni et al., 2011), and cardiovascular disease (Iwasaki et al., 2005; Qi et al., 2007).

Type 2 diabetes is a disease marked by chronic inflammation (Hotamisligil, 2006), and ferritin increases with inflammation. The question therefore arises whether high iron, whose best biomarker is high ferritin, causes diabetes or diabetes causes high ferritin. Several lines of evidence support the former causality. In the study of metabolic syndrome quoted above, for example, independent markers of inflammatory stress such as CRP did not account for the association of ferritin with diabetes (Jehn et al., 2004). Other studies have also concluded that the diabetes risk associated with high iron is not accounted for by HH or inflammation but rather is related to dietary iron overload (Fleming et al., 2001; Fleming et al., 2002). Two recent studies of gestational diabetes have observed that the increased risk is associated in particular with dietary heme iron, which is more efficiently absorbed than nonheme iron (Bowers et al., 2011; Qiu et al., 2011). The best evidence for the causality of iron, however, is those studies in which reversal of diabetes occurs with iron reduction (below).

Differences between the Diabetes Phenotype of Hemochromatosis and Dietary or Transfusional Iron Overload: Role of Adiponectin

An important dichotomy is evident when considering the phenotype of individuals with hemochromatosis compared to those with typical type 2 diabetes. Namely, in both humans and in the mouse models, prediabetic HH is associated with lower insulin levels but enhanced insulin sensitivity (McClain et al., 2006). The typical phenotype of subjects with type 2 diabetes and those with dietary and transfusional iron overload, however, is one of insulin resistance (Fernández-Real et al., 2002a).

Mouse models (Cooksey et al., 2004) and humans with HH exhibit significantly higher levels of adiponectin (Gabrielsen et al., 2012). Adiponectin is an adipokine, a secreted, hormone-like protein produced by adipocytes and causally linked to insulin sensitivity (Kubota et al., 2002). In contrast to HH, mice with dietary iron overload have *lower* adiponectin levels than mice on lower iron chows (Gabrielsen et al., 2012). This finding is explained by the high ferroportin expression in adipocytes (Gabrielsen et al., 2012). In the limited tissues expressing high levels of ferroportin such as macrophages,

Cell Metabolism
Review

decreased hepcidin in HH results in increased ferroportin expression, iron export, and, therefore, in decreased iron levels despite total body iron overload (Brink et al., 1976; Cairo et al., 1997; Knutson et al., 2005).

In dietary iron overload, by contrast, hepcidin levels rise and iron accumulates in cells that express ferroportin, including adipocytes, because ferroportin is downregulated. Thus, in healthy non-HH populations, there is a negative relationship between serum ferritin and adiponectin (Fargnoli et al., 2008; Forouhi et al., 2007; Gabrielsen et al., 2012; Mojiminiyi et al., 2008). A recent large study has also demonstrated not only that ferritin is inversely associated with adiponectin, but also that both of these markers are associated with adipocyte insulin resistance as defined by elevated serum nonesterified fatty acid levels despite elevated insulin (Wlazlo et al., 2013). Inflammation increases ferritin and decreases adiponectin production (Subauste and Burant, 2007), and adipose tissue is inflamed in diabetes (Trayhurn and Wood, 2005), but this does not fully account for the ferritin-adiponectin relationship. We have determined, for example, that normal-range serum ferritin levels are strongly and inversely associated with adiponectin independently of inflammation as assessed by serum levels of CRP, IL-6, or tumor necrosis factor α (Gabrielsen et al., 2012). These observations were made in large and independent cohorts of subjects with type 2 diabetes and of obese subjects with diabetes compared to equally obese individuals without metabolic syndrome. Ferritin predicts adiponectin levels significantly better than body mass index. The relationship of ferritin to adiponectin is weaker in females, probably because the range of ferritin values is significantly narrower and lower in females than in males. The data suggest that ferritin may be one determinant of the higher adiponectin levels seen in females (Arita et al., 1999) and provide a potential contributing reason for the decreased incidence of diabetes in women prior to menopause (Szmuilowicz et al., 2009).

The use by adipocytes of iron levels to regulate adiponectin suggests an endocrine role for adipocytes in coordinating organism-wide metabolic responses to iron availability, as they do for responses to overall macronutrient status. There is other evidence for crosstalk between iron and adipocyte metabolism. Insulin treatment, for example, increases iron uptake by increasing cell-surface expression of TfR1 in adipocytes (Davis et al., 1986; Tanner and Lienhard, 1987). Iron induces lipolysis in cultured adipocytes and modulates the lipolytic response to norepinephrine (Rumberger et al., 2004; Yamagishi et al., 2000). Adipocytes express not only common regulators of iron homeostasis such as ferritin and iron-regulatory proteins (Festa et al., 2000), but also iron-related proteins with restricted tissue expression (TfR2, HFE, and hepcidin) (Bekri et al., 2006; Farahani et al., 2004). In addition, expression of high levels of ferroportin in adipocytes allows them to serve an iron-sensing function with greater dynamic range and sensitivity, as reflected by the blunting of adiponectin response to dietary iron in animals with targeted deletion of the ferroportin gene in adipocytes (Gabrielsen et al., 2012).

Reduction of Iron as a Treatment for Diabetes

The previous data lead to the prediction that decrease of iron stores in dietary iron excess will be doubly beneficial to diabetes risk, increasing both insulin secretion, as in the studies of HH, and insulin sensitivity, through mechanisms that include increasing adiponectin. The β cell will have similar response and susceptibility to iron overload in both HH and dietary overload because of low or absent ferroportin (Hudson et al., 2010). In addition, β cells may be especially sensitive to iron because of high expression of DMT1 (Koch et al., 2003), which is needed for import of zinc for secretory packaging, but can also transport free serum iron whose levels will increase as transferrin approaches higher levels of iron saturation. Beneficial effects of phlebotomy have been demonstrated in a number of animal models of type 2 diabetes. Otsuka Long-Evans Tokushima Fatty (OLETF) rats that are phlebotomized or fed an iron-deficient diet exhibit lower hemoglobin A1c levels than controls (Minamiyama et al., 2010). Similar results are seen in the leptin-deficient *Ob/Ob* model of type 2 diabetes wherein low iron diets or iron chelators result in significant protection from diabetes that is related both to increased insulin secretion and sensitivity (Cooksey et al., 2010). In the latter study, the effects of lowering iron are long lasting and reversible and, importantly, are seen with levels of iron restriction that did not result in iron-deficiency anemia. Supporting these observations, iron-deficient veal calves and rats are more insulin sensitive than are iron sufficient controls and exhibit increased glucose utilization (Borel et al., 1993; Henderson et al., 1986; Hostettler-Allen et al., 1993).

Somewhat surprisingly, human data on the effects of iron depletion in common type 2 diabetes are scant. In relatively small and short-term studies of non-HH subjects either with or without known type 2 diabetes, phlebotomy improves insulin sensitivity, insulin secretion, and glycemia (Facchini, 1998; Fernández-Real et al., 2002b). Blood donors also exhibit increased insulin sensitivity and secretion, although there might be selection bias in these studies in terms of the population that donates blood (Fernández-Real et al., 2005). The study on the relation of iron to adiponectin, summarized in the previous section, also included a proof-of-concept study of a very small sample of prediabetic humans in which phlebotomy was performed to bring the individuals from the highest quartile of normal ferritin down to the lowest quartile (Gabrielsen et al., 2012). This intervention improved adiponectin, the area under the glucose curve, and the insulin disposition index, which is the product of insulin secretion and insulin sensitivity and a useful predictor of diabetes risk.

Phlebotomy also improves other factors associated with diabetes and the metabolic syndrome, including hypertriglyceridemia (Bofill et al., 1994), vascular reactivity (Fernández-Real et al., 2002c), and markers of nonalcoholic steatohepatitis (NASH) (Facchini et al., 2002). More recently, phlebotomy of 550–800 ml blood (1–1.5 units) from individuals with metabolic syndrome was shown to decrease blood pressure, fasting glucose, HbA1c, and the ratio of LDL to HDL cholesterol when measured 6 weeks after the first phlebotomy (Houschyar et al., 2012). There was a trend toward an increase in insulin sensitivity that was not significant ($p = 0.28$). As a cautionary note, however, the individuals in the NASH study gained weight with blood donation, and the OLETF rats on the iron deficient diet had higher blood triglyceride and cholesterol levels (Minamiyama et al., 2010). Both the weight gain and increased blood lipids are

consistent with the effects of iron on fat metabolism and energy expenditure, and the phenotypes of those with overt iron deficiency, to be described below. Larger and longer-term studies are required in humans to address both the beneficial and potential adverse effects of iron depletion, their dose responsiveness, and their longevity.

Iron, Obesity, and Lipid Metabolism

Most investigations into the effects of iron on metabolism have focused on glucose metabolism because of the important epidemiologic connections between pathologic iron overload and diabetes. These connections have been evident since the early descriptions of hemochromatosis and its subsequent link to tissue iron overload in the 19th century. There is evidence, however, that iron also affects lipid metabolism, adipocyte biology, and obesity. This is not surprising, given the effects of iron on adiponectin, the requirement for iron in the oxidation of lipids, and the potential additive effects of oxidative stress from lipid metabolism and excess iron.

There is a greater prevalence of iron deficiency in obese (39%) and overweight (12%) children and adolescents than normal weight children whose prevalence of iron deficiency is only 4% (Pinhas-Hamiel et al., 2003). The association of iron deficiency with obesity has been confirmed in other populations that include children and adults of both sexes (Cepeda-Lopez et al., 2011; Yanoff et al., 2007). The immediate question that arises is one of causality: the observations might simply be coincidental; for example the diets of many obese individuals may be enriched in iron-poor foods. Plausible cases for causality, in turn, can be made in both directions: normal or high iron stores might be needed to support higher rates of fatty acid oxidation so that iron-deficient individuals are less able to mobilize and use high fat, or, conversely, the inflammatory nature of obesity might trigger increased hepcidin levels that limit dietary iron absorption. Support for the latter hypothesis comes from a study that observed a 2-fold increase in the prevalence of iron deficiency in obese Mexican women and children compared to lean controls (Cepeda-Lopez et al., 2011). In this study, it was not dietary iron content but the inflammatory marker CRP, which was higher in the obese group, that was the best predictor of iron deficiency. Another study found body mass index to be associated with low serum iron but high ferritin, consistent with low-grade inflammation in obesity causing iron sequestration, perhaps mediated by hepcidin (Ausk and Ioannou, 2008). Other studies have found patterns both of primary iron deficiency and of inflammation-mediated iron sequestration in obese adults (Yanoff et al., 2007). Thus, the iron phenotype of obese individuals is likely heterogeneous.

Animal studies demonstrate that iron restriction can be a primary and independent cause of adiposity. Namely, rats fed an iron-deficient diet have increased fat mass, although there is a compensating loss of lean mass such that obesity per se does not develop (McClung et al., 2008). More recently, adipocyte-restricted overexpression of the protein mitoNEET, which sequesters iron sulfur clusters, was shown to lower adipocyte heme and mitochondrial iron and result in extreme obesity in *Ob/Ob* mice (Kusminski et al., 2012). The obesity, however, is well tolerated, and the mice remain insulin sensitive and nondiabetic. The phenotype is reminiscent of the "healthy obese" without metabolic syndrome who have lower ferritin levels that those with metabolic syndrome (Gabrielsen et al., 2012). Other studies have revealed further layers of complexity in the relationship between iron and obesity; for example, an obesogenic high-fat diet can cause decreased iron absorption in the gut, mediated by dysregulation of the oxidoreductases DCTB and hephaestin (Sonnweber et al., 2012).

The possible mechanisms underlying weight regulation by iron are therefore likely to be multifactorial. Iron is required for lipolysis in cultured adipocytes (Rumberger et al., 2004), and this may contribute to the observations that rats fed an iron-deficient diet (Stangl and Kirchgessner, 1998) and iron-deficient women (Ozdemir et al., 2007) have lower plasma levels of triglycerides. Another contributing factor to lower triglycerides is that high levels of iron augment fatty acid oxidation, as was shown in the HH mouse model ($Hfe^{-/-}$) (Huang et al., 2011). On normal chow, although $Hfe^{-/-}$ mice exhibit increased glucose uptake in skeletal muscle, glucose oxidation is decreased and the ratio of fatty acid to glucose oxidation is increased. When put onto a high-fat diet, the $Hfe^{-/-}$ mice exhibit increased fatty acid oxidation, are hypermetabolic, and are protected from obesity. In addition to promoting lipid oxidation, high dietary iron also stimulates lipogenesis (Baquer et al., 1982), so the net effects of iron on lipid metabolism are complex.

In addition to direct modulation of lipid metabolism pathways, the finding that iron regulates adiponectin secretion suggests the possibility that iron availability might also be used to coordinate metabolism by regulating other hormones important to fuel and energy homeostasis. Indeed, levels of the anorexigenic hormone leptin are low in thalassemia patients (Chaliasos et al., 2010), although this would be expected to contribute to greater caloric intake, not leanness, in iron-overloaded individuals. The effects of iron on adiponectin also cannot be simply reconciled with the actions of iron to increase fatty acid oxidation rates, since adiponectin promotes fatty acid oxidation but is decreased by iron. The decrease in adiponectin could be seen as a mechanism to compensate for the fact that iron can stimulate fatty acid oxidation directly (see below), thus protecting the organism from additive oxidative stressors. Clearly much more basic knowledge on the effects and mechanism of action of iron on these diverse pathways in multiple tissues is needed before we will understand the complex phenomena. Finally, an understanding of why both low and high iron are associated with obesity is needed: is there a modal dose-response curve for some of these effects, and are they related to independent and distinct mechanisms at the two ends of the spectrum of tissue iron levels?

Potential Molecular Mechanisms for Iron Regulation of Glucose Metabolism

The mechanisms underlying the effects of altering tissue iron on metabolism are just beginning to be understood. Given the many effects in multiple tissues already described and the involvement of iron and heme in processes as diverse as glucose and fat oxidation, hypoxia sensing (Semenza, 2012), CO and NO sensing, transcriptional regulation (Yin et al., 2007), generation of reactive oxygen species, and regulation of hormone levels, the effects of iron are likely to be protean. Furthermore, the effects will have dose thresholds that will differ across the range

Cell Metabolism
Review

from iron deficiency, through the broad range of normal, to iron excess.

Reactive Oxygen Species

Iron is capable of generating hydroxyl radicals from peroxide and can also inhibit antioxidant defenses such as SOD2 (Jouihan et al., 2008), although it is worth noting that iron deficiency is also associated with increased reactive oxygen species (ROS) (Walter et al., 2002). High iron has been linked to oxidative damage to DNA, lipids, and proteins that in turn has been implicated in cardiovascular disease, diabetes, atherosclerosis, and neurological degeneration as seen in Alzheimer's (Jomova and Valko, 2011). In the progression of diabetes ROS can cause both β cell failure and insulin resistance. β cells are particularly sensitive to ROS because of low expression of antioxidants such as catalase and SOD2, overexpression of which have been shown to increase β cell viability (Azevedo-Martins et al., 2003; Lenzen et al., 1996). ROS can cause β cell dysfunction by multiple mechanisms including decreased insulin gene expression secondary to decreased expression of transcription factors necessary for β cell differentiation, maintenance, and insulin gene transcription (Kaneto et al., 2010). ROS have also been reported to directly affect circulating human insulin by hydroxylation of phenylalanine residues that results in lower affinity binding to the insulin receptor (Montes-Cortes et al., 2010). Finally, ROS can induce insulin resistance through multiple mechanisms—for example, activation of FOXO1, which prevents downregulation of gluconeogenesis even in the presence of insulin signaling (Ponugoti et al., 2012).

The number of other potential targets of ROS that could contribute to diabetes is immense. It should be kept in mind that low levels of ROS also act as physiologic and normal cell signaling molecules that mediate cellular differentiation, survival, and metabolism (Ray et al., 2012). In mammals, for example, ROS generated by the electron transport complex III is released into the intermembrane space of mitochondria, where it can escape to the cytosol and activate PPARγ, C/EBPα, and adipocyte differentiation (Tormos et al., 2011). Other ROS signaling targets include the MAPK and PI3K pathways, wherein oxidation of cysteines in protein phosphatases results in activation (Ray et al., 2012). Thus, ROS generated by intermediate levels of iron may play a role in normal metabolic regulation, once again emphasizing the theme that the transition between signaling normal physiologic responses and pathophysiologic ones may be a subtle one and that the effects of iron are likely to be highly context dependent. Finally, it should be mentioned that iron is also capable of generating reactive nitrogen species that are also capable of triggering modification of macromolecules (Nappi and Vass, 1998).

Hypoxia-Inducible Factors

Hypoxia-inducible factors 1 and 2 (HIF-1 and HIF-2) regulate cellular response to low oxygen by upregulating transcription of a diverse set of proteins involved in angiogenesis, erythropoiesis, and glycolytic flux (reviewed in Semenza, 2012). HIFs also regulate iron metabolism, and under conditions of low iron HIF-2 upregulates DMT-1 and DCYTB, while HIF-1 upregulates DMT-1 and decreases ferritin (Romney et al., 2011; Shah et al., 2009). Conversely, cellular iron levels regulate HIF protein levels through control of prolyl hydroxylase (PHD) activity (Semenza, 2012). PHDs require iron and oxygen to hydroxylate HIF subunits to target them for degradation by von Hippel-Lindau (VHL) E3 ubiquitin ligase. Under conditions of low iron or low oxygen, PHDs are inactive and HIF is stabilized. As a result, β cells treated with an iron chelator increase Hif1α protein, while iron treatment decreases Hif1α (Cheng et al., 2010). Decreased Hif1α results in downregulation of its targets, including the glucose transporters Glut1 and Glut2, which in turn results in impaired glucose sensing and glucose-stimulated insulin secretion (Cheng et al., 2010). Mice with targeted deletion of *Vhl* in β cells develop basal hypoglycemia with increased insulin. When challenged with glucose, however, they have impaired glucose tolerance due to impaired glucose stimulated insulin secretion (Zehetner et al., 2008). The latter effect is explained by increased Hif-activated glucose uptake and glycolysis stimulating higher levels of ATP production and insulin secretion in the basal state, whereas with rising glucose there is less glucose oxidation resulting in less ATP and insulin secretion than in normal cells.

HIFs are also known to regulate energy utilization in muscle, liver, and fat by stimulating glycolysis and cellular glucose uptake to allow for a shift to glycolytic metabolism. Specifically, Hif-1α upregulates glucose transporters GLUT1 and GLUT3 and increases expression of hexokinase 1 and 2 (Aragonés et al., 2009). Hypoxia impacts insulin signaling in adipocytes by reducing the level of insulin receptor phosphorylation (Regazzetti et al., 2009). HIF also plays a role of increasing the inflammatory state of adipose tissue and increasing fibrosis through a HIF target enzyme lysyl oxidase (Halberg et al., 2009). Targeted disruption Hif-1α or Hif-1β in adipose tissue improves insulin signaling and decreases fat mass even when the mice are challenged with a high fat diet (Jiang et al., 2011). The integration of these and other effects of hypoxia on metabolism is seen in a disease of chronic pseudohypoxia, namely Chuvash polycythemia. Patients with Chuvash polycythemia are homozygous for a mutation in VHL that prevents HIF degradation, allowing it to be constitutively active (Ang et al., 2002). These patients have decreased circulating glucose, increased Glut1, and decreased hemoglobin A1c (McClain et al., 2013).

AMP-Activated Protein Kinase

The AMP-activated protein kinase (AMPK) pathway controls energy balance by sensing cellular energy status through its activation by an elevated ratio of AMP to ATP (Hardie, 2011). A large variety of hormonal signals and metabolic stresses such as glucose deprivation, ischemia, hypoxia, oxidative stress, and hyperosmotic stress activate AMPK, although not all of these work through altering the AMP:ATP ratio (Kahn et al., 2005). Activated AMPK stimulates glucose uptake and fatty acid oxidation in tissues and suppresses gluconeogenesis in liver (Long and Zierath, 2006). These are pathways that play important roles in the pathogenesis and treatment of diabetes and are also pathways that are affected by iron. Close coregulation of iron levels and metabolic parameters such as fuel preference is conserved from yeast to mammals, and in yeast this coregulation is mediated by the ortholog of AMPK, Snf1 (Haurie et al., 2003; Shakoury-Elizeh et al., 2010).

As described above, *Hfe*$^{-/-}$ mice demonstrate increased adiponectin concentrations. One of the principal targets mediating adiponectin action, AMPK, is activated in *Hfe*$^{-/-}$ mice (Huang et al., 2007), but iron can also activate AMPK independently of adiponectin. Although the mechanism for this activation is not

completely understood, plausible candidates include:(1) alterations in AMP/ATP ratios caused by iron-induced mitochondrial dysfunction (Jouihan et al., 2008), or (2) stimulation of the upstream activating kinase of AMPK, LKB1, by SIRT1-mediated deacetylation (Hou et al., 2008; Lan et al., 2008). SIRT1 is itself activated by oxidant stress and/or NAD (Alcendor et al., 2007; Brunet et al., 2004). These results serve further to illustrate the complexity of the association of iron and diabetes risk in that the effects of AMPK activation by iron on glucose disposal, gluconeogenesis, and lipid oxidation are generally antidiabetic. Thus, the integration of the pleiotropic effects of iron on diabetes risk in multiple tissues is not yet fully understood.

Iron-Responsive Elements

IRPs maintain cellular iron homeostasis through iron-regulated binding to IREs (reviewed in Anderson et al., 2012). IRP1 is known to have dual functions, both as an iron sensor and as a cytosolic aconitase when bound to iron sulfur clusters. In the mitochondrion, aconitase functions in the tricarboxylic acid (TCA) cycle, in which it catalyzes the reversible isomerization of citrate and isocitrate, but in the cytosol the production of citrate generates a substrate for ATP-citrate lyase. Cytosolic aconitase is also important in reducing $NADP^+$ to NADPH, a cofactor for enzymes involved in synthesis of glutathione, lipids, and cholesterol (Minard and McAlister-Henn, 2005). Mitochondrial aconitase is sensitive to iron because it contains four iron sulfur clusters and is downregulated by IRPs in low-iron conditions (Eisenstein and Ross, 2003). Thus, not only do IRPs control cellular iron metabolism but IRP-dependent regulation also has far-reaching metabolic effects through control of mitochondrial and cytosolic citrate levels. Abnormal IRP1 activity is seen in patients with Friedreich ataxia (Condò et al., 2010; Lobmayr et al., 2005), a human degenerative neuromuscular disease caused by a mutation in a mitochondrial protein, frataxin, which is thought to be an iron chaperone or storage protein (Babcock et al., 1997). In these patients, IRP1 aconitase activity is decreased, while IRP binding to IREs is increased. Interestingly, Friedreich ataxia is associated with increased prevalence of type 2 diabetes.

Epigenetic Effects of Iron

The Dutch Famine Birth Cohort Study's finding of increased prevalence of type 2 diabetes and metabolic syndrome in adults prenatally exposed to extreme caloric restriction has prompted investigations on the epigenetic impact of maternal nutrition on the metabolic state of offspring (Ravelli et al., 1998). Maternal iron intake impacts the metabolic programming of offspring, although this relationship may be complex, with factors such as the period of altered iron status and the direction of change (high or low iron) affecting the phenotype. In rats, prenatal iron deficiency increases susceptibility to high-fat-diet-induced obesity, glucose intolerance, and hypertension (Bourque et al., 2012). When not challenged with the high-fat diet, however, offspring of rat dams with dietary iron restriction have improved glucose tolerance and lower serum triglycerides although they also demonstrate higher systolic blood pressure (Lewis et al., 2001). Thus, the effects of iron on metabolic programming may be diet dependent, consistent with its effects on mediators such as AMPK. Human studies have also largely focused on maternal iron deficiency, not iron excess, and not in the context of diabetes risk. Anemia during the third trimester of pregnancy lowers systolic pressure in 7-year-old offspring (Brion et al., 2008). In contrast, iron supplementation in the first trimester was associated with increased blood pressure in offspring (Belfort et al., 2008). Collectively, these results indicate that dietary iron may be a factor in signaling the fed verse fasted state of an organism, which could signal epigenetic modifications to initiate an altered metabolic state that is compliant with nutritional availability. More research is needed in this field to assess the role of prenatal iron exposure in adult glucose homeostasis.

There are several possible mechanisms for iron control of epigenetic modification including regulation of the sirtuin (Sirt) family of histone deacetylases, the Jumonji C (JmjC)-domain-containing histone demethylases, or both (reviewed in Houtkooper et al., 2012; Takeuchi et al., 2006). Sirts couple lysine deacetylation with NAD hydrolysis. Because NAD is limiting for this reaction, it is one pathway through which metabolism can directly affect epigenetics. NAD can be recycled from nicotinamide or synthesized de novo through a pathway rate-limited by nicotinamide phosphoribosyltransferase (NAMPT, also known as visfatin). There is a positive association between circulating levels of NAMPT and levels of ferritin and prohepcidin (Fernández-Real et al., 2007), although the physiologic importance of circulating NAMPT is not fully understood, and prohepcidin levels poorly reflect those of mature hepcidin. Histone demethylation also affects gene expression in a manner dependent on iron and the metabolic state of the cell. The JmjC-domain family of demethylases removes mono- or dimethyl groups through iron- and α-ketoglutarate-dependent oxidation reactions. The importance of iron in this reaction is highlighted by treatment of endothelial cells by desferoxamine, an iron chelator, which decreases demethylase activity in Jmj-domain-containing protein 6 to a similar level as protein knockdown (Boeckel et al., 2011). Interestingly, deletion of JmjC-domain-containing histone demethylase 2 ($JHDM2a^{-/-}$) in mice leads to obesity hyperlipidemia, hyperinsulinemia, and hyperleptinemia (Inagaki et al., 2009).

The mechanisms outlined in this section do not represent an exhaustive catalog of all the pathways and mechanisms by which iron may contribute to diabetes risk. For example, one possible mediator of the effects of iron for which evidence is emerging is heme, which is involved in several regulatory nodes. For example,

- PGC-1α, a master transcriptional regulator of metabolic programs also regulates heme synthesis (Handschin et al., 2005; Yin et al., 2007);
- the regulation of circadian metabolic rhythm, disruption of which is a risk factor for diabetes, is dependent on several heme-containing proteins (Handschin et al., 2005; Yin et al., 2007);
- and heme and iron play a role in microRNA processing through regulation of Drosha/Pasha and Dicer microRNA processing complexes (Faller et al., 2007; Li et al., 2012).

Iron is also linked to diabetes through mitoNEET, an iron-sulfur cluster protein and postulated target of the antidiabetic thiazolidinediones (Colca et al., 2004; Wiley et al., 2007). Thiazolidinediones prevent mitochondrial iron accumulation, suggesting that they may act, in part, through regulation of cellular iron

Cell Metabolism
Review

stores (Zuris et al., 2012; Zuris et al., 2011). Finally, iron is essential for the multitude of pathways that require heme or iron sulfur clusters for activity including the electron transport chain, TCA cycle, and DNA repair (Rouault and Tong, 2009). These diverse cellular processes illustrate that the relationship between iron and metabolism is complex and more research is needed to further establish how iron overload or depletion may affect these pathways.

Summary

Epidemiologic observations in humans and experimental studies in animal models have established a clear association between tissue iron stores and diabetes risk. A subset of these studies suggests that the relation is causal, that is, high iron is sufficient to cause diabetes. At the same time, it is clear that iron has a multiplicity of effects in many tissues that can be either pro- or antidiabetic at the ends of the spectrum that runs from iron deficiency to iron excess. In the β cell, for example, excess iron is toxic, but there is clearly also a minimum level required for full metallation of the proteins needed for glucose oxidation and glucose sensing. Likewise, although iron overload is associated with diabetes risk, iron deficiency is associated with another major risk factor for diabetes, obesity. The phenotypes of iron excess and obesity are certainly not mutually exclusive, however, and it might be in fact that the combination of obesity and iron overload is particularly prone to causing diabetes through its resulting combination of insulin deficiency and insulin resistance. It is probably also the case that the full expression of these effects depends on environmental and genetic factors. For example, high iron-induced augmentation of fat oxidation may be protective of obesity in individuals consuming diets with modest fat content but may cause excessive oxidant stress and concomitantly greater diabetes risk in individuals consuming a high-fat diet. Clearly, much work is needed to address many unanswered questions such as the following:

- Can long-lasting protection or cure of diabetes be afforded to individuals with high iron, and, if so, what are optimal levels of tissue iron and how may they be assessed?
- What is the effect of the full range of "normal" iron concentrations on diverse metabolic processes in tissues including liver, fat, muscle, pancreas, gut, and brain?
- What are the molecular mechanisms for these effects and can they be targeted by approaches other than changing global iron levels?
- How might this knowledge be relevant to other diseases with important components of both metabolism and redox signaling/stress including cancer and neurodegenerative diseases?
- Do the known polymorphisms in genes regulating iron uptake, antioxidant defenses, and related regulatory pathways modify diabetes risk in humans?

ACKNOWLEDGMENTS

This work was supported by the NIH (DK081842 to D.M. and T32DK091317 to J.S.), the Research Service of the Veterans Administration, and the Marilyn Jane Robinson Foundation. The authors would like to acknowledge the assistance of Amnon Schlegel for assistance in reviewing the manuscript.

REFERENCES

Abraham, D., Rogers, J., Gault, P., Kushner, J.P., and McClain, D.A. (2006). Increased insulin secretory capacity but decreased insulin sensitivity after correction of iron overload by phlebotomy in hereditary haemochromatosis. Diabetologia *49*, 2546–2551.

Afkhami-Ardekani, M., and Rashidi, M. (2009). Iron status in women with and without gestational diabetes mellitus. J. Diabetes Complications *23*, 194–198.

Alcendor, R.R., Gao, S., Zhai, P., Zablocki, D., Holle, E., Yu, X., Tian, B., Wagner, T., Vatner, S.F., and Sadoshima, J. (2007). Sirt1 regulates aging and resistance to oxidative stress in the heart. Circ. Res. *100*, 1512–1521.

Anderson, C.P., Shen, M., Eisenstein, R.S., and Leibold, E.A. (2012). Mammalian iron metabolism and its control by iron regulatory proteins. Biochim. Biophys. Acta *1823*, 1468–1483.

Andrews, N.C., and Schmidt, P.J. (2007). Iron homeostasis. Annu. Rev. Physiol. *69*, 69–85.

Andriopoulos, B., Jr., Corradini, E., Xia, Y., Faasse, S.A., Chen, S., Grgurevic, L., Knutson, M.D., Pietrangelo, A., Vukicevic, S., Lin, H.Y., and Babitt, J.L. (2009). BMP6 is a key endogenous regulator of hepcidin expression and iron metabolism. Nat. Genet. *41*, 482–487.

Ang, S.O., Chen, H., Hirota, K., Gordeuk, V.R., Jelinek, J., Guan, Y., Liu, E., Sergueeva, A.I., Miasnikova, G.Y., Mole, D., et al. (2002). Disruption of oxygen homeostasis underlies congenital Chuvash polycythemia. Nat. Genet. *32*, 614–621.

Aragonés, J., Fraisl, P., Baes, M., and Carmeliet, P. (2009). Oxygen sensors at the crossroad of metabolism. Cell Metab. *9*, 11–22.

Arita, Y., Kihara, S., Ouchi, N., Takahashi, M., Maeda, K., Miyagawa, J., Hotta, K., Shimomura, I., Nakamura, T., Miyaoka, K., et al. (1999). Paradoxical decrease of an adipose-specific protein, adiponectin, in obesity. Biochem. Biophys. Res. Commun. *257*, 79–83.

Ausk, K.J., and Ioannou, G.N. (2008). Is obesity associated with anemia of chronic disease? A population-based study. Obesity (Silver Spring) *16*, 2356–2361.

Azevedo-Martins, A.K., Lortz, S., Lenzen, S., Curi, R., Eizirik, D.L., and Tiedge, M. (2003). Improvement of the mitochondrial antioxidant defense status prevents cytokine-induced nuclear factor-kappaB activation in insulin-producing cells. Diabetes *52*, 93–101.

Babcock, M., de Silva, D., Oaks, R., Davis-Kaplan, S., Jiralerspong, S., Montermini, L., Pandolfo, M., and Kaplan, J. (1997). Regulation of mitochondrial iron accumulation by Yfh1p, a putative homolog of frataxin. Science *276*, 1709–1712.

Baker, K.S., Ness, K.K., Steinberger, J., Carter, A., Francisco, L., Burns, L.J., Sklar, C., Forman, S., Weisdorf, D., Gurney, J.G., and Bhatia, S. (2007). Diabetes, hypertension, and cardiovascular events in survivors of hematopoietic cell transplantation: a report from the bone marrow transplantation survivor study. Blood *109*, 1765–1772.

Baquer, N.Z., Hothersall, J.S., Sochor, M., and McLean, P. (1982). Bioinorganic regulation of pathways of carbohydrate and lipid metabolism. 1. Effect of iron and manganese on the enzyme profile of pathways of carbohydrate metabolism in adipose tissue during development. Enzyme *27*, 61–68.

Beguin, Y. (2003). Soluble transferrin receptor for the evaluation of erythropoiesis and iron status. Clin. Chim. Acta *329*, 9–22.

Bekri, S., Gual, P., Anty, R., Luciani, N., Dahman, M., Ramesh, B., Iannelli, A., Staccini-Myx, A., Casanova, D., Ben Amor, I., et al. (2006). Increased adipose tissue expression of hepcidin in severe obesity is independent from diabetes and NASH. Gastroenterology *131*, 788–796.

Belfort, M.B., Rifas-Shiman, S.L., Rich-Edwards, J.W., Kleinman, K.P., Oken, E., and Gillman, M.W. (2008). Maternal iron intake and iron status during pregnancy and child blood pressure at age 3 years. Int. J. Epidemiol. *37*, 301–308.

Beutler, E., Felitti, V.J., Koziol, J.A., Ho, N.J., and Gelbart, T. (2002). Penetrance of 845G—> A (C282Y) HFE hereditary haemochromatosis mutation in the USA. Lancet *359*, 211–218.

Boeckel, J.N., Guarani, V., Koyanagi, M., Roexe, T., Lengeling, A., Schermuly, R.T., Gellert, P., Braun, T., Zeiher, A., and Dimmeler, S. (2011). Jumonji

domain-containing protein 6 (Jmjd6) is required for angiogenic sprouting and regulates splicing of VEGF-receptor 1. Proc. Natl. Acad. Sci. USA *108*, 3276–3281.

Bofill, C., Joven, J., Bages, J., Vilella, E., Sans, T., Cavallé, P., Miralles, R., Llobet, J., and Camps, J. (1994). Response to repeated phlebotomies in patients with non-insulin-dependent diabetes mellitus. Metabolism *43*, 614–620.

Borel, M.J., Beard, J.L., and Farrell, P.A. (1993). Hepatic glucose production and insulin sensitivity and responsiveness in iron-deficient anemic rats. Am. J. Physiol. *264*, E380–E390.

Borgna-Pignatti, C., Rugolotto, S., De Stefano, P., Piga, A., Di Gregorio, F., Gamberini, M.R., Sabato, V., Melevendi, C., Cappellini, M.D., and Verlato, G. (1998). Survival and disease complications in thalassemia major. Ann. N Y Acad. Sci. *850*, 227–231.

Borgna-Pignatti, C., Rugolotto, S., De Stefano, P., Zhao, H., Cappellini, M.D., Del Vecchio, G.C., Romeo, M.A., Forni, G.L., Gamberini, M.R., Ghilardi, R., et al. (2004). Survival and complications in patients with thalassemia major treated with transfusion and deferoxamine. Haematologica *89*, 1187–1193.

Bourque, S.L., Komolova, M., McCabe, K., Adams, M.A., and Nakatsu, K. (2012). Perinatal iron deficiency combined with a high-fat diet causes obesity and cardiovascular dysregulation. Endocrinology *153*, 1174–1182.

Bowers, K., Yeung, E., Williams, M.A., Qi, L., Tobias, D.K., Hu, F.B., and Zhang, C. (2011). A prospective study of prepregnancy dietary iron intake and risk for gestational diabetes mellitus. Diabetes Care *34*, 1557–1563.

Brink, B., Disler, P., Lynch, S., Jacobs, P., Charlton, R., and Bothwell, T. (1976). Patterns of iron storage in dietary iron overload and idiopathic hemochromatosis. J. Lab. Clin. Med. *88*, 725–731.

Brion, M.J., Leary, S.D., Smith, G.D., McArdle, H.J., and Ness, A.R. (2008). Maternal anemia, iron intake in pregnancy, and offspring blood pressure in the Avon Longitudinal Study of Parents and Children. Am. J. Clin. Nutr. *88*, 1126–1133.

Brunet, A., Sweeney, L.B., Sturgill, J.F., Chua, K.F., Greer, P.L., Lin, Y., Tran, H., Ross, S.E., Mostoslavsky, R., Cohen, H.Y., et al. (2004). Stress-dependent regulation of FOXO transcription factors by the SIRT1 deacetylase. Science *303*, 2011–2015.

Buysschaert, M., Paris, I., Selvais, P., and Hermans, M.P. (1997). Clinical aspects of diabetes secondary to idiopathic haemochromatosis in French-speaking Belgium. Diabetes Metab. *23*, 308–313.

Cairo, G., Recalcati, S., Montosi, G., Castrusini, E., Conte, D., and Pietrangelo, A. (1997). Inappropriately high iron regulatory protein activity in monocytes of patients with genetic hemochromatosis. Blood *89*, 2546–2553.

Cepeda-Lopez, A.C., Osendarp, S.J., Melse-Boonstra, A., Aeberli, I., Gonzalez-Salazar, F., Feskens, E., Villalpando, S., and Zimmermann, M.B. (2011). Sharply higher rates of iron deficiency in obese Mexican women and children are predicted by obesity-related inflammation rather than by differences in dietary iron intake. Am. J. Clin. Nutr. *93*, 975–983.

Chaliasos, N., Challa, A., Hatzimichael, E., Koutsouka, F., Bourantas, D.K., Vlahos, A.P., Siamopoulou, A., Bourantas, K.L., and Makis, A. (2010). Serum adipocytokine and vascular inflammation marker levels in Beta-thalassaemia major patients. Acta Haematol. *124*, 191–196.

Cheng, K., Ho, K., Stokes, R., Scott, C., Lau, S.M., Hawthorne, W.J., O'Connell, P.J., Loudovaris, T., Kay, T.W., Kulkarni, R.N., et al. (2010). Hypoxia-inducible factor-1alpha regulates beta cell function in mouse and human islets. J. Clin. Invest. *120*, 2171–2183.

Colca, J.R., McDonald, W.G., Waldon, D.J., Leone, J.W., Lull, J.M., Bannow, C.A., Lund, E.T., and Mathews, W.R. (2004). Identification of a novel mitochondrial protein ("mitoNEET") cross-linked specifically by a thiazolidinedione photoprobe. Am. J. Physiol. Endocrinol. Metab. *286*, E252–E260.

Condò, I., Malisan, F., Guccini, I., Serio, D., Rufini, A., and Testi, R. (2010). Molecular control of the cytosolic aconitase/IRP1 switch by extramitochondrial frataxin. Hum. Mol. Genet. *19*, 1221–1229.

Cooksey, R.C., Jouihan, H.A., Ajioka, R.S., Hazel, M.W., Jones, D.L., Kushner, J.P., and McClain, D.A. (2004). Oxidative stress, beta-cell apoptosis, and decreased insulin secretory capacity in mouse models of hemochromatosis. Endocrinology *145*, 5305–5312.

Cooksey, R.C., Jones, D., Gabrielsen, S., Huang, J., Simcox, J.A., Luo, B., Soesanto, Y., Rienhoff, H., Abel, E.D., and McClain, D.A. (2010). Dietary iron restriction or iron chelation protects from diabetes and loss of beta-cell function in the obese (ob/ob lep-/-) mouse. Am. J. Physiol. Endocrinol. Metab. *298*, E1236–E1243.

D'Alessio, F., Hentze, M.W., and Muckenthaler, M.U. (2012). The hemochromatosis proteins HFE, TfR2, and HJV form a membrane-associated protein complex for hepcidin regulation. J. Hepatol. *57*, 1052–1060.

Davis, R.J., Corvera, S., and Czech, M.P. (1986). Insulin stimulates cellular iron uptake and causes the redistribution of intracellular transferrin receptors to the plasma membrane. J. Biol. Chem. *261*, 8708–8711.

De Domenico, I., McVey Ward, D., and Kaplan, J. (2008). Regulation of iron acquisition and storage: consequences for iron-linked disorders. Nat. Rev. Mol. Cell Biol. *9*, 72–81.

Dmochowski, K., Finegood, D.T., Francombe, W., Tyler, B., and Zinman, B. (1993). Factors determining glucose tolerance in patients with thalassemia major. J. Clin. Endocrinol. Metab. *77*, 478–483.

Dongiovanni, P., Fracanzani, A.L., Fargion, S., and Valenti, L. (2011). Iron in fatty liver and in the metabolic syndrome: a promising therapeutic target. J. Hepatol. *55*, 920–932.

Eisenstein, R.S., and Ross, K.L. (2003). Novel roles for iron regulatory proteins in the adaptive response to iron deficiency. J. Nutr. *133*(5, Suppl 1), 1510S–1516S.

Facchini, F.S. (1998). Effect of phlebotomy on plasma glucose and insulin concentrations. Diabetes Care *21*, 2190.

Facchini, F.S., Hua, N.W., and Stoohs, R.A. (2002). Effect of iron depletion in carbohydrate-intolerant patients with clinical evidence of nonalcoholic fatty liver disease. Gastroenterology *122*, 931–939.

Faller, M., Matsunaga, M., Yin, S., Loo, J.A., and Guo, F. (2007). Heme is involved in microRNA processing. Nat. Struct. Mol. Biol. *14*, 23–29.

Farahani, P., Chiu, S., Bowlus, C.L., Boffelli, D., Lee, E., Fisler, J.S., Krauss, R.M., and Warden, C.H. (2004). Obesity in BSB mice is correlated with expression of genes for iron homeostasis and leptin. Obes. Res. *12*, 191–204.

Fargnoli, J.L., Fung, T.T., Olenczuk, D.M., Chamberland, J.P., Hu, F.B., and Mantzoros, C.S. (2008). Adherence to healthy eating patterns is associated with higher circulating total and high-molecular-weight adiponectin and lower resistin concentrations in women from the Nurses' Health Study. Am. J. Clin. Nutr. *88*, 1213–1224.

Feder, J.N., Gnirke, A., Thomas, W., Tsuchihashi, Z., Ruddy, D.A., Basava, A., Dormishian, F., Domingo, R., Jr., Ellis, M.C., Fullan, A., et al. (1996). A novel MHC class I-like gene is mutated in patients with hereditary haemochromatosis. Nat. Genet. *13*, 399–408.

Fernández-Real, J.M., López-Bermejo, A., and Ricart, W. (2002a). Cross-talk between iron metabolism and diabetes. Diabetes *51*, 2348–2354.

Fernández-Real, J.M., Peñarroja, G., Castro, A., García-Bragado, F., Hernández-Aguado, I., and Ricart, W. (2002b). Blood letting in high-ferritin type 2 diabetes: effects on insulin sensitivity and beta-cell function. Diabetes *51*, 1000–1004.

Fernández-Real, J.M., Peñarroja, G., Castro, A., García-Bragado, F., López-Bermejo, A., and Ricart, W. (2002c). Blood letting in high-ferritin type 2 diabetes: effects on vascular reactivity. Diabetes Care *25*, 2249–2255.

Fernández-Real, J.M., López-Bermejo, A., and Ricart, W. (2005). Iron stores, blood donation, and insulin sensitivity and secretion. Clin. Chem. *51*, 1201–1205.

Fernández-Real, J.M., Moreno, J.M., Chico, B., López-Bermejo, A., and Ricart, W. (2007). Circulating visfatin is associated with parameters of iron metabolism in subjects with altered glucose tolerance. Diabetes Care *30*, 616–621.

Festa, M., Ricciardelli, G., Mele, G., Pietropaolo, C., Ruffo, A., and Colonna, A. (2000). Overexpression of H ferritin and up-regulation of iron regulatory protein genes during differentiation of 3T3-L1 pre-adipocytes. J. Biol. Chem. *275*, 36708–36712.

Fleming, D.J., Jacques, P.F., Tucker, K.L., Massaro, J.M., D'Agostino, R.B., Sr., Wilson, P.W., and Wood, R.J. (2001). Iron status of the free-living, elderly

Framingham Heart Study cohort: an iron-replete population with a high prevalence of elevated iron stores. Am. J. Clin. Nutr. *73*, 638–646.

Fleming, D.J., Tucker, K.L., Jacques, P.F., Dallal, G.E., Wilson, P.W., and Wood, R.J. (2002). Dietary factors associated with the risk of high iron stores in the elderly Framingham Heart Study cohort. Am. J. Clin. Nutr. *76*, 1375–1384.

Ford, E.S., and Cogswell, M.E. (1999). Diabetes and serum ferritin concentration among U.S. adults. Diabetes Care *22*, 1978–1983.

Forouhi, N.G., Harding, A.H., Allison, M., Sandhu, M.S., Welch, A., Luben, R., Bingham, S., Khaw, K.T., and Wareham, N.J. (2007). Elevated serum ferritin levels predict new-onset type 2 diabetes: results from the EPIC-Norfolk prospective study. Diabetologia *50*, 949–956.

Gabrielsen, J.S., Gao, Y., Simcox, J.A., Huang, J., Thorup, D., Jones, D., Cooksey, R.C., Gabrielsen, D., Adams, T.D., Hunt, S.C., et al. (2012). Adipocyte iron regulates adiponectin and insulin sensitivity. J. Clin. Invest. *122*, 3529–3540.

Gamberini, M.R., De Sanctis, V., and Gilli, G. (2008). Hypogonadism, diabetes mellitus, hypothyroidism, hypoparathyroidism: incidence and prevalence related to iron overload and chelation therapy in patients with thalassaemia major followed from 1980 to 2007 in the Ferrara Centre. Pediatr. Endocrinol. Rev. *6*(*Suppl 1*), 158–169.

Ganz, T. (2011). Hepcidin and iron regulation, 10 years later. Blood *117*, 4425–4433.

Ganz, T., and Nemeth, E. (2009). Iron sequestration and anemia of inflammation. Semin. Hematol. *46*, 387–393.

Gillum, R.F. (2001). Association of serum ferritin and indices of body fat distribution and obesity in Mexican American men—the Third National Health and Nutrition Examination Survey. Int. J. Obes. Relat. Metab. Disord. *25*, 639–645.

Halberg, N., Khan, T., Trujillo, M.E., Wernstedt-Asterholm, I., Attie, A.D., Sherwani, S., Wang, Z.V., Landskroner-Eiger, S., Dineen, S., Magalang, U.J., et al. (2009). Hypoxia-inducible factor 1alpha induces fibrosis and insulin resistance in white adipose tissue. Mol. Cell. Biol. *29*, 4467–4483.

Handschin, C., Lin, J., Rhee, J., Peyer, A.K., Chin, S., Wu, P.H., Meyer, U.A., and Spiegelman, B.M. (2005). Nutritional regulation of hepatic heme biosynthesis and porphyria through PGC-1alpha. Cell *122*, 505–515.

Hardie, D.G. (2011). AMP-activated protein kinase: an energy sensor that regulates all aspects of cell function. Genes Dev. *25*, 1895–1908.

Hatunic, M., Finucane, F.M., Brennan, A.M., Norris, S., Pacini, G., and Nolan, J.J. (2010a). Effect of iron overload on glucose metabolism in patients with hereditary hemochromatosis. Metabolism *59*, 380–384.

Hatunic, M., Finucane, F.M., Norris, S., Pacini, G., and Nolan, J.J. (2010b). Glucose metabolism after normalization of markers of iron overload by venesection in subjects with hereditary hemochromatosis. Metabolism *59*, 1811–1815.

Haurie, V., Boucherie, H., and Sagliocco, F. (2003). The Snf1 protein kinase controls the induction of genes of the iron uptake pathway at the diauxic shift in Saccharomyces cerevisiae. J. Biol. Chem. *278*, 45391–45396.

Henderson, S.A., Dallman, P.R., and Brooks, G.A. (1986). Glucose turnover and oxidation are increased in the iron-deficient anemic rat. Am. J. Physiol. *250*, E414–E421.

Hentze, M.W., Muckenthaler, M.U., Galy, B., and Camaschella, C. (2010). Two to tango: regulation of Mammalian iron metabolism. Cell *142*, 24–38.

Hoffmeister, P.A., Storer, B.E., and Sanders, J.E. (2004). Diabetes mellitus in long-term survivors of pediatric hematopoietic cell transplantation. J. Pediatr. Hematol. Oncol. *26*, 81–90.

Hostettler-Allen, R., Tappy, L., and Blum, J.W. (1993). Enhanced insulin-dependent glucose utilization in iron-deficient veal calves. J. Nutr. *123*, 1656–1667.

Hotamisligil, G.S. (2003). Inflammatory pathways and insulin action. Int. J. Obes. Relat. Metab. Disord. *27*(*Suppl 3*), S53–S55.

Hotamisligil, G.S. (2006). Inflammation and metabolic disorders. Nature *444*, 860–867.

Hou, X., Xu, S., Maitland-Toolan, K.A., Sato, K., Jiang, B., Ido, Y., Lan, F., Walsh, K., Wierzbicki, M., Verbeuren, T.J., et al. (2008). SIRT1 regulates hepatocyte lipid metabolism through activating AMP-activated protein kinase. J. Biol. Chem. *283*, 20015–20026.

Houschyar, K.S., Lüdtke, R., Dobos, G.J., Kalus, U., Broecker-Preuss, M., Rampp, T., Brinkhaus, B., and Michalsen, A. (2012). Effects of phlebotomy-induced reduction of body iron stores on metabolic syndrome: results from a randomized clinical trial. BMC Med. *10*, 54.

Houtkooper, R.H., Pirinen, E., and Auwerx, J. (2012). Sirtuins as regulators of metabolism and healthspan. Nat. Rev. Mol. Cell Biol. *13*, 225–238.

Hramiak, I.M., Finegood, D.T., and Adams, P.C. (1997). Factors affecting glucose tolerance in hereditary hemochromatosis. Clin. Invest. Med. *20*, 110–118.

Huang, J., Gabrielsen, J.S., Cooksey, R.C., Luo, B., Boros, L.G., Jones, D.L., Jouihan, H.A., Soesanto, Y., Knecht, L., Hazel, M.W., et al. (2007). Increased glucose disposal and AMP-dependent kinase signaling in a mouse model of hemochromatosis. J. Biol. Chem. *282*, 37501–37507.

Huang, J., Jones, D., Luo, B., Sanderson, M., Soto, J., Abel, E.D., Cooksey, R.C., and McClain, D.A. (2011). Iron overload and diabetes risk: a shift from glucose to Fatty Acid oxidation and increased hepatic glucose production in a mouse model of hereditary hemochromatosis. Diabetes *60*, 80–87.

Hudson, D.M., Curtis, S.B., Smith, V.C., Griffiths, T.A., Wong, A.Y., Scudamore, C.H., Buchan, A.M., and MacGillivray, R.T. (2010). Human hephaestin expression is not limited to enterocytes of the gastrointestinal tract but is also found in the antrum, the enteric nervous system, and pancreatic beta-cells. Am. J. Physiol. Gastrointest. Liver Physiol. *298*, G425–G432.

Inagaki, T., Tachibana, M., Magoori, K., Kudo, H., Tanaka, T., Okamura, M., Naito, M., Kodama, T., Shinkai, Y., and Sakai, J. (2009). Obesity and metabolic syndrome in histone demethylase JHDM2a-deficient mice. Genes Cells *14*, 991–1001.

Iwasaki, T., Nakajima, A., Yoneda, M., Yamada, Y., Mukasa, K., Fujita, K., Fujisawa, N., Wada, K., and Terauchi, Y. (2005). Serum ferritin is associated with visceral fat area and subcutaneous fat area. Diabetes Care *28*, 2486–2491.

Jaruratanasirikul, S., Chareonmuang, R., Wongcharnchailert, M., Laosombat, V., Sangsupavanich, P., and Leetanaporn, K. (2008). Prevalence of impaired glucose metabolism in beta-thalassemic children receiving hypertransfusions with a suboptimal dosage of iron-chelating therapy. Eur. J. Pediatr. *167*, 873–876.

Jehn, M., Clark, J.M., and Guallar, E. (2004). Serum ferritin and risk of the metabolic syndrome in U.S. adults. Diabetes Care *27*, 2422–2428.

Jiang, R., Manson, J.E., Meigs, J.B., Ma, J., Rifai, N., and Hu, F.B. (2004). Body iron stores in relation to risk of type 2 diabetes in apparently healthy women. JAMA *291*, 711–717.

Jiang, C., Qu, A., Matsubara, T., Chanturiya, T., Jou, W., Gavrilova, O., Shah, Y.M., and Gonzalez, F.J. (2011). Disruption of hypoxia-inducible factor 1 in adipocytes improves insulin sensitivity and decreases adiposity in high-fat diet-fed mice. Diabetes *60*, 2484–2495.

Jomova, K., and Valko, M. (2011). Advances in metal-induced oxidative stress and human disease. Toxicology *283*, 65–87.

Jouihan, H.A., Cobine, P.A., Cooksey, R.C., Hoagland, E.A., Boudina, S., Abel, E.D., Winge, D.R., and McClain, D.A. (2008). Iron-mediated inhibition of mitochondrial manganese uptake mediates mitochondrial dysfunction in a mouse model of hemochromatosis. Mol. Med. *14*, 98–108.

Kahn, B.B. (1998). Type 2 diabetes: when insulin secretion fails to compensate for insulin resistance. Cell *92*, 593–596.

Kahn, S.E. (2003). The relative contributions of insulin resistance and beta-cell dysfunction to the pathophysiology of Type 2 diabetes. Diabetologia *46*, 3–19.

Kahn, B.B., Alquier, T., Carling, D., and Hardie, D.G. (2005). AMP-activated protein kinase: ancient energy gauge provides clues to modern understanding of metabolism. Cell Metab. *1*, 15–25.

Kaneto, H., Katakami, N., Matsuhisa, M., and Matsuoka, T.A. (2010). Role of reactive oxygen species in the progression of type 2 diabetes and atherosclerosis. Mediators Inflamm. *2010*, 453892.

Knutson, M.D., Oukka, M., Koss, L.M., Aydemir, F., and Wessling-Resnick, M. (2005). Iron release from macrophages after erythrophagocytosis is up-regulated by ferroportin 1 overexpression and down-regulated by hepcidin. Proc. Natl. Acad. Sci. USA *102*, 1324–1328.

Koch, R.O., Zoller, H., Theuri, I., Obrist, P., Egg, G., Strohmayer, W., Vogel, W., and Weiss, G. (2003). Distribution of DMT 1 within the human glandular system. Histol. Histopathol. *18*, 1095–1101.

Kriska, A.M., Saremi, A., Hanson, R.L., Bennett, P.H., Kobes, S., Williams, D.E., and Knowler, W.C. (2003). Physical activity, obesity, and the incidence of type 2 diabetes in a high-risk population. Am. J. Epidemiol. *158*, 669–675.

Kubota, N., Terauchi, Y., Yamauchi, T., Kubota, T., Moroi, M., Matsui, J., Eto, K., Yamashita, T., Kamon, J., Satoh, H., et al. (2002). Disruption of adiponectin causes insulin resistance and neointimal formation. J. Biol. Chem. *277*, 25863–25866.

Kusminski, C.M., Holland, W.L., Sun, K., Park, J., Spurgin, S.B., Lin, Y., Askew, G.R., Simcox, J.A., McClain, D.A., Li, C., and Scherer, P.E. (2012). MitoNEET-driven alterations in adipocyte mitochondrial activity reveal a crucial adaptive process that preserves insulin sensitivity in obesity. Nat. Med. *18*, 1539–1549.

Lan, F., Cacicedo, J.M., Ruderman, N., and Ido, Y. (2008). SIRT1 modulation of the acetylation status, cytosolic localization, and activity of LKB1. Possible role in AMP-activated protein kinase activation. J. Biol. Chem. *283*, 27628–27635.

Lenzen, S., Drinkgern, J., and Tiedge, M. (1996). Low antioxidant enzyme gene expression in pancreatic islets compared with various other mouse tissues. Free Radic. Biol. Med. *20*, 463–466.

Lewis, R.M., Petry, C.J., Ozanne, S.E., and Hales, C.N. (2001). Effects of maternal iron restriction in the rat on blood pressure, glucose tolerance, and serum lipids in the 3-month-old offspring. Metabolism *50*, 562–567.

Li, Y., Lin, L., Li, Z., Ye, X., Xiong, K., Aryal, B., Xu, Z., Paroo, Z., Liu, Q., He, C., and Jin, P. (2012). Iron homeostasis regulates the activity of the microRNA pathway through poly(C)-binding protein 2. Cell Metab. *15*, 895–904.

Liuzzi, J.P., Aydemir, F., Nam, H., Knutson, M.D., and Cousins, R.J. (2006). Zip14 (Slc39a14) mediates non-transferrin-bound iron uptake into cells. Proc. Natl. Acad. Sci. USA *103*, 13612–13617.

Lobmayr, L., Brooks, D.G., and Wilson, R.B. (2005). Increased IRP1 activity in Friedreich ataxia. Gene *354*, 157–161.

Long, Y.C., and Zierath, J.R. (2006). AMP-activated protein kinase signaling in metabolic regulation. J. Clin. Invest. *116*, 1776–1783.

Lowell, B.B., and Shulman, G.I. (2005). Mitochondrial dysfunction and type 2 diabetes. Science *307*, 384–387.

Mackenzie, B., Ujwal, M.L., Chang, M.H., Romero, M.F., and Hediger, M.A. (2006). Divalent metal-ion transporter DMT1 mediates both H+ -coupled Fe2+ transport and uncoupled fluxes. Pflugers Arch. *451*, 544–558.

Mastrogiannaki, M., Matak, P., Keith, B., Simon, M.C., Vaulont, S., and Peyssonnaux, C. (2009). HIF-2alpha, but not HIF-1alpha, promotes iron absorption in mice. J. Clin. Invest. *119*, 1159–1166.

McClain, D.A., Abraham, D., Rogers, J., Brady, R., Gault, P., Ajioka, R., and Kushner, J.P. (2006). High prevalence of abnormal glucose homeostasis secondary to decreased insulin secretion in individuals with hereditary haemochromatosis. Diabetologia *49*, 1661–1669.

McClain, D.A., Abuelgasim, K.A., Nouraie, M., Salomon-Andonie, J., Niu, X., Miasnikova, G., Polyakova, L.A., Sergueeva, A., Okhotin, D.J., Cherqaoui, R., et al. (2013). Decreased serum glucose and glycosylated hemoglobin levels in patients with Chuvash polycythemia: a role for HIF in glucose metabolism. J. Mol. Med. *91*, 59–67.

McClung, J.P., Andersen, N.E., Tarr, T.N., Stahl, C.H., and Young, A.J. (2008). Physical activity prevents augmented body fat accretion in moderately iron-deficient rats. J. Nutr. *138*, 1293–1297.

Mendler, M.H., Turlin, B., Moirand, R., Jouanolle, A.M., Sapey, T., Guyader, D., Le Gall, J.Y., Brissot, P., David, V., and Deugnier, Y. (1999). Insulin resistance-associated hepatic iron overload. Gastroenterology *117*, 1155–1163.

Merkel, P.A., Simonson, D.C., Amiel, S.A., Plewe, G., Sherwin, R.S., Pearson, H.A., and Tamborlane, W.V. (1988). Insulin resistance and hyperinsulinemia in patients with thalassemia major treated by hypertransfusion. N. Engl. J. Med. *318*, 809–814.

Messina, M.F., Lombardo, F., Meo, A., Miceli, M., Wasniewska, M., Valenzise, M., Ruggeri, C., Arrigo, T., and De Luca, F. (2002). Three-year prospective evaluation of glucose tolerance, beta-cell function and peripheral insulin sensitivity in non-diabetic patients with thalassemia major. J. Endocrinol. Invest. *25*, 497–501.

Meynard, D., Kautz, L., Darnaud, V., Canonne-Hergaux, F., Coppin, H., and Roth, M.P. (2009). Lack of the bone morphogenetic protein BMP6 induces massive iron overload. Nat. Genet. *41*, 478–481.

Minamiyama, Y., Takemura, S., Kodai, S., Shinkawa, H., Tsukioka, T., Ichikawa, H., Naito, Y., Yoshikawa, T., and Okada, S. (2010). Iron restriction improves type 2 diabetes mellitus in Otsuka Long-Evans Tokushima fatty rats. Am. J. Physiol. Endocrinol. Metab. *298*, E1140–E1149.

Minard, K.I., and McAlister-Henn, L. (2005). Sources of NADPH in yeast vary with carbon source. J. Biol. Chem. *280*, 39890–39896.

Moirand, R., Adams, P.C., Bicheler, V., Brissot, P., and Deugnier, Y. (1997). Clinical features of genetic hemochromatosis in women compared with men. Ann. Intern. Med. *127*, 105–110.

Mojiminiyi, O.A., Marouf, R., and Abdella, N.A. (2008). Body iron stores in relation to the metabolic syndrome, glycemic control and complications in female patients with type 2 diabetes. Nutr. Metab. Cardiovasc. Dis. *18*, 559–566.

Monahan, B.J., Villén, J., Marguerat, S., Bähler, J., Gygi, S.P., and Winston, F. (2008). Fission yeast SWI/SNF and RSC complexes show compositional and functional differences from budding yeast. Nat. Struct. Mol. Biol. *15*, 873–880.

Montes-Cortes, D.H., Hicks, J.J., Ceballos-Reyes, G.M., Garcia-Sanchez, J.R., Medina-Navarro, R., and Olivares-Corichi, I.M. (2010). Chemical and functional changes of human insulin by in vitro incubation with blood from diabetic patients in oxidative stress. Metabolism *59*, 935–942.

Nappi, A.J., and Vass, E. (1998). Hydroxyl radical formation resulting from the interaction of nitric oxide and hydrogen peroxide. Biochim. Biophys. Acta *1380*, 55–63.

Nelson, R., Chawla, M., Connolly, P., and LaPorte, J. (1978). Ferritin as an index of bone marrow iron stores. South. Med. J. *71*, 1482–1484.

Nemeth, E., Tuttle, M.S., Powelson, J., Vaughn, M.B., Donovan, A., Ward, D.M., Ganz, T., and Kaplan, J. (2004). Hepcidin regulates cellular iron efflux by binding to ferroportin and inducing its internalization. Science *306*, 2090–2093.

Nemeth, E., Roetto, A., Garozzo, G., Ganz, T., and Camaschella, C. (2005). Hepcidin is decreased in TFR2 hemochromatosis. Blood *105*, 1803–1806.

Ozdemir, A., Sevinç, C., Selamet, U., and Türkmen, F. (2007). The relationship between iron deficiency anemia and lipid metabolism in premenopausal women. Am. J. Med. Sci. *334*, 331–333.

Pietrangelo, A. (2010). Hereditary hemochromatosis: pathogenesis, diagnosis, and treatment. Gastroenterology *139*, 393–408, 408, e1–e2.

Pinhas-Hamiel, O., Newfield, R.S., Koren, I., Agmon, A., Lilos, P., and Phillip, M. (2003). Greater prevalence of iron deficiency in overweight and obese children and adolescents. Int. J. Obes. Relat. Metab. Disord. *27*, 416–418.

Ponugoti, B., Dong, G., and Graves, D.T. (2012). Role of forkhead transcription factors in diabetes-induced oxidative stress. Exp. Diabetes Res. *2012*, 939751.

Qi, L., van Dam, R.M., Rexrode, K., and Hu, F.B. (2007). Heme iron from diet as a risk factor for coronary heart disease in women with type 2 diabetes. Diabetes Care *30*, 101–106.

Qiu, C., Zhang, C., Gelaye, B., Enquobahrie, D.A., Frederick, I.O., and Williams, M.A. (2011). Gestational diabetes mellitus in relation to maternal dietary heme iron and nonheme iron intake. Diabetes Care *34*, 1564–1569.

Radisky, D.C., Babcock, M.C., and Kaplan, J. (1999). The yeast frataxin homologue mediates mitochondrial iron efflux. Evidence for a mitochondrial iron cycle. J. Biol. Chem. *274*, 4497–4499.

Ravelli, A.C., van der Meulen, J.H., Michels, R.P., Osmond, C., Barker, D.J., Hales, C.N., and Bleker, O.P. (1998). Glucose tolerance in adults after prenatal exposure to famine. Lancet *351*, 173–177.

Ray, P.D., Huang, B.W., and Tsuji, Y. (2012). Reactive oxygen species (ROS) homeostasis and redox regulation in cellular signaling. Cell. Signal. *24*, 981–990.

Regazzetti, C., Peraldi, P., Grémeaux, T., Najem-Lendom, R., Ben-Sahra, I., Cormont, M., Bost, F., Le Marchand-Brustel, Y., Tanti, J.F., and Giorgetti-Peraldi, S. (2009). Hypoxia decreases insulin signaling pathways in adipocytes. Diabetes *58*, 95–103.

Romney, S.J., Newman, B.S., Thacker, C., and Leibold, E.A. (2011). HIF-1 regulates iron homeostasis in Caenorhabditis elegans by activation and inhibition of genes involved in iron uptake and storage. PLoS Genet. *7*, e1002394.

Rossetti, L., Giaccari, A., and DeFronzo, R.A. (1990). Glucose toxicity. Diabetes Care *13*, 610–630.

Rouault, T.A., and Tong, W.H. (2009). Tangled up in red: intertwining of the heme and iron-sulfur cluster biogenesis pathways. Cell Metab. *10*, 80–81.

Rumberger, J.M., Peters, T., Jr., Burrington, C., and Green, A. (2004). Transferrin and iron contribute to the lipolytic effect of serum in isolated adipocytes. Diabetes *53*, 2535–2541.

Semenza, G.L. (2012). Hypoxia-inducible factors in physiology and medicine. Cell *148*, 399–408.

Shah, Y.M., Matsubara, T., Ito, S., Yim, S.H., and Gonzalez, F.J. (2009). Intestinal hypoxia-inducible transcription factors are essential for iron absorption following iron deficiency. Cell Metab. *9*, 152–164.

Shakoury-Elizeh, M., Protchenko, O., Berger, A., Cox, J., Gable, K., Dunn, T.M., Prinz, W.A., Bard, M., and Philpott, C.C. (2010). Metabolic response to iron deficiency in Saccharomyces cerevisiae. J. Biol. Chem. *285*, 14823–14833.

Sharifi, F., Nasab, N.M., and Zadeh, H.J. (2008). Elevated serum ferritin concentrations in prediabetic subjects. Diab. Vasc. Dis. Res. *5*, 15–18.

Shayeghi, M., Latunde-Dada, G.O., Oakhill, J.S., Laftah, A.H., Takeuchi, K., Halliday, N., Khan, Y., Warley, A., McCann, F.E., Hider, R.C., et al. (2005). Identification of an intestinal heme transporter. Cell *122*, 789–801.

Sonnweber, T., Ress, C., Nairz, M., Theurl, I., Schroll, A., Murphy, A.T., Wroblewski, V., Witcher, D.R., Moser, P., Ebenbichler, C.F., et al. (2012). High-fat diet causes iron deficiency via hepcidin-independent reduction of duodenal iron absorption. J. Nutr. Biochem. *23*, 1600–1608.

Stangl, G.I., and Kirchgessner, M. (1998). Different degrees of moderate iron deficiency modulate lipid metabolism of rats. Lipids *33*, 889–895.

Subauste, A.R., and Burant, C.F. (2007). Role of FoxO1 in FFA-induced oxidative stress in adipocytes. Am. J. Physiol. Endocrinol. Metab. *293*, E159–E164.

Szmuilowicz, E.D., Stuenkel, C.A., and Seely, E.W. (2009). Influence of menopause on diabetes and diabetes risk. Nat Rev Endocrinol *5*, 553–558.

Takeuchi, T., Watanabe, Y., Takano-Shimizu, T., and Kondo, S. (2006). Roles of jumonji and jumonji family genes in chromatin regulation and development. Dev. Dyn. *235*, 2449–2459.

Tanner, L.I., and Lienhard, G.E. (1987). Insulin elicits a redistribution of transferrin receptors in 3T3-L1 adipocytes through an increase in the rate constant for receptor externalization. J. Biol. Chem. *262*, 8975–8980.

Toomajian, C., Ajioka, R.S., Jorde, L.B., Kushner, J.P., and Kreitman, M. (2003). A method for detecting recent selection in the human genome from allele age estimates. Genetics *165*, 287–297.

Tormos, K.V., Anso, E., Hamanaka, R.B., Eisenbart, J., Joseph, J., Kalyanaraman, B., and Chandel, N.S. (2011). Mitochondrial complex III ROS regulate adipocyte differentiation. Cell Metab. *14*, 537–544.

Trayhurn, P., and Wood, I.S. (2005). Signalling role of adipose tissue: adipokines and inflammation in obesity. Biochem. Soc. Trans. *33*, 1078–1081.

Tuomainen, T.P., Nyyssönen, K., Salonen, R., Tervahauta, A., Korpela, H., Lakka, T., Kaplan, G.A., and Salonen, J.T. (1997). Body iron stores are associated with serum insulin and blood glucose concentrations. Population study in 1,013 eastern Finnish men. Diabetes Care *20*, 426–428.

Vogiatzi, M.G., Macklin, E.A., Trachtenberg, F.L., Fung, E.B., Cheung, A.M., Vichinsky, E., Olivieri, N., Kirby, M., Kwiatkowski, J.L., Cunningham, M., et al.; Thalassemia Clinical Research Network. (2009). Differences in the prevalence of growth, endocrine and vitamin D abnormalities among the various thalassaemia syndromes in North America. Br. J. Haematol. *146*, 546–556.

Walter, P.B., Knutson, M.D., Paler-Martinez, A., Lee, S., Xu, Y., Viteri, F.E., and Ames, B.N. (2002). Iron deficiency and iron excess damage mitochondria and mitochondrial DNA in rats. Proc. Natl. Acad. Sci. USA *99*, 2264–2269.

Wang, R.H., Li, C., Xu, X., Zheng, Y., Xiao, C., Zerfas, P., Cooperman, S., Eckhaus, M., Rouault, T., Mishra, L., and Deng, C.X. (2005). A role of SMAD4 in iron metabolism through the positive regulation of hepcidin expression. Cell Metab. *2*, 399–409.

Weatherall, D.J. (1998). Pathophysiology of thalassaemia. Baillieres Clin. Haematol. *11*, 127–146.

Wiley, S.E., Murphy, A.N., Ross, S.A., van der Geer, P., and Dixon, J.E. (2007). MitoNEET is an iron-containing outer mitochondrial membrane protein that regulates oxidative capacity. Proc. Natl. Acad. Sci. USA *104*, 5318–5323.

Wilson, J.G., Lindquist, J.H., Grambow, S.C., Crook, E.D., and Maher, J.F. (2003). Potential role of increased iron stores in diabetes. Am. J. Med. Sci. *325*, 332–339.

Wlazlo, N., van Greevenbroek, M.M., Ferreira, I., Jansen, E.H., Feskens, E.J., van der Kallen, C.J., Schalkwijk, C.G., Bravenboer, B., and Stehouwer, C.D. (2013). Iron Metabolism Is Associated With Adipocyte Insulin Resistance and Plasma Adiponectin: The Cohort on Diabetes and Atherosclerosis Maastricht (CODAM) study. Diabetes Care *36*, 309–315.

Yamagishi, H., Okazaki, H., Shimizu, M., Izawa, T., and Komabayashi, T. (2000). Relationships among serum triacylglycerol, fat pad weight, and lipolysis in iron-deficient rats. J. Nutr. Biochem. *11*, 455–460.

Yanoff, L.B., Menzie, C.M., Denkinger, B., Sebring, N.G., McHugh, T., Remaley, A.T., and Yanovski, J.A. (2007). Inflammation and iron deficiency in the hypoferremia of obesity. Int J Obes (Lond) *31*, 1412–1419.

Yin, L., Wu, N., Curtin, J.C., Qatanani, M., Szwergold, N.R., Reid, R.A., Waitt, G.M., Parks, D.J., Pearce, K.H., Wisely, G.B., and Lazar, M.A. (2007). Rev-erbalpha, a heme sensor that coordinates metabolic and circadian pathways. Science *318*, 1786–1789.

Zehetner, J., Danzer, C., Collins, S., Eckhardt, K., Gerber, P.A., Ballschmieter, P., Galvanovskis, J., Shimomura, K., Ashcroft, F.M., Thorens, B., et al. (2008). PVHL is a regulator of glucose metabolism and insulin secretion in pancreatic beta cells. Genes Dev. *22*, 3135–3146.

Zuris, J.A., Harir, Y., Conlan, A.R., Shvartsman, M., Michaeli, D., Tamir, S., Paddock, M.L., Onuchic, J.N., Mittler, R., Cabantchik, Z.I., et al. (2011). Facile transfer of [2Fe-2S] clusters from the diabetes drug target mitoNEET to an apo-acceptor protein. Proc. Natl. Acad. Sci. USA *108*, 13047–13052.

Zuris, J.A., Ali, S.S., Yeh, H., Nguyen, T.A., Nechushtai, R., Paddock, M.L., and Jennings, P.A. (2012). NADPH inhibits [2Fe-2S] cluster protein transfer from diabetes drug target MitoNEET to an apo-acceptor protein. J. Biol. Chem. *287*, 11649–11655.

CHAPTER 3

IRON REGULATES GLUCOSE HOMEOSTASIS IN LIVER AND MUSCLE VIA AMP-ACTIVATED KINASE IN MICE

Reprint of: Huang J, Simcox JA, Mitchell CM, Jones D, Cox J, Luo B, Cooksey R, LazloB, and DA McClain. (2013). Iron regulates glucose homeostasis in liver and muscle via AMP-activated protein kinase in mice. FASEB. Reprinted with permission from FASEB.

I contributed to this manuscript by involvement with experimental design and preparation of the manuscript. Additionally, I measured nonheme iron, transferrin transcript, ferritin Western blots in the skeletal muscle, immunoprecipitation and blotting of acetylated LKB1 in liver, and Western blots of total and acetylated p53.

The FASEB Journal article fj.12-216929. Published online March 20, 2013.

The FASEB Journal • Research Communication

Iron regulates glucose homeostasis in liver and muscle *via* AMP-activated protein kinase in mice

Jingyu Huang,[*,†] Judith Simcox,[*,†] T. Creighton Mitchell,[*,†] Deborah Jones,[*,†] James Cox,[*,†] Bai Luo,[*,†] Robert C. Cooksey,[*,†,‡] Laszlo G. Boros,[§,‖] and Donald A. McClain[*,†,‡,1]

*Department of Medicine and †Department of Biochemistry, University of Utah School of Medicine, Salt Lake City, Utah, USA; ‡Veterans Affairs Medical Center, Research Service, Salt Lake City, Utah, USA; §Sidmap LLC, Los Angeles, California, USA, and ‖Department of Pediatrics, Los Angeles Biomedical Research Institute at the Harbor–University of California Los Angeles Medical Center, Torrance, CA, USA

ABSTRACT **Excess iron is associated with hepatic damage and diabetes in humans, although the detailed molecular mechanisms are not known. To investigate how iron regulates glucose homeostasis, we fed C57BL/6J male mice with high-iron (HI) diets (2 or 20 g Fe/kg chow). Mice fed an HI diet exhibited elevated AMP-activated protein kinase (AMPK) activity and impaired insulin signaling in skeletal muscle and liver. Consistent with the increased AMPK activity, glucose uptake was enhanced in mice fed an HI diet. The effects of improved glucose tolerance induced by HI feeding were abolished in transgenic mice with expression of muscle specific dominant-negative AMPK. Glucose output was suppressed in the liver of wild-type mice fed an HI diet, due to decreased expression of gluconeogenic genes and decreased substrate (lactate) from peripheral glycolysis. Iron activated AMPK by increasing deacetylase and decreasing LKB1 acetylation, in turn stimulating the phosphorylation of LKB1 and AMPK. The effects of HI diet were abrogated by treatment of the mice with *N*-acetyl cysteine, suggesting a redox-dependent mechanism for increasing deacetylase activity. In addition, tissue from iron-fed mice exhibited an elevated AMP/ATP ratio, further contributing to AMPK activation. In summary, a diet high in iron improves glucose tolerance by activating AMPK through mechanisms that include deacetylation.—Huang J., Simcox, J., Mitchell, T. C., Jones, D., Cox, J., Luo, B., Cooksey, R. C., Boros, L. G., McClain, D. A. Iron regulates glucose homeostasis in liver and muscle *via* AMP-activated protein kinase in mice. *FASEB J.* 27, 000–000 (2013). www.fasebj.org**

Key Words: AMPK · insulin signaling · acetylation

IRON PLAYS A CRITICAL ROLE in numerous biological pathways. It is a key factor in the reduction-oxidation (redox) reactions of oxidative phosphorylation in the respiratory chain and in the binding of oxygen to hemoglobin and myoglobin. The biological significance of iron largely depends on its transition ability, which, in biological systems, often involves the 1-electron redox reactions between its ferric (3+) and ferrous (2+) forms. In addition to its beneficial properties, free reduced iron is also toxic because of its participation in Fenton redox chemistry: Reduced iron reacts with hydrogen peroxide (H_2O_2) or lipid peroxides to produce highly reactive radicals that can damage lipids, proteins, and nucleic acids.

A large body of evidence demonstrates that iron overload is associated with development of cirrhosis and diabetes in humans (1–5), although the molecular mechanisms by which iron affects intracellular signaling and homeostatic systems are not fully understood. Many studies of iron-associated cirrhosis and diabetes have focused on hereditary hemochromatosis (HH), a genetic disease characterized by iron overload of many tissues (6). The majority of patients with HH have mutations in the *HFE* gene (7). Recent studies have reported that the prevalence of diabetes in adults with HH is 13–23% and that of impaired glucose tolerance is 15–30%, which represents a 2- to 4-fold increase over a comparable reference population of Northern European descent (5, 8). Mice with targeted deletion of the *Hfe* gene ($Hfe^{-/-}$) recapitulate the biochemical abnormalities and histopathology of human HH (9). Insulin secretion, for example, is decreased both in $Hfe^{-/-}$

Abbreviations: ACC, acetyl-CoA carboxylase; AMPK, AMP-activated protein kinase; AMPK-DN, dominant-negative AMP-activated protein kinase; AUC_G, area under the curve for glucose; G6Pase, glucose-6-phosphatase; GAPDH, glyceraldehyde-3-phosphate dehydrogenase; HH, hereditary hemochromatosis; HI, high iron; LI, low iron; MHI, moderately high iron; NAC, *N*-acetylcysteine; NC, normal chow; Pepck, phosphoenolpyruvate carboxykinase; Rpl13a, ribosomal protein L13a; Tfrc, transferrin receptor 1; WT, wild type

[1] Correspondence: Division of Endocrinology, 30 N. 2030 East, Salt Lake City, UT 84132, USA. E-mail donald.mcclain@hsc.utah.edu

doi: 10.1096/fj.12-216929

This article includes supplemental data. Please visit *http://www.fasebj.org* to obtain this information.

mice (10) and in human HH subjects (5). Increased gluconeogenesis and metabolic inflexibility in *Hfe*$^{-/-}$ mice also contribute to the risk of diabetes (3). These defects, however, are well compensated in *Hfe*$^{-/-}$ mice, as evidenced by improved rather than impaired glucose tolerance (11).

We have shown previously that AMP-activated protein kinase (AMPK) signaling was activated in *Hfe*$^{-/-}$ mice (11). AMPK controls energy balance at the cellular and organismal levels (12). AMPK is a sensor of cellular energy status and is activated by an elevated ratio of AMP or ADP to ATP (13). A large variety of hormonal signals and metabolic stresses, such as glucose deprivation, ischemia, hypoxia, oxidative stress, and hyperosmotic stress, activate AMPK, although not all of these signal through an increased cellular AMP:ATP and/or ADP:ATP ratio (12, 14). Activated AMPK stimulates glucose uptake and fatty acid oxidation in peripheral tissues and suppresses gluconeogenesis in liver, pathways that play important roles in the pathogenesis and treatment of diabetes (15).

In our previous study of AMPK signaling in *Hfe*$^{-/-}$ mice (11), the causality between the effects of iron and AMPK were not established, nor were the pathways fully explicated that linked those effects to changes in metabolism. Furthermore, important differences are apparent in the distributions of tissue iron in HH compared to dietary iron overload (16) and in the phenotypes resulting from these two sources of iron overload (17). Because dietary iron overload is a more important risk factor for diabetes in the general population than HH, we therefore also sought to determine whether the same effects of iron as were observed in HH would be seen in mice fed high-iron (HI) diets. Here we show that iron affects glucose tolerance in mice through its activation of AMPK in liver and muscle through mechanisms that include LKB1 deacetylation.

MATERIALS AND METHODS

Experimental animals

C57/Bl6J wild-type (WT) mice (3 mo old) were fed a normal chow (NC) diet or an HI diet for 2 mo. Normal chow (Harlan Teklad TD-8656; Harlan Bioproducts, Indianapolis, IN, USA) contains 4.5% of calories as fat and 0.5 g/kg of carbonyl iron. The moderately high iron (MHI) and HI diets contain 4.5% of calories as fat and either 2 or 20 g/kg of carbonyl iron. An additional group of mice fed a low-iron (LI) diet (4–6 mg/kg chow) were used in the stable isotope studies. Mice with muscle-specific expression of a dominant-negative AMPK were kindly provided by Morris Birnbaum (University of Pennsylvania, Philadelphia, PA, USA). Procedures were approved by the Institutional Animal Care and Use Committee of the University of Utah.

Quantification of transcript levels by RT-PCR

Quantitative RT-PCR was performed with a Light Cycler (Roche Diagnostics, Basel, Switzerland) as described previously (11). The following primers were used (designed using Primer3 software; http://www.simgene.com): phosphoenolpyruvate carboxykinase (Pepck), 5′-TTGGAGAGAATGCTCGTGTG and 5′-TGGAGAACAGCTGACTGGTG; glucose-6-phosphatase (G6Pase), 5′-AGGAAGGATGGAGGAAGGAA and 5′-TGGAACCAGATGGGAAAGAG; transferrin receptor 1 (Tfrc), 5′-CAGTCCAGCTGGCAAAGATT and 5′-GTCCAGTGTGGGAACAGGTC; and ribosomal protein L13a (Rpl13a), 5′-GGAGAAACGGAAGGAAAAGG and 5′-ACAGGAGCAGTGCCTAAGGA. Messenger RNA levels of specific genes were normalized to Rpl13a levels for the same sample. Rp113a normalized to the cDNA template amount did not show any variation with chow iron content.

Tissue nonheme iron determination

Tissue nonheme iron was quantified as described previously (18). Briefly, after digestion in trichloroacetic acid at 65°C, tissue extracts were added to the chromogen reagent containing bathophenanthroline sulfonate. Optical density was read at 535 nm and compared to iron standards.

Ex vivo glucose uptake into isolated soleus muscle

2-Deoxy-D-glucose uptake was measured as described previously (19).

Glucose and pyruvate tolerance testing

After 6 h of food withdrawal, mice were injected intraperitoneally with 1 mg/g body weight of glucose in 0.9% saline. Glucose levels were measured from tail vein blood with a glucometer (Elite; Bayer Corp., Tarrytown, NY, USA) at 0, 5, 15, 30, 60, and 120 min. Extra tail blood (30 μl) was collected at 0 and 30 min for insulin measurement. For pyruvate tolerance testing, after overnight food withdrawal, blood glucose was measured with a glucometer before and after intraperitoneal injection of sodium pyruvate (2 mg/g body weight) at 0, 5, 15, 30, 60, and 120 min.

Stable isotope tracer studies

Stable isotope studies were performed as described previously (11).

Deacetylase activity

Tissue deacetylase activity was measured in nuclear extracts using an assay kit from Enzo Life Sciences (Farmingdale, NY, USA).

Measurement of AMP and ATP

Approximately 20 mg of frozen tissue was transferred to chilled (−20°C) bead mill tubes containing 1.4-mm ceramic beads. Cold (−20°C) 90% methanol (500 μl) containing the internal standard NAD (1 mg/ml) was added, and the tubes were placed into a Omni BeadRuptor 24 (Omni International, Kennesaw, GA, USA) and homogenized at 6.5 m/s^2 for 30 s. These tubes were then incubated for 60 min at −20°C and centrifuged (4°C) for 10 min at 20,000 *g* to precipitate the proteins. The supernatant was reserved, and a second extraction step was performed in the same manner as the first but with 60% methanol (−20°C). The supernatants were combined and vacuum dried.

Two Shimadzu LC10AD VP pumps and a CTO-10AS column oven (Shimadzu Corp., Kyoto, Japan) were used for HPLC separation. Detection was accomplished using a

PE Sciex 365 triple-quadrupole mass spectrometer (Perkin Elmer Sciex, Framingham, MA, USA) modified with an Ionics EP10+ source (Ionics, Bolton, ON, Canada). Prior to LC-MS analysis to each dried sample was added 48 μl of 10 mM sodium phosphate buffer (pH 7.0) followed by 2 μl of 2-vinylpyridine. The sample was allowed to incubate at room temperature for 30 min, followed by the addition of 50 μl of 20 mM ammonium formate buffer (pH 9.2) containing 7.5 mM *N*-butyl amine. After centrifuging at 20,000 *g* for 5 min, 20 μL of each sample was injected onto a Phenomenex Gemini-NX C18 (150×3mm; 3 μm particle size, 110A pore size; Phenomenex, Torrance, CA, USA) fitted with a Phenomenex security guard precolumn. For HPLC separation, solvent A contained 20 mM ammonium formate and 7.5 mM *N*-dibutylamine in ultrapure water, and solvent B contained 7.5 mM *N*-dibutlyamine in MS-grade methanol. The initial column conditions were 5% B for 3 min, followed by a gradient elution to 90% B over 20 min. This was held for 1 min, then brought back to 5% B over 2 min. The column was then equilibrated for an additional 10 min. Data were recorded using Analyst 1.4.2 software (Sciex) with final peak heights recorded in Excel (Microsoft, Redmond, WA, USA). Data were normalized to weight and internal standard.

Tissue culture

Mouse C2C12 myoblast cells were grown in MEMα (Invitrogen, Carlsbad, CA, USA) plus 10% fetal bovine serum and 1% penicillin/streptomycin/glutamine. Myoblast differentiation was induced by 2% heat-inactivated horse serum at ~70% confluence. The induction medium was changed every other day for 4 consecutive days. Differentiated C2C12 myotube cells were treated overnight with various concentrations of ferrous sulfate. After 2 h incubation, cells were washed with PBS and harvested.

Western blotting

Age-matched (5 mo) male mice were euthanized. Hindlimb muscle and liver were collected, and tissue homogenates were prepared for Western blot analysis. Levels of total and/or phosphorylated proteins were detected by immunoblotting using the following antibodies: acetyl-CoA carboxylase (ACC; Ser79; Cell Signaling Technology, Danvers, MA, USA), AMPK (Thr172; Cell Signaling Technology), ferritin (Abcam, Cambridge, MA, USA), p53-Lys382 (Cell Signaling Technology), Akt (Cell Signaling Technology), and IRS2 (Abcam). Signals quantified by densitometry were normalized to glyceraldehyde-3-phosphate dehydrogenase (GAPDH) levels (Santa Cruz Biotechnology, Santa Cruz, CA, USA) or, in the case of pAMPK, to total AMPK protein.

Statistical procedures

Descriptive statistics are presented as averages ± SEM. A 2-tailed Student's *t* test was used to compare the differences between groups.

RESULTS

AMPK is activated by excess iron in muscle

We first determined whether skeletal muscle of mice fed an HI diet (20 g Fe/kg) accumulated excess iron. Ferritin, a marker for tissue iron stores, was increased 2.1-fold in skeletal muscle from mice fed an HI diet compared to control mice fed an NC diet (500 mg Fe/kg; NC=0.48±0.16, HI=0.98±0.11 arbitrary density units, n=4/group, P<0.05; **Fig. 1*A***). The Western blots were normalized to GAPDH, and although iron deficiency up-regulates that protein, iron excess has been shown to have no effect on GAPDH expression (20). Consistent with that finding, we saw no systematic variation of GAPDH mRNA levels in our Western blots (see figures), whose gels were also normalized by equal protein loading.

Ferritin represents a sequestered pool of iron with very little turnover, so to verify that iron fluxes remain high in muscle from mice fed the HI diet, we also measured transcript levels of the transferrin receptor *Tfrc*. *Tfrc* mRNA contains iron-responsive elements (IREs) in its 3′ untranslated region that result in decreased *Tfrc* mRNA levels as intracellular bioavailable iron levels increase (21). *Tfrc* transcript levels decreased by 47% in muscle from mice fed the HI diet (P< 0.001; Fig. 1*B*). Finally, we directly assessed nonheme iron levels in muscle, and they were increased by 22% in skeletal muscle from mice fed the HI chow (P<0.05; Fig. 1*C*).

The phosphorylated form of AMPK was increased 2.7-fold in muscle from mice fed the HI diet (20 g Fe/kg; NC=4.06±0.33, HI=10.80±1.36 arbitrary density units, n=4/group, P<0.01; Fig. 1*D*). We confirmed activation of AMPK by examining phosphorylation of an AMPK downstream target, ACC. ACC also showed a 3.1-fold increase in phosphorylation in muscle (pAMPK: NC=4.1±0.6, HI=10.8±1.4 arbitrary density units, P<0.01; pACC: NC=5.0±0.5, HI=15.9±3.0 arbitrary density units, P=0.02; n=3–4/group; Fig. 1*D*). More modest elevations of dietary iron (2g Fe/kg, compared to NC, 500 mg Fe/kg) could also activate AMPK. The phosphorylated forms of AMPK and ACC were increased by 1.8- and 5.4-fold, respectively, in skeletal muscle from mice fed the MHI diet (2 g Fe/kg, P<0.05; Supplemental Fig. S1).

To further demonstrate that activation of AMPK was induced directly by iron rather than hormonal or indirect metabolic effects of iron, cultured and differentiated C2C12 myotubes were treated with different concentrations of iron, and phosphorylation of AMPK was examined by Western blotting. At 1 μM $FeSO_4$, levels of pAMPK and pACC were increased by 1.25- and 3.0-fold, respectively, compared to C2C12 myotubes cultured in iron-free MEMα (pAMPK: iron-free=8.0±0.5, 1 μM $FeSO_4$=10.0±0.4 arbitrary density units, P<0.05; pACC: iron-free=9.8±1.5, 1 μM $FeSO_4$=29.8±9.4 arbitrary density units, P=0.02; Fig. 1*E*). Dose-response analysis revealed no significant stimulation at 100 nM $FeSO_4$ and maximal stimulation at 1 μM $FeSO_4$ (Fig. 1*F*). A time-course study revealed no increase of AMPK at 1 h, but near maximal stimulation at 4 h that was maintained through 12 h (not shown). We determined nonheme iron levels in the cells, and they were increased 3.9-fold in the iron-treated cells (1.38±0.10 *vs.* 0.35±0.05 arbitrary units normalized to cell number, n=4/group, P=0.0001).

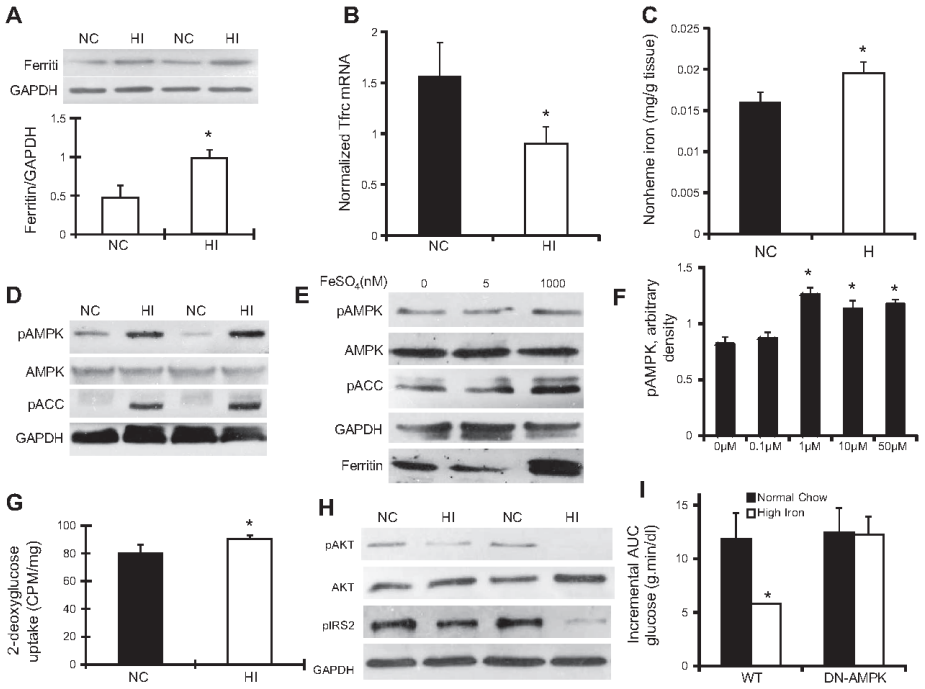

Figure 1. Iron activates AMPK and leads to increased glucose uptake in skeletal muscle of C57BL/6J male mice fed an HI diet. *A*) Hindlimb muscle was collected from age-matched (5-mo-old) male WT mice fed an NC diet (500 mg Fe/kg) or an HI diet (20 g Fe/kg). Ferritin and GAPDH were detected by Western blotting (n=4). Densitometric data from 4 independent data points were normalized to GAPDH and quantitated for statistical analysis (see text). *P< 0.05). *B*) Normalized *Tfrc* mRNA levels were determined in skeletal muscle of mice fed NC or HI diets (n=18/group). *P< 0.001. *C*) Tissue nonheme iron levels were determined in skeletal muscle of mice fed NC or HI diets (n=18/group). *P< 0.05. *D*) Skeletal muscle from WT mice fed NC or HI diets were analyzed by Western blotting for activated pAMPK, total AMPK, pACC, and GAPDH (n=3–4; P<0.01 for pAMPK, P=0.02 for pACC). *E*) C2C12 cells were differentiated into myoblasts and cultured in iron-free MEMα (n=3, P<0.05). Extracts of C2C12 cells grown in different iron concentrations overnight were prepared for Western blot analysis of pAMPK, total AMPK, pACC, and GAPDH. *F*) Dose response of pAMPK as a function of medium iron concentration. Cells were treated as in *E* (n=4/group). *P< 0.01. *G*) Soleus muscle from 5-mo-old male WT mice fed HI or NC diets was incubated with 2-[^{3}H] deoxy-D-glucose in the presence of 13.3 nM insulin. Results for glucose uptake are corrected for extracellular tissue absorption using mannitol and normalized to muscle weight (n=6–8). *P< 0.05). *H*) Skeletal muscles from WT mice fed NC or HI diets were analyzed by Western blotting for pAKT, total AKT, pIRS2, and GAPDH (n=4–5 for pAKT, P<0.05; n=4 for pIRS2, P=0.16). *I*) Control C57BL/6J WT mice, or mice with expression of dominant-negative AMPK (AMPK-DN) in skeletal muscle, were either maintained on NC diet or fed an HI diet for 8 wk. Intraperitoneal glucose tolerance testing was then performed, and area under the curve (AUC) for glucose was calculated (n=11–12, P=0.89 for AMPK-DN mice). *P< 0.05.

Glucose uptake is increased despite decreased insulin signaling in muscle of mice fed an HI diet

Isolated soleus muscles from mice fed the HI diet exhibited a significant increase in 2-deoxyglucose uptake after insulin stimulation compared to control mice fed the NC diet (NC=80.2±6.0, HI=90.5±2.3 cpm/mg, P<0.05; Fig. 1*G*). The augmentation of glucose uptake was not explained by increased insulin signaling; rather, phosphorylation of AKT and its downstream target IRS2 were decreased by 60% (NC=0.52±0.11, HI=0.21±0.05 arbitrary density units, n=4–5/group, P<0.05) and 53% (NC=0.69±0.16, HI=0.32±0.15 arbitrary density units, n=4/group, P=0.16), respectively, in skeletal muscle of mice fed the HI diet compared to control mice fed the NC diet (Fig. 1*H*).

AMPK mediates the effects of iron on glucose homeostasis *in vivo*

In order to prove that AMPK activation mediates iron-regulated glucose homeostasis *in vivo*, we fed the HI diet (20 g Fe/kg) to mice expressing a dominant-negative AMPK (AMPK-DN) in skeletal muscle. WT mice fed the HI diet for 8 wk exhibited a 51% decrease in the incremental area under the curve for glucose

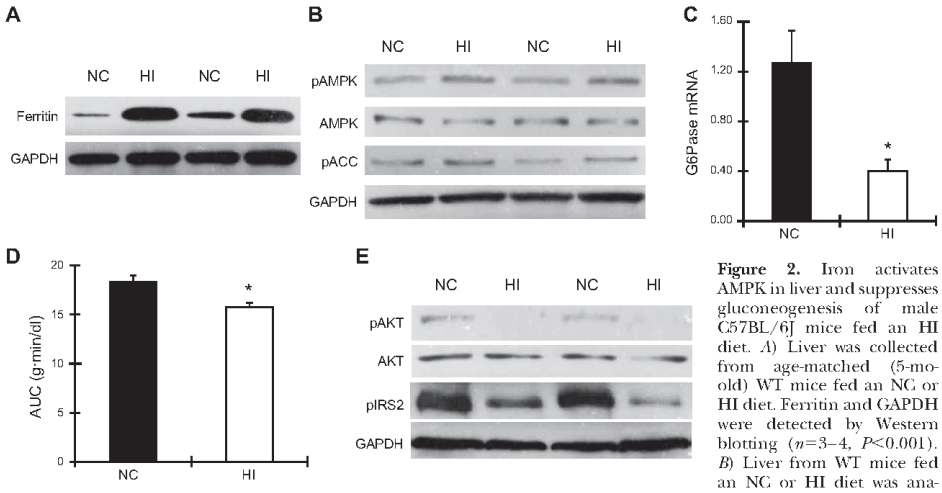

Figure 2. Iron activates AMPK in liver and suppresses gluconeogenesis of male C57BL/6J mice fed an HI diet. *A*) Liver was collected from age-matched (5-mo-old) WT mice fed an NC or HI diet. Ferritin and GAPDH were detected by Western blotting (n=3–4, P<0.001). *B*) Liver from WT mice fed an NC or HI diet was analyzed by Western blotting for pAMPK, total AMPK, pACC, and GAPDH (n=3–4; P<0.05 for pAMPK and P=0.11 for pACC). *C*) Expression of mRNA for the gluconeogenesic gene *G6pase* in liver of WT mice fed an NC or HI diet was examined by quantatitive RT-PCR (n=4). *P < 0.05. *D*) Pyruvate tolerance testing of WT mice fed an NC or HI diet was performed by measuring blood glucose after injection of 2 mg pyruvate/g body weight. AUC for glucose was calculated (n=4–5). *P < 0.05. *E*) Liver from mice fed an NC or HI diet was analyzed by Western blotting for pAKT, total AKT, pIRS2, and GAPDH. (n=3–4; P=0.001 for pAKT, P<0.001 for pIRS2).

(AUC_G) after intraperitoneal glucose challenge (NC=11.8±2.4, HI=5.8±0.1 g·min/dl, n=4/group, P<0.05; Fig. 1*I*). AMPK-DN mice, by contrast, showed no augmentation of glucose uptake after 8 wk of HI diet (NC=12.4±2.2, HI=12.2±1.7 g·min/dl, n=3–4/group, P=0.95; Fig. 1*I*). The same pattern was seen with total AUC_G as with incremental AUC_G, namely a statistically significant decrease in AUC_G in WT mice fed the HI diet but no difference in the AMPK-DN mice (not shown).

AMPK is activated by iron in liver

We also examined AMPK activity in liver. We first confirmed that liver in mice fed the HI diet was iron overloaded. Ferritin was elevated by 3.8-fold in liver from mice fed the HI diet compared to mice fed the NC diet (NC=20.7±1.0, HI=5.4±1.7 arbitrary density units, n=3–4/group, P<0.001; **Fig. 2*A***). The phosphorylated form of AMPK was increased 1.9-fold (NC=0.42±0.03, HI=0.83±0.11 arbitrary density units, n=3–4/group, P<0.05) and ACC was increased 2.0-fold (NC=0.22±0.06, HI=0.43±0.08 arbitrary density units, n=3–4 /group, P=0.11) in liver from mice fed the HI diet (Fig. 2*B*).

Decreased hepatic glucose output in liver of mice fed an HI diet despite decreased insulin signaling

Because AMPK is known to suppress hepatic gluconeogenesis, we examined gluconeogenesis-related gene expression in liver by quantitative RT-PCR. *G6Pase* mRNA was decreased by 70% (P<0.05; Fig. 2*C*), and *Pepck* mRNA level was decreased by 25% although not significantly (P=0.14, data not shown). We further confirmed decreased gluconeogenesis by performing pyruvate tolerance testing. Mice fed the HI diet exhibited a 14% decrease in AUC_G after intraperitoneal pyruvate challenge (P<0.05; Fig. 2*D*).

We next examined hepatic glucose metabolism using stable isotope-based dynamic metabolic profiling (SiDMAP) tracer studies. Intraperitoneal glucose tolerance testing was performed using [U-$^{13}C_6$]-D-glucose. Consistent with the data above, mice fed the HI diet exhibited a 13% decrease in hepatic glucose output compared with mice fed the NC diet (P=0.05; **Table 1**) and a 15.8% decrease compared with mice fed the LI diet (P<0.05; Table 1). Because intracellular lactate is one of the precursors contributing to hepatic glucose output, we examined the glucose-derived lactate fraction in liver. Mice fed the HI diet trended toward a decrease in hepatic lactate compared with mice fed the NC diet (18%, P=0.12; Table 1) and exhibited a 28.4% decrease compared with mice fed the LI diet (P<0.05; Table 1). Glucose-derived plasma lactate, the source of glucose production *via* Cori cycling, was 9.2% lower in mice fed the HI diet compared with mice fed the NC diet (P<0.01; Table 1) and 13.5% lower compared with mice fed the LI diet (P<0.001; Table 1). Liver lactate from glycolysis in mice fed the HI diet was 3.5% lower compared with mice fed the NC diet P<0.01; Table 1) and 3.4% lower compared with mice fed the LI diet (P<0.01; Table 1).

TABLE 1. *Metabolic fate of glucose in a 13C isotoplome-wide association study (IWAS) matrix*

Treatment	MHI	NC	LI
Hepatic glucose output, glucose-derived/z242 ^{13}C-labeled fraction	45.13 ± 5.81	51.85 ± 3.28*	53.58 ± 2.8*
Hepatic lactate level, glucose-derived ^{13}C-labeled lactate	6.69 ± 0.67	8.12 ± 1.99#	9.34 ± 2.00*
Plasma lactate, glucose-derived ^{13}C-labeled lactate	19.07 ± 1.39	21 ± 1.15**	22.05 ± 1.97***
Liver lactate from glycolysis, glucose-derived M3 ^{13}C-lactate	78.86 ± 0.53	81.77 ± 2.15**	81.64 ± 1.33***

Metabolic fate of glucose after intraperitoneal challenge with [U-$^{13}C_6$]D-glucose substrate by its cross-labeling of plasma and liver metabolic products according to IWAS in WT C57BL/6J mice fed NC diet (500 mg Fe/kg), MHI diet (2 g Fe/kg), and LI diet (35 mg Fe/kg); $n = 3$/group. *$P \leq 0.05$, **$P < 0.01$, ***$P < 0.001$ *vs.* HI diet; #$P = 0.12$ *vs.* HI diet (not significant).

To determine whether the decreased hepatic glucose production was mediated by augmented insulin action, insulin signaling in liver was examined by Western blotting. Phosphorylation of AKT and IRS2 were lower by 68 and 72%, respectively, in liver of mice fed the HI diet (pAKT: NC= 8.7±1.0, HI=2.7±0.4 arbitrary density units, n=3/group, P=0.01; IRS2: NC=16.3±0.2, HI=4.6±1.1 arbitrary density units, n=3–4/group, P<0.05; Fig. 2*E*).

Mechanism for activation of AMPK in skeletal muscle and liver of mice fed an HI diet

We next examined the mechanisms by which iron activated AMPK. Because the phosphorylated form and activity of AMPK are regulated by LKB1, which in turn is regulated by acetylation (22, 23), we measured LKB1 acetylation in liver and skeletal muscle. LKB1 acetylation was decreased by 53% in skeletal muscle (NC=15.5±0.8, HI=7.2±0.3 arbitrary density units, P<0.001; **Fig. 3*A***) and by 36% in liver of mice fed the HI diet (NC=1.48±0.03, HI=0.95±0.09 arbitrary density units, n=3/group, P<0.01; Fig. 3*B*). We also directly assessed lysine deacetylase activity in muscle and liver. Deacetylase activity in tissues of mice fed the HI diet was increased 2.0-fold in skeletal muscle (P<0.02) and 1.6-fold (P<0.05) in liver (Fig. 3*C*). We also assessed SIRT1 activity directly by assessing the acetylation of p53 at Lys382 (24). Acetylation of p53 was decreased in muscle tissue of mice fed the HI diet (P<0.01; Fig. 3*D*). Because deacetylation of p53 results in its degradation (25), we also assessed total p53, and its levels, too, were decreased in HI (P<0.005; Fig. 3*D*). Treatment with the sirtuin inhibitors nicotinamide or splitomicin abolished the increased phosphorylation of AMPK induced by iron treatment of C2C12 cells (Fig. 3*E*).

Because an increased AMP/ATP ratio is also known to increase AMPK activity, we measured AMP and ATP levels in skeletal muscle and liver. The AMP/ATP ratio was increased by 2.7-fold in skeletal muscle (P<0.05; Fig. 3*F*) and by 2.0-fold in liver (P<0.05; Fig. 3*F*) of mice fed the HI diet.

Iron overload may result in increased oxidative stress, which in turn regulates SIRT1 activity (26). We therefore determined whether oxidative stress was enhanced in skeletal muscle with dietary iron overload. Protein carbonyl levels, a commonly used indicator of protein oxidation (27) were increased by 2-fold (P<0.01; **Fig. 4*A***) and 5.4-fold (P<0.05; Fig. 4*A*) in skeletal muscle and liver, respectively, of mice fed the HI diet. We next determined whether increased oxidative stress mediated iron-induced AMPK activation and also improved glucose tolerance. Similar to the study depicted in Fig. 1*H*, mice fed the HI diet for 8 wk exhibited a 48% decrease in the incremental AUC_G after intraperitoneal glucose challenge compared to mice fed the NC diet (P<0.001; Fig. 4*B*). After concomitant treatment for 8 wk with the antioxidant *N*-acetyl cysteine (NAC), however, no difference was observed in AUC_G between mice fed the NC and HI diets (P=0.36). Both groups of NAC-treated mice had significantly lower incremental AUC_G than control mice fed the NC diet (P<0.01), but this was largely the effect of significantly higher fasting glucose levels in the NAC-treated animals (NAC=151±5, control=127±6 mg/dl, P<0.01; data not shown) rather than decreased glucose excursions. Thus, the total AUC_G did not differ between control and NAC-treated mice (P=0.52; data not shown). The increased protein carbonyl level in muscle and liver of mice fed the HI diet was also normalized after 8 wk of NAC treatment (P=0.49 and P=0.57 for NC *vs.* HI in muscle and liver, respectively; Fig. 4*C*), as was the increased phosphorylation of AMPK (P=0.61 and P=0.78; Fig. 4*D*).

DISCUSSION

Our previous studies in a mouse model of HH have shown that iron-overloaded *Hfe*$^{-/-}$ mice exhibit elevated AMPK activity in skeletal muscle (11), although it was not determined whether the AMPK activation was induced by iron or other secondary iron-independent signaling pathways. The mechanism of the activation of AMPK by iron and the subsequent changes in glucose homeostasis were also unknown, as was the status of insulin signaling. We report here that high dietary iron in WT mice activates AMPK in liver and muscle. This stimulation is mediated by redox signaling and decreased LKB1 acetylation, thus increasing LKB1 activity to phosphorylate and activate AMPK. Activated AMPK overruns dampened insulin signaling, increasing glucose uptake in muscle and suppressing gluconeogenesis in liver, contributing to the improved glucose tolerance observed in mice fed an HI diet. That AMPK is largely responsible is demonstrated by the lack of the effects of iron in muscle of mice expressing AMPK-DN in that tissue.

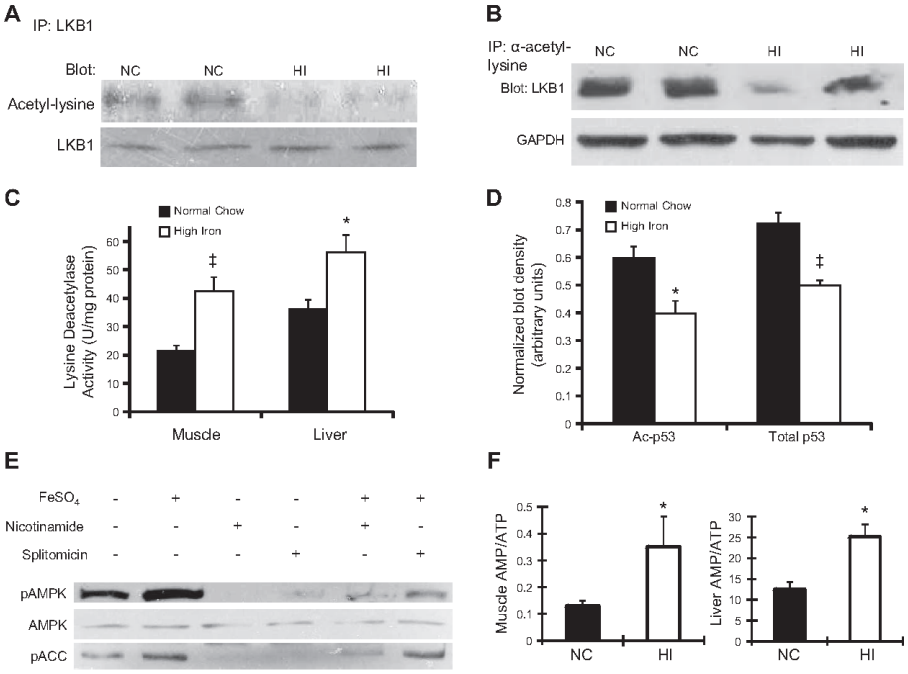

Figure 3. Iron activates AMPK through deacetylation of LKB1. *A*) Lysates of skeletal muscle from WT mice fed an NC or HI diet were incubated and precipitated by anti-LKB1. Pulldown was analyzed by Western blotting for anti-acetylated lysine (53% decrease, $n=3$/group, $P<0.001$). Anti-LKB1 was blotted as a loading control. *B*) Lysates of liver from WT mice fed an NC or HI diet were incubated and precipitated by anti-acetylated lysine. Pulldown was analyzed by Western blotting for LKB1 (36% decrease, $n=3$, $P<0.01$). Anti-GAPDH was blotted for normalizaton. *C*) Lysine deacetylase activity was measured in liver and muscle (2.0-fold increase in muscle, $n=3$/group; 1.6-fold increase in liver, $n=3$/group). $^{*}P < 0.05$; $^{‡}P < 0.02$. *D*) Western blotting for p53 acetylation at Lys382 (left bars) and total p53 (right bars) normalized to actin ($n=5$–6/group). $^{*}P < 0.01$, $^{‡}P < 0.005$. *E*) Differentiated C2C12 myotubes were grown with or without 1 μM $FeSO_4$ overnight. These cells were also incubated with or without 10 mM nicotinamide or 100 μM splitomicin overnight. Cell lysates were prepared for Western blot analysis of pAMPK, total AMPK, phosphorylated ACC, and GAPDH. *F*) AMP and ATP in skeletal muscle (left panel, $n=3$–5) and liver (right panel, $n=3$) of WT mice on NC or HI were measured by LC-MS-MS-MS. $^{*}P < 0.05$.

Iron entry into cells and bioavailable iron levels within cells are tightly regulated (28), so it was first necessary to determine whether skeletal muscle does accumulate excess iron with increased dietary intake, as has been previously demonstrated with HH (3, 11). Iron loading in muscle was demonstrated by 3 independent methods: increased ferritin protein levels, indicating increased iron stores in cells; decreased transferrin receptor levels, indicating higher levels of bioavailable iron flux; and increased total nonheme iron levels. These data demonstrate conclusively that despite the multiple pathways for regulation of iron and negative feedback regulation of dietary iron absorption mediated by hepcidin (28), those systems are not sufficient to prevent overload in muscle with chronic dietary excess of iron.

Numerous studies have demonstrated that in both humans and mouse models, iron overload is associated with diabetes and other markers of metabolic syndrome, such as steatohepatitis (1–5, 11, 29). The current study demonstrates that iron inhibits insulin signaling in muscle and liver, but also exerts compensatory beneficial metabolic effects by up-regulating AMPK activity. These effects were seen after feeding mice excess iron for only 2 mo, and with 2- to 4-fold elevations of ferritin and iron levels in muscle and liver. The majority of these studies were performed in mice fed a diet containing 20 g/kg elemental iron, but similar effects were seen in mice fed 1/10 that amount, only 4-fold more than normal rodent chow. "Normal" human serum ferritin values vary over a 10- to 15-fold range, suggesting that the current results are applicable to individuals with modest degrees of excess iron, such as can be seen with dietary excess. Of note, the effects of high iron on hepatic glucose handling are not attributable to overt liver damage: Mice fed these diets did not develop hepato-

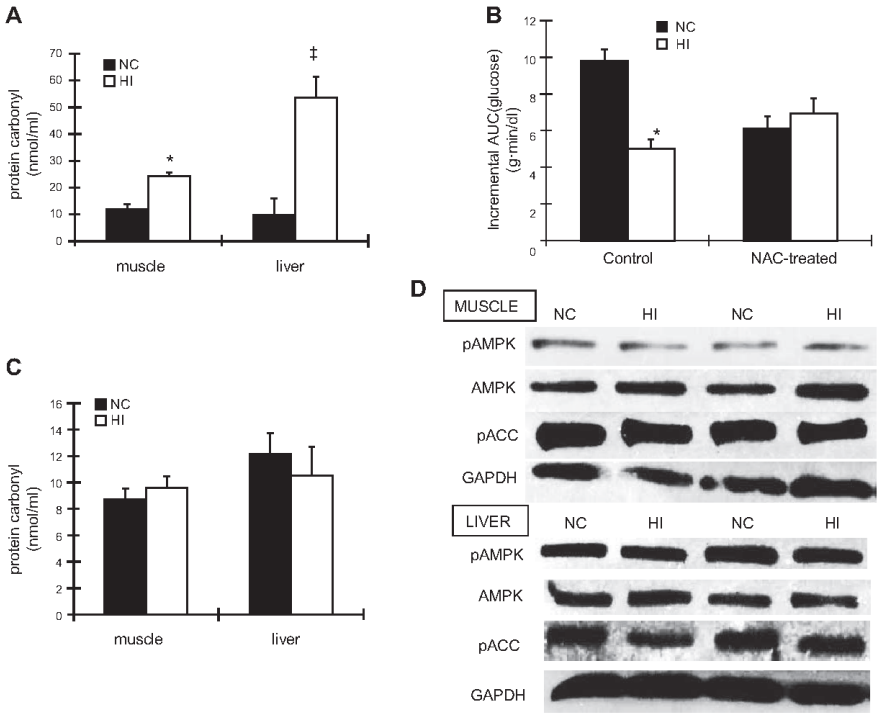

Figure 4. Iron induces oxidative stress, and treatment of mice with antioxidants reverses the effect of HI diet on AMPK and glucose tolerance. *A*) Protein carbonyl levels in skeletal muscle (left panel, $n=3$–5) and liver (right panel, $n=3$) of WT mice fed an NC or HI diet were measured. $^{*}P < 0.01$; $^{\ddagger}P < 0.05$. *B*) WT mice fed an NC or HI diet were treated with or without 10 mg/ml *N*-acetylcysteine (NAC; pH 7.0) for 2 mo. Glucose tolerance test was then performed, and incremental AUC for glucose was calculated ($n=5$; $P<0.01$ for mice with NAC treatment). $^{*}P = 0.05$. *C*) After 2 mo of 10 mg/ml NAC treatment, protein carbonyl levels in skeletal muscle and liver of WT mice fed an NC or HI diet were measured ($n=5$; $P=0.49$ in skeletal muscle, $P=0.57$ in liver). *D*) After 2 mo of 10 mg/ml NAC treatment, skeletal muscle and liver from mice fed an NC or HI diet were analyzed by Western blotting for pAMPK, total AMPK, pACC, and GAPDH ($n=3$–4, $P=0.61$ for pAMPK in muscle; $n=4$, $P=0.78$ for pAMPK in liver).

toxicity, as evidenced by increased serum levels of transaminases (data not shown), and it is also known that the *Hfe*$^{-/-}$ mouse model is resistant to the hepatofibrotic complications of iron overload that are seen in humans (30).

Although the observed effects of iron were to decrease glycemia in mice, over time other effects of excess iron are diabetogenic, for example, decreased insulin secretion, metabolic inflexibility, and mitochondrial dysfunction (10). These effects of iron overload in the development of diabetes would be particularly detrimental when combined with conditions causing insulin resistance, such as obesity or a high fat-diet. Finally, it is possible that the balance of the competing effects of AMPK activation compared to decreased insulin signaling may be different in humans or change over time. Thus, the final integrated effects of iron on diabetes risk are likely to be complex and modified by species, age, weight, diet, and multiple other variables.

The current studies were undertaken because of significant differences between dietary iron overload and HH, for example, in the tissue distribution of iron overload in the two conditions. Iron overload occurs in liver and muscle tissues both of *Hfe*$^{-/-}$ mice and of mice fed HI diets. Iron levels in adipose tissue (17) and macrophages (16) of *Hfe*$^{-/-}$ mice, by contrast, are lower than in WT mice, based on the fact that the lower hepcidin levels in HH result in increased expression of the iron export channel ferroportin (31, 32). Thus, tissues with relatively high ferroportin expression are paradoxically iron underloaded in HH, whereas high hepcidin in dietary iron overload lead to increased iron levels in those same tissues. In addition, in contrast to the decreased insulin signaling in liver of WT mice fed an HI diet, insulin signaling in liver of *Hfe*$^{-/-}$ mice was

enhanced (3). This may be related to increased adiponectin levels in the *Hfe*$^{-/-}$ mice but decreased levels with dietary iron excess, related to the different adipocyte iron levels in the two conditions (17). In addition, macrophage iron loading on HI diets could contribute to macrophage inflammation that could, in turn, impair insulin signaling (33).

We demonstrate that one of the mechanisms of AMPK activation by iron is through the deacetylation of LKB1, one of the upstream stimulating kinases of AMPK. Deacetylation of LKB1 is largely mediated by SIRT1 (22, 23), and the decreased acetylation of the SIRT1 target p53 (24) argues that activation of SIRT1 is contributing to the observed effects. Consistent with a role of SIRT1 in responding to iron and activating AMPK, activation of SIRT1 attenuates oxidant-induced pathways (34) and mimics a low-energy state to signal increased fatty acid oxidation, a pathway also stimulated by AMPK (35). Other sirtuins, however, also modulate the LKB1/AMPK pathway (36), so we cannot be sure that other deacetylases do not contribute to the effects of iron on LKB1 acetylation. The pharmacologic effects of nicotinamide and splitomicin observed in the C2C12 cells argue that if other deacetylases are involved, they are likely to be other sirtuin family members rather than a non-NAD-dependent deacetylase. AMPK in yeast is itself activated by decreased acetylation (37), arguing that direct modulation of AMPK might add to LKB1-mediated changes in dietary iron overload. Other potential consequences of sirtuin activation by iron are possible and remain to be determined.

The sirtuins are known to respond to oxidative stress, and the experiments on the NAC-treated mice support that signaling by redox state of the tissue is playing a role in mediating the observed effects. Oxidant stress is known to increase in iron overload (10, 38). It should also be noted that factors other than enhanced skeletal muscle glucose uptake are contributing to the phenotype of the NAC-treated mice. Fasting glucose levels, for example, are significantly higher, and it may be speculated that diminished redox-dependent signaling of AMPK and its suppression of hepatic glucose production (Table 1) is a factor.

In summary, the current results and previous studies demonstrate that iron exerts significant effects across several tissues to exert effects on glucose homeostasis and diabetes risk. This system-wide association study (SWAS) greatly assists in the ultimate description of the effects of iron on metabolism, which include a complex set of dose-sensitive effects across several tissues, reflecting both beneficial and detrimental effects and both its toxic potential and regulatory actions.

The authors thank Dr. Morris Birnbaum (University of Pennsylvania, Philadelphia, PA, USA) for the AMPK-DN mice. This work was supported by the U.S. National Institutes of Health (RO1DK081842, D.M.; 1T32DK091317, J.S.), the Research Service of the U.S. Department of Veterans Affairs, and the Marilyn Jane Robinson Foundation.

REFERENCES

1. Rajpathak, S. N., Wylie-Rosett, J., Gunter, M. J., Negassa, A., Kabat, G. C., Rohan, T. E., and Crandall, J. (2009) Biomarkers of body iron stores and risk of developing type 2 diabetes. *Diabetes Obes. Metab.* **11,** 472–479
2. Fernandez-Real, J. M., Lopez-Bermejo, A., and Ricart, W. (2002) Cross-talk between iron metabolism and diabetes. *Diabetes* **51,** 2348–2354
3. Huang, J., Jones, D., Luo, B., Sanderson, M., Soto, J., Abel, E. D., Cooksey, R. C., and McClain, D. A. (2011) Iron overload and diabetes risk: a shift from glucose to fatty acid oxidation and increased hepatic glucose production in a mouse model of hereditary hemochromatosis. *Diabetes* **60,** 80–87
4. Dongiovanni, P., Fracanzani, A. L., Fargion, S., and Valenti, L. (2011) Iron in fatty liver and in the metabolic syndrome: a promising therapeutic target. *J. Hepatol.* **55,** 920–932
5. McClain, D., Abraham, D., Rogers, J., Brady, R., Gault, P., Ajioka, R., and Kushner, J. (2006) High prevalence of abnormal glucose homeostasis secondary to decreased insulin secretion in individuals with hereditary haemochromatosis. *Diabetologia* **49,** 1661–1669
6. Pietrangelo, A. (2010) Hereditary hemochromatosis: pathogenesis, diagnosis, and treatment. *Gastroenterology* **139,** 393–408, e391–e392
7. Feder, J. N., Gnirke, A., Thomas, W., Tsuchihashi, Z., Ruddy, D. A., Basava, A., Dormishian, F., Domingo, R., Jr., Ellis, M. C., Fullan, A., Hinton, L. M., Jones, N. L., Kimmel, B. E., Kronmal, G. S., Lauer, P., Lee, V. K., Loeb, D. B., Mapa, F. A., McClelland, E., Meyer, N. C., Mintier, G. A., Moeller, N., Moore, T., Morikang, E., Prass, C. E., Quintana, L., Starnes, S. M., Schatzman, R. C., Brunke, K. J., Drayna, D. T., Risch, N. J., Bacon, B. R., and Wolff, R. K. (1996) A novel MHC class I-like gene is mutated in patients with hereditary haemochromatosis. *Nat. Genet.* **13,** 399–408
8. Hatunic, M., Finucane, F. M., Brennan, A. M., Norris, S., Pacini, G., and Nolan, J. J. (2010) Effect of iron overload on glucose metabolism in patients with hereditary hemochromatosis. *Metabolism* **59,** 380–384
9. Zhou, X. Y., Tomatsu, S., Fleming, R. E., Parkkila, S., Waheed, A., Jiang, J., Fei, Y., Brunt, E. M., Ruddy, D. A., Prass, C. E., Schatzman, R. C., O'Neill, R., Britton, R. S., Bacon, B. R., and Sly, W. S. (1998) HFE gene knockout produces mouse model of hereditary hemochromatosis. *Proc. Natl. Acad. Sci. U. S. A.* **95,** 2492–2497
10. Cooksey, R. C., Jouihan, H. A., Ajioka, R. S., Hazel, M. W., Jones, D. L., Kushner, J. P., and McClain, D. A. (2004) Oxidative stress, beta-cell apoptosis, and decreased insulin secretory capacity in mouse models of hemochromatosis. *Endocrinology* **145,** 5305–5312
11. Huang, J., Gabrielsen, J. S., Cooksey, R. C., Luo, B., Boros, L. G., Jones, D. L., Jouihan, H. A., Soesanto, Y., Knecht, L., Hazel, M. W., Kushner, J. P., and McClain, D. A. (2007) Increased glucose disposal and AMP-dependent kinase signaling in a mouse model of hemochromatosis. *J. Biol. Chem.* **282,** 37501–37507
12. Kahn, B. B., Alquier, T., Carling, D., and Hardie, D. G. (2005) AMP-activated protein kinase: ancient energy gauge provides clues to modern understanding of metabolism. *Cell Metab.* **1,** 15–25
13. Xiao, B., Sanders, M. J., Underwood, E., Heath, R., Mayer, F. V., Carmena, D., Jing, C., Walker, P. A., Eccleston, J. F., Haire, L. F., Saiu, P., Howell, S. A., Aasland, R., Martin, S. R., Carling, D., and Gamblin, S. J. (2011) Structure of mammalian AMPK and its regulation by ADP. *Nature* **472,** 230–233
14. Fryer, L. G., Parbu-Patel, A., and Carling, D. (2002) Protein kinase inhibitors block the stimulation of the AMP-activated protein kinase by 5-amino-4-imidazolecarboxamide riboside. *FEBS Lett.* **531,** 189–192
15. Long, Y. C., and Zierath, J. R. (2006) AMP-activated protein kinase signaling in metabolic regulation. *J. Clin. Invest.* **116,** 1776–1783

16. Sullivan, J. L. (2007) Macrophage iron, hepcidin, and atherosclerotic plaque stability. *Exp. Biol. Med. (Maywood)* **232,** 1014–1020
17. Gabrielsen, J. S., Gao, Y., Simcox, J. A., Huang, J., Thorup, D., Jones, D., Cooksey, R. C., Gabrielsen, D., Adams, T. D., Hunt, S. C., Hopkins, P. N., Cefalu, W. T., and McClain, D. A. (2012) Adipocyte iron regulates adiponectin and insulin sensitivity. *J. Clin. Invest.* **122,** 3529–3540
18. Huberman, A., and Perez, C. (2002) Nonheme iron determination. *Anal. Biochem.* **307,** 375–378
19. Holland, W. L., Brozinick, J. T., Wang, L. P., Hawkins, E. D., Sargent, K. M., Liu, Y., Narra, K., Hoehn, K. L., Knotts, T. A., Siesky, A., Nelson, D. H., Karathanasis, S. K., Fontenot, G. K., Birnbaum, M. J., and Summers, S. A. (2007) Inhibition of ceramide synthesis ameliorates glucocorticoid-, saturated-fat-, and obesity-induced insulin resistance. *Cell Metab.* **5,** 167–179
20. Quail, E. A., and Yeoh, G. C. (1995) The effect of iron status on glyceraldehyde 3-phosphate dehydrogenase expression in rat liver. *FEBS Lett.* **359,** 126–128
21. Casey, J. L., Hentze, M. W., Koeller, D. M., Caughman, S. W., Rouault, T. A., Klausner, R. D., and Harford, J. B. (1988) Iron-responsive elements: regulatory RNA sequences that control mRNA levels and translation. *Science* **240,** 924–928
22. Hou, X., Xu, S., Maitland-Toolan, K. A., Sato, K., Jiang, B., Ido, Y., Lan, F., Walsh, K., Wierzbicki, M., Verbeuren, T. J., Cohen, R. A., and Zang, M. (2008) SIRT1 regulates hepatocyte lipid metabolism through activating AMP-activated protein kinase. *J. Biol. Chem.* **283,** 20015–20026
23. Lan, F., Cacicedo, J. M., Ruderman, N., and Ido, Y. (2008) SIRT1 modulation of the acetylation status, cytosolic localization, and activity of LKB1. Possible role in AMP-activated protein kinase activation. *J. Biol. Chem.* **283,** 27628–27635
24. Solomon, J. M., Pasupuleti, R., Xu, L., McDonagh, T., Curtis, R., DiStefano, P. S., and Huber, L. J. (2006) Inhibition of SIRT1 catalytic activity increases p53 acetylation but does not alter cell survival following DNA damage. *Mol. Cell. Biol.* **26,** 28–38
25. Ito, A., Kawaguchi, Y., Lai, C. H., Kovacs, J. J., Higashimoto, Y., Appella, E., and Yao, T. P. (2002) MDM2-HDAC1-mediated deacetylation of p53 is required for its degradation. *EMBO J.* **21,** 6236–6245
26. Brunet, A., Sweeney, L. B., Sturgill, J. F., Chua, K. F., Greer, P. L., Lin, Y., Tran, H., Ross, S. E., Mostoslavsky, R., Cohen, H. Y., Hu, L. S., Cheng, H. L., Jedrychowski, M. P., Gygi, S. P., Sinclair, D. A., Alt, F. W., and Greenberg, M. E. (2004) Stress-dependent regulation of FOXO transcription factors by the SIRT1 deacetylase. *Science* **303,** 2011–2015
27. Stadtman, E. R., and Oliver, C. N. (1991) Metal-catalyzed oxidation of proteins. Physiological consequences. *J. Biol. Chem.* **266,** 2005–2008
28. Andrews, N. C., and Schmidt, P. J. (2007) Iron homeostasis. *Ann. Rev. Physiol.* **69,** 69–85
29. Ford, E. S., and Cogswell, M. E. (1999) Diabetes and serum ferritin concentration among U.S. adults. *Diabetes Care* **22,** 1978–1983
30. Lebeau, A., Frank, J., Biesalski, H. K., Weiss, G., Srai, S. K., Simpson, R. J., McKie, A. T., Bahram, S., Gilfillan, S., and Schumann, K. (2002) Long-term sequelae of HFE deletion in C57BL/6 x 129/O1a mice, an animal model for hereditary haemochromatosis. *Eur. J. Clin. Invest.* **32,** 603–612
31. Nemeth, E., Roetto, A., Garozzo, G., Ganz, T., and Camaschella, C. (2004) Hepcidin is decreased in TFR2-hemochromatosis. *Blood* **105,** 1803–1806
32. Nemeth, E., Tuttle, M. S., Powelson, J., Vaughn, M. B., Donovan, A., Ward, D. M., Ganz, T., and Kaplan, J. (2004) Hepcidin regulates cellular iron efflux by binding to ferroportin and inducing its internalization. *Science* **306,** 2090–2093
33. Shoelson, S. E., Lee, J., and Goldfine, A. B. (2006) Inflammation and insulin resistance. *J. Clin. Invest.* **116,** 1793–1801
34. Kume, S., Haneda, M., Kanasaki, K., Sugimoto, T., Araki, S., Isono, M., Isshiki, K., Uzu, T., Kashiwagi, A., and Koya, D. (2006) Silent information regulator 2 (SIRT1) attenuates oxidative stress-induced mesangial cell apoptosis via p53 deacetylation. *Free Rad. Biol. Med.* **40,** 2175–2182
35. Feige, J. N., Lagouge, M., Canto, C., Strehle, A., Houten, S. M., Milne, J. C., Lambert, P. D., Mataki, C., Elliott, P. J., and Auwerx, J. (2008) Specific SIRT1 activation mimics low energy levels and protects against diet-induced metabolic disorders by enhancing fat oxidation. *Cell Metab.* **8,** 347–358
36. Pillai, V. B., Sundaresan, N. R., Kim, G., Gupta, M., Rajamohan, S. B., Pillai, J. B., Samant, S., Ravindra, P. V., Isbatan, A., and Gupta, M. P. (2010) Exogenous NAD blocks cardiac hypertrophic response via activation of the SIRT3-LKB1-AMP-activated kinase pathway. *J. Biol. Chem.* **285,** 3133–3144
37. Lu, J. Y., Lin, Y. Y., Sheu, J. C., Wu, J. T., Lee, F. J., Chen, Y., Lin, M. I., Chiang, F. T., Tai, T. Y., Berger, S. L., Zhao, Y., Tsai, K. S., Zhu, H., Chuang, L. M., and Boeke, J. D. (2011) Acetylation of yeast AMPK controls intrinsic aging independently of caloric restriction. *Cell* **146,** 969–979
38. Jouihan, H. A. C. P., Cooksey, R. C., Hoagland, E. A., Boudina, S., Abel, E. D., Winge, D. R., McClain, D. A. (2008) Iron-mediated inhibition of mitochondrial manganese uptake mediates mitochondrial dysfunction in a mouse model of hemochromatosis. *Mol. Med.* **14,** 98–108

Received for publication November 9, 2012.
Accepted for publication March 11, 2013.

CHAPTER 4

DIETARY IRON CONTROLS CIRCADIAN RHYTHM OF HEPATIC GLUCOSE METABOLISM THROUGH HEME SYNTHESIS

Abstract

The circadian rhythm of the liver is important in the maintenance of glucose homeostasis, and disruption of this rhythm is associated with type 2 diabetes risk. Feeding is one factor that sets the circadian clock in peripheral tissues, but relatively little is known about the role of specific dietary components in that regard. We have assessed the effects of dietary iron on the circadian rhythm of gluconeogenesis. Dietary iron affects circadian glucose metabolism through heme-mediated regulation of the interaction of Rev-Erbα with its cosuppressor NCOR. Loss of regulated heme synthesis was achieved by aminolevulinic acid (ALA) treatment of mice or cultured cells, to bypass the rate-limiting enzyme in hepatic heme synthesis, ALAS1. ALA treatment abolishes differences in hepatic glucose production and in the expression of gluconeogenic enzymes seen with variation of dietary iron. The differences among diets are also lost with inhibition of heme synthesis by treatment with isonicotinylhydrazine (INH). Heme levels respond to dietary iron through modulation of the level of PGC-1α, a transcriptional activator of ALAS1. Treatment of mice with the antioxidant n-

acetylcysteine (NAC) diminishes the PGC-1α variation observed among the iron diets, suggesting that iron may be acting through reactive oxygen species signaling to regulate PGC-1α. Together, these studies show that dietary iron alters the circadian rhythm of metabolism through control of intracellular heme synthesis.

Introduction

Circadian rhythms are endogenous cycles of behavioral and physiological processes that are set by external signals called zeitgebers. Light is the zeitgeber for the central clock of the suprachiasmatic nucleus (SCN) that controls circadian movement, feeding behavior, and thermoregulation (Buhr *et al.*, 2010). These contribute to the synchronization of clocks in peripheral tissues, but peripheral clocks also entrain to non-SCN zeitgebers. Notably, the liver is entrained to food intake and can become dyssynchronous from the SCN (Damiola *et al.*, 2000; Stokkan *et al.*, 2001). Such dyssynchrony may contribute to the observed association between metabolic dysregulation and altered sleep rhythms or night shift work (Huang *et al.*, 2011).

The precise contribution of specific nutrients to setting the hepatic clock is incompletely understood. One micronutrient, iron, has significant effects on metabolism. Iron affects metabolic regulation through multiple mechanisms, including effects on AMP-dependent kinase, fuel preference, insulin secretion, and regulation of the insulin-sensitizing adipokine, adiponectin (Huang *et al.* 2007, Gabrielsen *et al.* 2012). Iron overload and excess dietary iron are also significant risk factors for diabetes (Fernandez-Real *et al.*, 2002; Bowers *et al.*, 2011; Qui *et al.*, 2011; Simcox and McClain, 2013). Iron is a particularly attractive candidate for contributing to changes in circadian metabolism: Not only is iron an essential component of several proteins involved with electron

transport and metabolism, but several circadian transcription factors bind heme. Heme, for example, is necessary for the formation of the complex of nuclear receptor subfamily 1 group d member 1 (Rev-Erbα) with Nuclear Receptor Co-Repressor 1 (NCOR), part of the negative arm of the circadian transcriptional feedback loop (Li *et al.*, 2007, Raghuram *et al*., 2009). Heme has also been reported to bind Clock and Per2, although the functional relevance of this binding is unknown (Kaasik & Lee, 2004; Kitanishi *et al.*, 2008; Airola *et al.*, 2010; Lukat-Rogers *et al.*, 2010).

To test the hypothesis that dietary iron intake may affect circadian metabolic rhythms, we fed mice chow with various iron concentrations, creating tissue iron levels within the range found from normal variation in human diets. We demonstrate that dietary iron content affects gluconeogenesis and circadian rhythm through modifying hepatic heme levels with concordant changes in Rev-Erbα binding to NCOR. Iron elicits these effects through Peroxisome Proliferator-Activated Receptor Coactivator 1 (PGC-1α)-mediated regulation of the rate-limiting enzyme of heme synthesis in non-erythroid cells, aminolevulinic acid synthase (ALAS1).

Results

Dietary iron affects circadian glucose metabolism

To assess the effects of dietary iron on circadian glucose utilization, we performed glucose tolerance tests (GTTs) at 6-hour intervals in separate cohorts of fasted (6-hour) C57BL/6J male mice fed high (H, 2g iron/kg chow), high normal (HN, 500mg iron/kg chow), or low normal (LN, 35mg iron/kg chow) iron diets for 6 weeks. These levels of dietary iron allowed normal hemoglobin concentrations and red blood cell volumes (hematocrit) to be maintained, but did lead to significant differences in total

liver iron concentraions, with an ~3-fold difference between mice fed the LN compared to H iron diets (Table 4.1). Fasting glucose and area under the glucose curve (AUCg) during glucose tolerance testing varied significantly with time, as has been reported previously (Ben-Dyke *et al.*, 1971; Zimmet *et al.*, 1974). Additionally, glucose values differed among the dietary groups, with significant differences in fasting glucose values at ZT18 and in AUCg at ZT0 and ZT12 (4.S.1A and B).

To elucidate the mechanism behind these differences in glucose, we first measured *ad libitum* circulating insulin levels and saw no variation between the diets that would explain the changes in glucose metabolism (Table 4.1). We next assessed gluconeogenesis because it is a major contributor to serum glucose concentrations, and its dysregulation is seen early in diabetes. We have previously reported that high dietary iron significantly decreases gluconeogenesis (Huang *et al.*, 2013). We validated these data with an *in vivo* measure of gluconeogenesis, the pyruvate tolerance test (PTT), performed at ZT12 when mice normally begin feeding and down regulate gluconeogenesis (Figure 4.1A and B). Mice fed the LN diet exhibited higher levels of blood glucose in response to pyruvate injection compared to mice on the HN or H diets. Variations in glucagon did not account for these differences (Table 4.1). The LN-fed mice weighed 1.8 and 1.2 g more than the HN- and H-fed mice, respectively (Table 4.1). This difference in weight, however, did not account for the differences in PTT as weight and AUCg were not significantly correlated across all individuals (p=.3944, not shown).

We next assessed the transcript levels of gluconeogenic genes in the livers of the mice on the different iron diets. Consistent with the AUCg after pyruvate tolerance testing, the mRNA levels of phosphoenolpyruvate carboxykinase (PEPCK) exhibited a

significantly greater peak in mice on the LN diet when compared to the H- and HN-fed mice (Figure 4.1C). Glucose-6-phosphatase (G6Pase) peak levels trended higher in the LN compared to the H group (Figure 4.1D). For both transcripts, the magnitude of the variation over the 24-hour period is less in the H-fed mice compared to the LN group. The HN group is similar to the H group for PEPCK and to the LN group for G6Pase. Feeding behavior did not differ significantly among these groups (4.S.1C).

Iron alters Rev-Erbα repressor complex formation and activity

Because the parameters of glucose homeostasis exhibited temporal fluctuations that were dependent on dietary iron content, we next examined circadian regulatory factors that are associated with iron. Rev-Erbα is a member of the circadian regulon that directly inhibits PEPCK and G6Pase expression. This repressive activity requires heme for Rev-Erbα to bind NCOR to form the repressor complex (Yin *et al.*, 2007). We assessed complex formation at ZT14, a time when circadian repression of gluconeogenic enzyme expression is beginning to manifest, by performing an immunoprecipitation of Rev-Erbα followed by immunoblotting for NCOR. We observed a direct correlation of complex formation with increased dietary iron (Figure 4.2A and B), consistent with the observed decreases in gluconeogenesis and levels of gluconeogenic enzyme transcripts with higher dietary iron. Complex formation correlated with occupancy at ZT14 of the PEPCK and G6Pase promoters by NCOR, as revealed by chromatin immunoprecipitation (ChIP) (Figure 4.2 C and D). At ZT14, we did not observe variations in Rev-Erbα transcript or proteins between the diets (4.S.2A and B).

Dietary iron alters heme levels and temporal expression of enzymes involved in heme synthesis and degradation

The heme dependence of Rev-Erbα/NCOR repressor complex formation prompted us to measure hepatic heme levels. Mice were maintained on the various iron diets for 9 weeks then sacrificed. Their livers were perfused with PBS to remove red blood cells, and total heme levels were assessed by HPLC (Figure 4.3A and 4.S.3A). A pyridine hemochromagen assay was performed to determine levels of heme b, the form that binds Rev-Erbα (Figure 4.3B and 4.S.3B) (Li *et al.*, 2011). In all three assays, heme was highest in the H-fed mice at ZT12, which was the time at which we observed arise in Rev-Erbα/NCOR complex formation (Figure 4.2B and D). Conversely, at ZT0, heme levels were highest in the LN-fed mice and significantly lower in the HN- and H-fed mice (4.S.3A and 3B)). The net result of these changes is that heme b levels show higher circadian variation in mice fed higher iron diets, as reflected in the ZT12/ZT0 ratios (LN=.778, HN=1.69, and H=3.02). This same pattern of variation was observed in the total heme, and in addition, the LN total heme levels peaked at ZT0 while the HN and H heme levels peaked at ZT12 (not shown). Peak transcript levels of ALAS1 (Figure 4.3E) increase with increased heme at ZT10, and heme oxygenase 1 (HO-1), an enzyme necessary for heme catabolism (4.S.3C), also increased with increasing dietary iron at ZT18.

If ALAS-1-mediated changes in heme levels are driving the changes in Rev-Erbα/NCOR association, we hypothesized that bypassing ALAS-1 should increase heme levels and abrogate the effects of dietary iron on gluconeogenesis. Conversely, inhibiting

heme synthesis should decrease heme levels, likewise limiting the effects of dietary iron but with an opposite effect on gluconeogenesis. Treatment of mice with the product of ALAS1, aminolevulinic acid (ALA) has been shown to increase heme levels in the liver and erythrocytes (Phillips *et al.*, 2000). Mice were therefore fed the LN, HN, and H iron diets for 9 weeks; for the last 3 weeks before harvest, they were concurrently treated with 2mg/mL ALA in their drinking water. No variations in water intake were observed between treated vs control mice (not shown). At the end of this period, we determined heme levels in perfused liver by HPLC. Heme levels increased in all three diets (Figure 4.4A). Heme b levels showed a similar trend (4.S.2). We performed PTTs on the ALA treated and control mice at ZT12; ALA treatment abolished differences between the LN-, HN-, and H-fed mice (Figure 4.4B). ALA treatment also diminished the differences in PEPCK and G6Pase mRNA levels observed in the control mice with the various iron diets (Figure 4.4C and D). In general, the effect of ALA treatment was to decrease the PTT-AUCg and transcript levels in the LN mice toward the levels seen in the mice on the higher iron diets. Furthermore, IP of Rev-Erbα in ALA treated and control livers showed increased NCOR coprecipitation with ALA treatment in all groups (Figure 4.4E). The relative effect of ALA treatment on Rev-Erbα/NCOR complex formation was greatest in the LN mice, while the H-fed mice showed no effect of ALA treatment. The data are consistent with heme synthesis being limiting for circadian rhythmicity on lower iron diets but less so on the higher iron diets.

Isonicotinylhydrazine (isoniazid, INH) inhibits heme synthesis by decreasing pyridoxine, a cofactor for ALAS1. Mice were fed the iron diets for 8 weeks and then treated with INH in their drinking water for 10 days while continuing the iron diets. No

variations in water intake were observed in treated compared to control mice (data not shown). PTT was performed after 5 days of INH treatment, and tissues were harvested after 10 days. The results were the converse of those observed on ALA: The effect of INH was to increase the lower AUCg seen in the HN and H diets to a level resembling that observed in the mice on LN diet (Figure 4.4H). Similar effects were noted for PEPCK and G6Pase transcript levels (Figure 4.4I and J) seen in the HN and H diets up to those observed in the mice on the LN diet, also consistent with the hypothesis that heme is mediating the effects of dietary iron; the effects of inhibiting heme synthesis with INH were less marked in the LN mice who started with lower heme levels than in the HN and H groups that started with higher heme levels. The INH treatment also decreased Rev-Erb□/NCOR complex formation in all of the iron diets, with the greatest relative effect seen in the H group (Figure 4.4K and 4L).

Dietary iron acts directly on the hepatocyte to alter gluconeogenesis

To determine if dietary iron directly affects hepatocyte glucose production as opposed to exerting more indirect (e.g., hormonal) effects, we treated HepG2 cells with ferric ammonium citrate (FAC). Cells were grown for 12 hours in control DMEM or DMEM with 10μM FAC, with or without treatment of ALA or INH. We then set a circadian rhythm in the cells with 100nM dexamethasone (DXS) shock (Balsilobre *et al*., 2000). The results were concordant with *in vivo* results. At the peak expression of PEPCK and G6Pase, non-iron-treated cells exhibited a greater PEPCK and G6Pase expression compared to the FAC treated cells (Figure 4.5A and B). These differences were largely ablated with ALA or INH treatment of the cells. ALA treatment brings

PEPCK and G6Pase transcript levels down in non-iron-treated cells, close to those observed in the FAC-treated cells (Figure 4.5A and B, left panels). Conversely, INH increases transcript levels in the FAC treated cells, close to those observed in non-iron-treated cells (Figure 4.5A and B). During the peak times, we also assessed NCOR association with Rev-Erbα through a coimmunoprecipitation and were able to recapitulate the trends observed in the animals: FAC treatment increased association of NCOR and Rev-Erbα (Figure 4.5C and D, middle panel). ALA treatment increased complex formation to levels seen in the FAC-treated cells, while INH treatment decreased association to levels seen in the non-iron-treated cells (Figure 4.5C and 5D).

Variations in heme synthesis are due to differences in PGC-1α expression related to altered oxidative signaling in mice on the different iron diets

PGC-1α regulation of ALAS1 transcription (Estall *et al.*, 2009) led us to explore its possible regulation by iron to explain the differences in heme synthesis between the iron diets. In mice, both PGC-1α transcript and protein levels increased with increasing dietary iron (Figure 4.6A-C). In HepG2 cells, partial silencing of PGC-1α by siRNA treatment (Figure 4.6D) ablated the differences in ALAS1, PEPCK, and G6Pase that occurred with FAC treatment (Figure 4.6E, 6F, and 6G).

PGC-1α is up regulated by reactive oxygen species (ROS) (Wu *et al.*, 1999; Lin *et al.*, 2005; Marmolino *et al.*, 2010), and iron is known to create ROS through fenton chemistry. Therefore, we explored oxidative signaling as a mechanism through which dietary iron up regulates PGC-1α. Cellular oxidative markers differed temporally among the diets, with lower GSH levels (Figure 4.7A) and NADPH/NADP+ ratios (Figure 4.7B)

in the H fed mice. To blunt differences in oxidant levels among mice on the iron diets, we treated them with the antioxidant N-acetylcysteine (NAC). Mice began their respective iron diets at 3 months of age and remained on the diets for 9 weeks, at which time they were split into a control and NAC treated group. The NAC treatment was administered in the drinking water of the animals for 10 days at levels of 40mM. No variation in water intake was observed between the treated group and control (not shown). The livers of the mice were harvested at ZT12. NAC treatment abolished differences in PGC-1α, PEPCK, G6Pase, ALAS1, GSH, and NADPH/NADP+ ratios between the diets (Figure 4.7C-7H).

Discussion

Iron is a risk factor for several parameters of metabolic syndrome. For example, a high serum ferritin level, a marker of tissue iron stores, is associated with insulin resistance and type 2 diabetes (Ford and Cogswell, 1999; Forouhi *et al.,* 2007). Likewise, high iron is associated with gestational diabetes, high triglyceride levels, steatohepatitis, and cardiovascular risk (Kiechl *et al.*, 1994; Tuomainen *et al.*, 1998; Qui *et al.*, 2011; Kim *et al.*, 2013). Another hallmark of metabolic syndrome, obesity, is more prevalent in individuals with iron deficiency, although there is conflicting evidence as to whether this is related to low iron causing obesity or obesity causing decreased iron absorption (Pinhas-Hamiel *et al.*, 2003; Sonnweber *et al.*, 2012). This relationship between iron and metabolic syndrome highlights the role of iron as both a structural component of proteins involved in fuel metabolism and bioenergetics, and as a cellular regulator of metabolic pathways such as adiponectin transcription and AMPK activity (Gabrielsen *et al.,* 2012; Huang *et al*., 2013). We show herein yet another role of iron in metabolism, namely that dietary iron affects the circadian rhythm of hepatic gluconeogenesis by altering heme

synthesis that in turn affects the activity of a key component of the circadian machinery, Rev-Erbα.

Besides being a crucial component of the circadian clock, Rev-Erbα regulates many aspects of glucose and lipid metabolism, including acting as a negative transcriptional regulator of gluconeogenic enzymes. Decreased Rev-Erbα expression is associated with hyperglycemia and obesity in mice and humans (Yin *et al.,* 2007; Cho *et al.*, 2012; Delezie *et al.*, 2012; Goumidi *et al.*, 2012). Previous work has shown that Rev-Erbα activity is dependent on the formation of a repressor complex with NCOR, which requires heme (Yin *et al.*, 2007). We verified the dependence of this complex formation on heme availability, and further showed that liver heme levels are increased in a circadian fashion with increased dietary iron. The results demonstrate that heme availability is altered by dietary iron and is a regulating factor in the circadian rhythm of hepatic gluconeogenesis. While heme is known to be required for Rev-Erbα/NCOR complex formation, the observations that heme availability is limiting for that process in normal physiologic circumstances has not been previously shown.

The changes in heme levels observed with increased dietary iron are not due to limiting amounts of iron for metalation of heme but rather by the regulation of heme synthesis by ALAS1. This is revealed by the facts that bypassing ALAS1 with ALA, or inhibiting heme synthesis by INH, abrogated the effects of dietary iron. If iron itself were limiting in the LN diet, for example, ALA would not be able to increase heme-dependent formation of the Rev-Erbα/NCOR complex in mice on that diet. Furthermore, mice on the lower levels of dietary iron show no evidence of systemic iron deficiency, in that they have normal red blood cell counts and blood hemoglobin levels and breed normally

(Table 4.1). ALAS-1 itself exhibits a circadian rhythm controlled by PGC-1α and its binding partners NRF-1 or FOXO1 (Handschin *et al.*, 2005). We confirmed this circadian rhythmicity in the current study and show that the magnitude of its excursions is significantly altered by dietary iron. The regulation of ALAS1 is not mediated directly by iron responsive proteins, as it is for the erythroid form of the enzyme ALAS2 (Ajioka *et al.*, 2006). Rather, iron drives increased PGC-1α expression that in turn transcriptionally activates ALAS-1. This was demonstrated by the fact that the effects of iron on ALAS-1, PEPCK, and G6Pase were not seen after knockdown of PGC-1α.

A decrease in PGC-1α transcript and protein levels in the skeletal muscle of rats fed iron deficient diet has been previously observed, although the mechanism of this change was not determined (Han *et al.*, 2011). We demonstrate that iron regulation of PGC-1α occurs at least in part through oxidant sensing pathways. Mice on the higher iron diets show evidence of changes in intracellular redox state as revealed by decreased GSH and decreased NADPH/NADP ratios. Treatment of mice with the antioxidant N-acetyl cysteine eliminated the variation seen in PGC-1α, ALAS-1, PEPCK, and G6Pase among the different iron diets. The levels of GSH and NADPH/NADP ratio significantly varied between the iron diets at specific time points, and treatment with NAC ablated the differences between the groups. These data suggest that dietary iron is acting through ROS to exert effects upon heme synthesis and subsequently gluconeogenesis. Recent research has focused on ROS not solely as potentially damaging or toxic entities, but also as an intracellular signaling pathway by which the bioenergetic and metabolic status of the cell is sensed for purposes of altering processes such as fuel choice, stress response, mitophagy, and cell cycle regulation (Ray *et al.*, 2012; Tormos *et al.*, 2011).

Average PEPCK and G6Pase transcript levels are greater in mice fed the LN iron diet compared to the H-fed group. The levels of G6Pase transcripts in the HN mice, however, are similar to those of the LN mice, while the levels of PEPCK in the HN mice are similar to the H-fed mice (Figure 1E and 1F). This variation in response to iron may be due to other signaling pathways: Differential regulation of PEPCK and G6Pase, for example, is also signaled by insulin and by the forkhead transcription factors (Barthel and Schmoll, 2003). Thus, the variation in these responses, in the differences of PEPCK and G6Pase promoter occupancy seen in the ChIP assays, and in the incomplete effects of ALA and INH treatments on heme and levels and gluconeogenic transcripts (Figures 4.3 and 4.4) highlight the fact that the regulation of gluconeogenesis is multifactorial, complex, and responsive to many influences beyond iron and oxidative stress.

We chose the specific levels of iron in the diets employed in this study for several reasons. The LN diet is derived from the dietary recommendations of the American Institute of Nutrition as specified in their AIN93G diet, which has levels of iron and other nutrients that are sufficient for normal growth, pregnancy, and lactation (Reeves *et al.*, 1993). This diet is commonly used as the normal chow in laboratories that investigate the effects of iron on physiology and development (Jang *et al.,* 2000; Reeves *et al*., 2004; Nam and Knutson, 2012). The level of iron in the HN diet is based on other "normal" diets commonly used in animal facilities, with batches of these diets ranging in iron content from 300mg/kg to 600mg/kg (Committee on animal nutrition, 1995). The H diet was selected because the mice have liver iron stores that are only modestly increased above that seen on the "normal" chows, namely 2-fold (Table 4.1). This is within the 4–fold range seen in hepatic iron among humans without specific iron-related pathology

(Milman *et al.*, 1986; Catiella *et al*., 2012). Serum ferritin, the most commonly used measure of tissue iron stores, varies over a range of ~15-fold in normal humans (Koziol *et al.*, 2001). Thus, our results demonstrate that iron exerts regulatory influences on metabolism even within its "normal" range.

Previous work on iron and metabolism has concentrated on pathologic iron overload. Hereditary hemochromatosis and β-thalassemia, for example, have long been known to be associated with type 2 diabetes (Brittenham *et al.,* 1994; Cooksey *et al*., 2004; Hatunic *et al.*, 2010). More recently, however, it has become clear that increased diabetes risk is also seen with more modest levels of iron excess such as are seen in normal individuals with higher levels of dietary iron intake or in those taking iron supplements (Jiang *et al.,* 2004; Bowers *et al.*, 2011; Qui *et al.*, 2011). On the surface, this correlation of high iron with increased diabetes risk appears contradictory to our results of high iron being associated with improved glucose tolerance and hepatic glucose production. However, type 2 diabetes is a multifactorial disease involving insulin resistance (most often related to obesity), insulin deficiency, and metabolic abnormalities in multiple tissues. Thus, prodiabetic effects of iron on insulin production and adipokines may over time overwhelm other apparently antidiabetic effects such as those observed on hepatic gluconeogenesis (Jouhani *et al.*, 2008; Gabrielsen *et al.*, 2012). It is also possible, however, that the increased magnitude of circadian variation in hepatic gluconeogenesis seen in the high iron fed mice could be prodiabetic under certain circumstances. For example, in situations of nightshift work, sleep disturbance, or snacking during the night, all of which are associated with increased diabetes risk (Huang *et al.*, 2011; Hatori *et al.,*

2012), it might be expected that individuals with higher iron would suffer greater dyssynchrony and disruption of normal metabolic regulation.

Besides its effects on ROS and heme availability, the effects of iron on metabolism are likely to be widespread and not explained by a single mechanism. We have previously shown, for example, regulation of insulin production, adiponectin, and AMP-dependent kinase by iron (Jouihan *et al.,* 2008; Gabrielsen *et al.* 2012; Huang *et al.,* 2013). The current studies suggest yet other possible effects of iron. In the INH treated mice, for example, even with complete ablation of the differences in heme levels in mice on the three diets, there were still differences noted in the Rev-Erbα repressor complex formation. This suggests that there may be factors other than heme by which iron alters Rev-Erbα/NCOR complex formation. The drosophila Rev-Erbα homologue E75 is regulated by nitric oxide (NO) (Cáceres et al., 2011), and transcript levels of nitric oxide synthase, the rate-limiting enzyme in NO synthesis, were increased with increasing dietary iron at certain time points (not shown). Further, the redox state of thiols within the heme-binding pocket of proteins such as Rev-Erbα also regulates heme binding (Ragsdale and Gupta, 2011; Shimizu, 2012). Therefore, the altered redox state of the cells seen in the various iron diets may also play a role in heme binding to Rev-Erbα. Finally, the activities of other heme-binding proteins such as Rev-Erbβ, another member of the Rev-ErbA family of transcription factors, are also likely to be altered by dietary iron. Thus, future studies to assess these pathways are justified, as are the effects of iron on other metabolic pathways such as lipid synthesis and in other tissues.

Although our work has focused on one metabolic process, hepatic gluconeogenesis in mammals, the effects of iron on circadian rhythms are also seen in

plants (Chen *et al.*, 2013) and insects (Mandilaras and Missirlis, 2012), and they are manifest in multiple organ systems and tissues, including the central clock of the SCN. Iron deficiency in mice, for example, alters thermoregulation, behavior, and monoamine metabolism and dopamine transporter expression in the central nervous system (Youdim *et al.,* 1981; Bianco *et al.*, 2009). Furthermore, knockdown of the drosophila homologue of ferritin in circadian neurons disrupts the molecular components of the central clock (Mandilaras and Missirlis, 2012). Other studies have shown that heme synthesis by the liver is capable of affecting pineal gland secretion of melatonin, suggesting that dietary iron will have further, perhaps sweeping, effects on physiology beyond that of hepatic control of gluconeogenesis (Puy *et al.,* 1996).

In summary, we have demonstrated that one mechanism through which dietary iron is able to regulate the core molecular clock in the liver is through regulation of heme synthesis. This novel role of iron provides another mechanism through which iron acts to regulate glucose metabolism. The studies suggest mechanisms that may underlie the interplay among iron, altered circadian rhythms, metabolic regulation, and diabetes risk.

Materials and methods

Animal studies

Three-month-old male C57BL6/J mice were fed diets of 35 mg/kg, 500 mg/kg, or 2 g/kg carbonyl iron (Harlan Teklad Madison, WI) for 6 weeks before *in vivo* physiological testing and 9 weeks before sacrifice. The animals were maintained on a 12-hour light/dark cycle. Treatment of mice was with 2mg/mL ALA (Frontier Scientific #A167), 1mg/mL INH (Sigma Aldrich #I3377), or 6.5mg/mL NAC (Sigma Aldrich

#A9165) in their drinking water and adjusted to pH 7. ALA treatment began after 6 weeks on diet and continued for 3 weeks concurrent with continued time on diet. Mice were treated with NAC or INH for 10 days after 8 weeks on diet. Prior to GTT, mice were fasted for 6 hours and then challenged with 1mg glucose per gram body weight through IP injection. Mice were not fasted prior to PTT because fasting has been shown to modulate circadian control of hepatic gluconeogenesis. For PTT, mice were challenged with 2mg pyruvate per gram body weight through IP injection. Procedures were approved by the Institutional Animal Care and Use Committee of the University of Utah and the Veterans Administration.

Cell culture

HepG2 cells (ATCC) were maintained in Dulbecco's Modified Eagle Medium: Nutrient Mixture F-12 supplemented (DMEM/F12) with 10% fetal bovine serum and 1% primocin. The cells were plated on 6 well plates overnight and then treated with 10μM FAC, 2mM ALA, 1mM INH or a PBS no treatment control for 12 hours. After the drug or iron treatment, the plate was synchronized with a 100nM dexamethasone (DXS) shock for 1-hour; after this time, the media was removed, the cells washed with PBS 2x, and DMEM/F12 with treatment was replaced. Cells were harvested at 4-hour intervals from the time of shock for 48 hours. Knockdown of PGC-1α was accomplished by PGC-1α siRNA from Santa Cruz Biotech (sc-38885), following the company's general protocol with control siRNA (sc-37007) and transfection reagent (sc-29528).

RT-PCR

RNA was isolated from liver samples using RNeasy Mini Kit (Qiagen) and bead mill tubes with 1.44mm ceramic beads; cDNA synthesis was performed with superscript III first-strand synthesis system (Invitrogen). Measurement of both RNA and cDNA was performed by nanodrop (EPOCH), and quantification of cDNA was performed by real-time PCR analysis using the Power SYBR Green Master Mix (Applied Biosciences). Primers were designed using the NIH facilitated Mouse Primer Depot (Simcox, 2009-2014 http://mouseprimerdepot.nci.nih.gov/).

Western blotting

Antibodies used included Rev-Erbα (Santa Cruz Biotechnologies Inc.), NCOR, β-actin (Cell Signaling), and PGC-1α (Abcam). The Criterion running and transfer system with precast gels was used (BioRad).

Heme measurement

Heme was measured by pyridine hemochrome spectrophotometric assay and HPLC as described (Sinclair *et al.*, 1999). In the pyridine hemochrome assay, heme was extracted from tissue samples with 500mM NaOH and samples were normalized to protein concentrations and brought up to 600µL volume after which pyridine was added to make a 40% solution. Initial wave scans were performed from 450 to 620nm using an Ultrospec 3000 spectrophotometer; this was repeated after addition of 1M potassium ferricyanide and sodium dithionite crystals. Data were collected with Biochrom DC software and analyzed using published extinction coefficients (Trumpower and Berry, 1987). For reverse phase HPLC measurements, liver samples were homogenized in

Acetone acidified with 2.5% HCl, filtered (0.45uM) and HPLC measurements performed on a Waters 2690 pump with C18 reverse phase column (39X300mm Waters μBondapak) and C18 precolumn (Water 2690; Water 996 phospho-diode array detector). Samples (0.125ul) were eluted over a 15-minute period using a linear gradient of 60% buffer A (.56mM NH4H2PO4, ph 7.0) to 100 % buffer B (100% Methanol), visualized with a Waters 996 phospho diode array detector at 400nm and quantified with external standards.

ChIP

ChIP studies were performed as previously described using the Simple ChIP kit with company modifications for tissue samples (Cell Signaling Technology; Gabrielsen *et al*., 2012). Liver samples were homogenized in bead mill tubes with 1.44mm ceramic beads and then cross-linked for 20 minutes with 1% formaldehyde, the crosslinking was stopped with glycine, and the lysates were sonicated 3x for 20 seconds using a sonic dismembrator (Fisher Scientific). Lysates were precleared with salmon sperm blocked protein A/G agarose beads (Millipore). Each sample IP was performed in duplicate. NCOR, Igg, or Histone H3 antibody (Cell signaling) was applied for 1 hour at room temperature. DNA was released from protein-DNA complexes by proteinase K digestion and quantified by real-time PCR for the enrichment at the PEPCK and G6Pase promoter as well as using GAPDH and the PEPCK gene as negative controls using the Power SYBR Green Master Mix (Applied Biosciences; Yin *et al.*, 2007). Occupancy was quantified to standard control and normalized to input control.

Coimmunoprecipitation

Liver protein lysates isolated in a standard HEPES lysis buffer were precleared with Protein A/G PLUS-Agarose beads (Santa Cruz Biotechnical Inc.). Rev-Erbα antibody (Santa Cruz Biotechnical Inc.) or a negative control Igg (Cell signaling) in 1x PBS was incubated with end over end mixing for 4 hours at 4˚C with Protein A/G PLUS-Agarose beads. The beads were washed 5x with PBSCM (PBS buffer (100 mM sodium phosphate, 150 mM NaCl, pH 7.2) with 1 mM CaCl2 + 1 mM MgCl2). The protein lysate samples were then incubated with the beads overnight. Following protein incubation, the beads were washed 5x with PBSCM and then samples were eluted with sample loading buffer and incubation at 100˚C for 5 minutes.

Metabolite measurement

This procedure was done as previously described (Huang *et al.*, 2013). Briefly, 20mg of freeze clamped tissue was homogenized in bead mill tubes containing 500µL of cold 90% MeOH containing internal standards. After a 20,000xg centrifugation, the supernatant was collected and a second extraction step was performed on the pellet with a cold 60% MeOH solution. The supernatants were combined and vacuum dried. Two Shimadzu LC10AD VP pumps and a CTO-10AS column oven were used for HPLC separation. Detection was accomplished using a PE Sciex 365 triple quadrupole mass spectrometer modified with an Ionics EP10+ source. Samples were reconstituted with the addition of 48 uL of 10 mM sodium phosphate buffer (pH 7.0) followed by 2 µL of 2-vinylpyridine, and after a 30-minute room temperature incubation, 50 µL of 20 mM ammonium formate buffer pH 9.2 containing 7.5 mM N-butyl amine was added. After centrifuging at 20,000xg for 5 minutes, twenty µL of each sample was injected onto a

Phenomenex (Torrance, CA) Gemini-NX C18 (150x3mm; 3 um particle size, 110A pore size) fitted with a Phenomenex security guard precolumn. Data were recorded using Analyst 1.4.2 software with final peak heights recorded in Excel. Data were normalized to weight and internal standard.

Statistics

Statistics were done using JMP pro statistical package using ANOVA with a Tukey-Kramer post hoc analysis to determine differences between groups. Results are presented as the mean ± the standard error of the mean.

References

Airola, M.V., Du, J., Dawson, J.H., and Crane, B.R. (2010). Heme binding to the Mammalian circadian clock protein period 2 is nonspecific. Biochemistry 49, 4327-4338.

Ajioka, R.S., Phillips, J.D., and Kushner, J.P. (2006). Biosynthesis of heme in mammals. Biochim Biophys Acta 1763, 723-736.

Anderson, C.P., Shen, M., Eisenstein, R.S., and Leibold, E.A. (2012). Mammalian iron metabolism and its control by iron regulatory proteins. Biochim Biophys Acta.

Balsalobre, A., Brown, S.A., Marcacci, L., Tronche, F., Kellendonk, C., Reichardt, H.M., Schutz, G., and Schibler, U. (2000). Resetting of circadian time in peripheral tissues by glucocorticoid signaling. Science 289, 2344-2347.

Ben-Dyke, R. (1971). Diurnal variation of oral glucose tolerance in volunteers and laboratory animals. Diabetologia 7, 156-159.

Berry, E.A., and Trumpower, B.L. (1987). Simultaneous determination of hemes a, b, and c from pyridine hemochrome spectra. Anal Biochem 161, 1-15.

Bianco, L.E., Unger, E.L., Earley, C.J., and Beard, J.L. (2009). Iron deficiency alters the day-night variation in monoamine levels in mice. Chronobiology international 26, 447-463.

Bowers, K., Yeung, E., Williams, M.A., Qi, L., Tobias, D.K., Hu, F.B., and Zhang, C. (2011). A prospective study of prepregnancy dietary iron intake and risk for gestational diabetes mellitus. Diabetes Care 34, 1557-1563.

Buhr, E.D., Yoo, S.H., and Takahashi, J.S. (2010). Temperature as a universal resetting cue for mammalian circadian oscillators. Science 330, 379-385.

Cable, E.E., Miller, T.G., and Isom, H.C. (2000). Regulation of heme metabolism in rat hepatocytes and hepatocyte cell lines: delta-aminolevulinic acid synthase and heme oxygenase are regulated by different heme-dependent mechanisms. Arch Biochem Biophys 384, 280-295.

Caceres, L., Necakov, A.S., Schwartz, C., Kimber, S., Roberts, I.J., and Krause, H.M. (2011). Nitric oxide coordinates metabolism, growth, and development via the nuclear receptor E75. Genes Dev 25, 1476-1485.

Castiella, A., Alustiza, J.M., Zapata, E., Emparanza, J.I., Otazua, P., Zubiaurre, L., and Aguirre, A. (2012). Mild hepatic iron overload in dysmetabolic hyperferritinemia: MRI may overestimate the liver iron concentration values. Annals of hematology 91, 961.

Chalmers, J.G. (1965). The Effect of Isoniazid on the Clearance of Pyruvic and Alpha-Oxoglutaric Acids in the Urine of Mice, Meriones Lybicus and Rats. British journal of cancer 19, 430-432.

Chen, Y.Y., Wang, Y., Shin, L.J., Wu, J.F., Shanmugam, V., Tsednee, M., Lo, J.C., Chen, C.C., Wu, S.H., and Yeh, K.C. (2013). Iron is involved in the maintenance of circadian period length in Arabidopsis. Plant physiology 161, 1409-1420.

Cho, H., Zhao, X., Hatori, M., Yu, R.T., Barish, G.D., Lam, M.T., Chong, L.W., DiTacchio, L., Atkins, A.R., Glass, C.K., Liddle, C., Auwerx, J., Downes, M., Panda, S., and Evans, R.M. (2012). Regulation of circadian behaviour and metabolism by REV-ERB-alpha and REV-ERB-beta. Nature 485, 123-127.

Cooksey, R.C., Jouihan, H.A., Ajioka, R.S., Hazel, M.W., Jones, D.L., Kushner, J.P., and McClain, D.A. (2004). Oxidative stress, beta-cell apoptosis, and decreased insulin secretory capacity in mouse models of hemochromatosis. Endocrinology 145, 5305-5312.

Damiola, F., Le Minh, N., Preitner, N., Kornmann, B., Fleury-Olela, F., and Schibler, U. (2000). Restricted feeding uncouples circadian oscillators in peripheral tissues from the central pacemaker in the suprachiasmatic nucleus. Genes Dev 14, 2950-2961.

Delezie, J., Dumont, S., Dardente, H., Oudart, H., Grechez-Cassiau, A., Klosen, P., Teboul, M., Delaunay, F., Pevet, P., and Challet, E. (2012). The nuclear receptor REV-ERBalpha is required for the daily balance of carbohydrate and lipid metabolism. Faseb J 26, 3321-3335.

Estall, J.L., Ruas, J.L., Choi, C.S., Laznik, D., Badman, M., Maratos-Flier, E., Shulman, G.I., and Spiegelman, B.M. (2009). PGC-1alpha negatively regulates hepatic FGF21 expression by modulating the heme/Rev-Erb(alpha) axis. Proc Natl Acad Sci U S A 106, 22510-22515.

Fan, W., Imamura, T., Sonoda, N., Sears, D.D., Patsouris, D., Kim, J.J., and Olefsky, J.M. (2009). FOXO1 transrepresses peroxisome proliferator-activated receptor gamma transactivation, coordinating an insulin-induced feed-forward response in adipocytes. J Biol Chem 284, 12188-12197.

Fernandez-Real, J.M., Lopez-Bermejo, A., and Ricart, W. (2002). Cross-talk between iron metabolism and diabetes. Diabetes 51, 2348-2354.

Ford, E.S., and Cogswell, M.E. (1999). Diabetes and serum ferritin concentration among U.S. adults. Diabetes Care 22, 1978-1983.

Forouhi, N.G., Harding, A.H., Allison, M., Sandhu, M.S., Welch, A., Luben, R., Bingham, S., Khaw, K.T., and Wareham, N.J. (2007). Elevated serum ferritin levels predict new-onset type 2 diabetes: results from the EPIC-Norfolk prospective study. Diabetologia 50, 949-956.

Gabrielsen, J.S., Gao, Y., Simcox, J.A., Huang, J., Thorup, D., Jones, D., Cooksey, R.C., Gabrielsen, D., Adams, T.D., Hunt, S.C., Hopkins, P.N., Cefalu, W.T., and McClain, D.A. (2012). Adipocyte iron regulates adiponectin and insulin sensitivity. J Clin Invest.

Goumidi, L., Grechez, A., Dumont, J., Cottel, D., Kafatos, A., Moreno, L.A., Molnar, D., Moschonis, G., Gottrand, F., Huybrechts, I., Dallongeville, J., Amouyel, P., Delaunay, F., and Meirhaeghe, A. (2013). Impact of REV-ERB alpha gene polymorphisms on obesity phenotypes in adult and adolescent samples. Int J Obes (Lond) 37, 666-672.

Gupta, N., and Ragsdale, S.W. (2011). Thiol-disulfide redox dependence of heme binding and heme ligand switching in nuclear hormone receptor rev-erb{beta}. J Biol Chem 286, 4392-4403.

Han, D.H., Hancock, C.R., Jung, S.R., Higashida, K., Kim, S.H., and Holloszy, J.O. (2011). Deficiency of the mitochondrial electron transport chain in muscle does not cause insulin resistance. PloS one 6, e19739.

Handschin, C., Lin, J., Rhee, J., Peyer, A.K., Chin, S., Wu, P.H., Meyer, U.A., and Spiegelman, B.M. (2005). Nutritional regulation of hepatic heme biosynthesis and porphyria through PGC-1alpha. Cell 122, 505-515.

Hatori, M., Vollmers, C., Zarrinpar, A., DiTacchio, L., Bushong, E.A., Gill, S., Leblanc, M., Chaix, A., Joens, M., Fitzpatrick, J.A., Ellisman, M.H., and Panda, S. (2012). Time-restricted feeding without reducing caloric intake prevents metabolic diseases in mice fed a high-fat diet. Cell Metab 15, 848-860.

Hatunic, M., Finucane, F.M., Brennan, A.M., Norris, S., Pacini, G., and Nolan, J.J. (2010). Effect of iron overload on glucose metabolism in patients with hereditary hemochromatosis. Metabolism 59, 380-384.

Huang, J., Jones, D., Luo, B., Sanderson, M., Soto, J., Abel, E.D., Cooksey, R.C., and McClain, D.A. (2011a). Iron overload and diabetes risk: a shift from glucose to Fatty

Acid oxidation and increased hepatic glucose production in a mouse model of hereditary hemochromatosis. Diabetes 60, 80-87.

Huang, J., Simcox, J., Mitchell, T.C., Jones, D., Cox, J., Luo, B., Cooksey, R.C., Boros, L.G., and McClain, D.A. (2013). Iron regulates glucose homeostasis in liver and muscle via AMP-activated protein kinase in mice. Faseb J.

Huang, W., Ramsey, K.M., Marcheva, B., and Bass, J. (2011b). Circadian rhythms, sleep, and metabolism. J Clin Invest 121, 2133-2141.

Jiang, R., Manson, J.E., Meigs, J.B., Ma, J., Rifai, N., and Hu, F.B. (2004). Body iron stores in relation to risk of type 2 diabetes in apparently healthy women. Jama 291, 711-717.

Jouihan HA, C.P., Cooksey RC, Hoagland EA, Boudina S, Abel ED, Winge DR, McClain DA (2008). Iron-mediated inhibition of mitochondrial manganese uptake mediates mitochondrial dysfunction in a mouse model of hemochromatosis. Mol Med 14, 98-108.

Kaasik, K., and Lee, C.C. (2004). Reciprocal regulation of haem biosynthesis and the circadian clock in mammals. Nature 430, 467-471.

Kiechl, S., Aichner, F., Gerstenbrand, F., Egger, G., Mair, A., Rungger, G., Spogler, F., Jarosch, E., Oberhollenzer, F., and Willeit, J. (1994). Body iron stores and presence of carotid atherosclerosis. Results from the Bruneck Study. Arteriosclerosis and thrombosis : a journal of vascular biology / American Heart Association 14, 1625-1630.

Kim, J., Jia, X., Buckett, P.D., Liu, S., Lee, C.H., and Wessling-Resnick, M. (2013). Iron loading impairs lipoprotein lipase activity and promotes hypertriglyceridemia. Faseb J 27, 1657-1663.

Kitanishi, K., Igarashi, J., Hayasaka, K., Hikage, N., Saiful, I., Yamauchi, S., Uchida, T., Ishimori, K., and Shimizu, T. (2008). Heme-binding characteristics of the isolated PAS-A domain of mouse Per2, a transcriptional regulatory factor associated with circadian rhythms. Biochemistry 47, 6157-6168.

Koziol, J.A., Ho, N.J., Felitti, V.J., and Beutler, E. (2001). Reference centiles for serum ferritin and percentage of transferrin saturation, with application to mutations of the HFE gene. Clinical chemistry 47, 1804-1810.

Lazzarino, G., Nuutinen, M., Tavazzi, B., Di Pierro, D., and Giardina, B. (1989). A method for preparing freeze-clamped tissue samples for metabolite analyses. Anal Biochem 181, 239-241.

Liang, H., and Ward, W.F. (2006). PGC-1alpha: a key regulator of energy metabolism. Advances in physiology education 30, 145-151.

Lin, J.D. (2009). Minireview: the PGC-1 coactivator networks: chromatin-remodeling and mitochondrial energy metabolism. Mol Endocrinol 23, 2-10.

Lukat-Rodgers, G.S., Correia, C., Botuyan, M.V., Mer, G., and Rodgers, K.R. (2010). Heme-based sensing by the mammalian circadian protein CLOCK. Inorganic chemistry 49, 6349-6365.

Mandilaras, K., and Missirlis, F. (2012). Genes for iron metabolism influence circadian rhythms in Drosophila melanogaster. Metallomics : integrated biometal science 4, 928-936.

Marmolino, D., Manto, M., Acquaviva, F., Vergara, P., Ravella, A., Monticelli, A., and Pandolfo, M. (2010). PGC-1alpha down-regulation affects the antioxidant response in Friedreich's ataxia. PloS one 5, e10025.

McClain, D., Abraham, D., Rogers, J., Brady, R., Gault, P., Ajioka, R., and Kushner, J. (2006). High prevalence of abnormal glucose homeostasis secondary to decreased insulin secretion in individuals with hereditary haemochromatosis. Diabetologia 49, 1661-1669.

Milman, N., Graudal, N., Hegnhoj, J., Christoffersen, P., and Pedersen, N.S. (1994). Relationships among serum iron status markers, chemical and histochemical liver iron content in 117 patients with alcoholic and non-alcoholic hepatic disease. Hepato-gastroenterology 41, 20-24.

Olivieri, N.F., Brittenham, G.M., McLaren, C.E., Templeton, D.M., Cameron, R.G., McClelland, R.A., Burt, A.D., and Fleming, K.A. (1998). Long-term safety and effectiveness of iron-chelation therapy with deferiprone for thalassemia major. N Engl J Med 339, 417-423.

Phillips, J.D., Jackson, L.K., Bunting, M., Franklin, M.R., Thomas, K.R., Levy, J.E., Andrews, N.C., and Kushner, J.P. (2001). A mouse model of familial porphyria cutanea tarda. Proc Natl Acad Sci U S A 98, 259-264.

Pinhas-Hamiel, O., Newfield, R.S., Koren, I., Agmon, A., Lilos, P., and Phillip, M. (2003). Greater prevalence of iron deficiency in overweight and obese children and adolescents. Int J Obes Relat Metab Disord 27, 416-418.

Potts-Kant, E.N., Li, Z., Tighe, R.M., Lindsey, J.Y., Frush, B.W., Foster, W.M., and Hollingsworth, J.W. (2012). NAD(P)H:quinone oxidoreductase 1 protects lungs from oxidant-induced emphysema in mice. Free radical biology & medicine 52, 705-715.

Puigserver, P., and Spiegelman, B.M. (2003). Peroxisome proliferator-activated receptor-gamma coactivator 1 alpha (PGC-1 alpha): transcriptional coactivator and metabolic regulator. Endocr Rev 24, 78-90.

Puy, H., Deybach, J.C., Bogdan, A., Callebert, J., Baumgartner, M., Voisin, P., Nordmann, Y., and Touitou, Y. (1996). Increased delta aminolevulinic acid and

decreased pineal melatonin production. A common event in acute porphyria studies in the rat. J Clin Invest 97, 104-110.

Qiu, C., Zhang, C., Gelaye, B., Enquobahrie, D.A., Frederick, I.O., and Williams, M.A. (2011). Gestational diabetes mellitus in relation to maternal dietary heme iron and nonheme iron intake. Diabetes Care 34, 1564-1569.

Raghuram, S., Stayrook, K.R., Huang, P., Rogers, P.M., Nosie, A.K., McClure, D.B., Burris, L.L., Khorasanizadeh, S., Burris, T.P., and Rastinejad, F. (2007). Identification of heme as the ligand for the orphan nuclear receptors REV-ERBalpha and REV-ERBbeta. Nature structural & molecular biology 14, 1207-1213.

Ray, P.D., Huang, B.W., and Tsuji, Y. (2012). Reactive oxygen species (ROS) homeostasis and redox regulation in cellular signaling. Cellular signalling 24, 981-990.

Reeves, P.G., Nielsen, F.H., and Fahey, G.C., Jr. (1993). AIN-93 purified diets for laboratory rodents: final report of the American Institute of Nutrition ad hoc writing committee on the reformulation of the AIN-76A rodent diet. J Nutr 123, 1939-1951.

Rhee, J., Inoue, Y., Yoon, J.C., Puigserver, P., Fan, M., Gonzalez, F.J., and Spiegelman, B.M. (2003). Regulation of hepatic fasting response by PPARgamma coactivator-1alpha (PGC-1): requirement for hepatocyte nuclear factor 4alpha in gluconeogenesis. Proc Natl Acad Sci U S A 100, 4012-4017.

Shimizu, T. (2012). Binding of cysteine thiolate to the Fe(III) heme complex is critical for the function of heme sensor proteins. Journal of inorganic biochemistry 108, 171-177.

Simcox, J.A., and McClain, D.A. (2013). Iron and diabetes risk. Cell Metab 17, 329-341.

Sinclair, P.R., Gorman, N., and Jacobs, J.M. (2001). Measurement of heme concentration. Curr Protoc Toxicol Chapter 8, Unit 8 3.

Sonnweber, T., Ress, C., Nairz, M., Theurl, I., Schroll, A., Murphy, A.T., Wroblewski, V., Witcher, D.R., Moser, P., Ebenbichler, C.F., Kaser, S., and Weiss, G. (2012). High-fat diet causes iron deficiency via hepcidin-independent reduction of duodenal iron absorption. J Nutr Biochem.

Stokkan, K.A., Yamazaki, S., Tei, H., Sakaki, Y., and Menaker, M. (2001). Entrainment of the circadian clock in the liver by feeding. Science 291, 490-493.

Tormos, K.V., Anso, E., Hamanaka, R.B., Eisenbart, J., Joseph, J., Kalyanaraman, B., and Chandel, N.S. (2011). Mitochondrial complex III ROS regulate adipocyte differentiation. Cell Metab 14, 537-544.

Torrance, J.D., and Bothwell, T.H. (1968). A simple technique for measuring storage iron concentrations in formalinised liver samples. The South African journal of medical sciences 33, 9-11.

Tuomainen, T.P., Punnonen, K., Nyyssonen, K., and Salonen, J.T. (1998). Association between body iron stores and the risk of acute myocardial infarction in men. Circulation 97, 1461-1466.

Wu, Z., Puigserver, P., Andersson, U., Zhang, C., Adelmant, G., Mootha, V., Troy, A., Cinti, S., Lowell, B., Scarpulla, R.C., and Spiegelman, B.M. (1999). Mechanisms controlling mitochondrial biogenesis and respiration through the thermogenic coactivator PGC-1. Cell 98, 115-124.

Yin, L., Wu, N., Curtin, J.C., Qatanani, M., Szwergold, N.R., Reid, R.A., Waitt, G.M., Parks, D.J., Pearce, K.H., Wisely, G.B., and Lazar, M.A. (2007). Rev-erbalpha, a heme sensor that coordinates metabolic and circadian pathways. Science 318, 1786-1789.

Youdim, M.B., Yehuda, S., and Ben-Uriah, Y. (1981). Iron deficiency-induced circadian rhythm reversal of dopaminergic-mediated behaviours and thermoregulation in rats. European journal of pharmacology 74, 295-301.

Zimmet, P.Z., Wall, J.R., Rome, R., Stimmler, L., and Jarrett, R.J. (1974). Diurnal variation in glucose tolerance: associated changes in plasma insulin, growth hormone, and non-esterified fatty acids. British medical journal 1, 485-488.

Table 4.1 Physiologic factors of metabolism and iron.

Variables	LN	HN	H
Hemoglobin (g/dL)	16.475 ± 0.534	15.575 ± 1.355	16.725 ± 1.686
Hematocrit (%)	47.995 ± 1.628	45.3275 ± 3.403	47.56 ± 4.030
Insulin (ng/mL)	1.7366 ± 0.651	1.5240 ± 0.450	2.1566 ± 0.385
Glucagon (pg/mL)	67.16 ± 5.51	60.43 ± 5.49	78.07 ± 8.743
Body weight (g)	29.89 ± 0.27***	28.09 ± 0.25	28.65 ± 0.176
Total liver iron (ppm/mg protein)	1.75 ± 0.25*	2.39 ± 0.32	5.25 ± 0.45**

Body weight is measured as n=72 per group. Iron was measured by ICP-OES, Optima 3100XL; PerkinElmer MS n=12 per group, ZT10. *p<.05, **p<.01, and ***p<.001. Hemoglobin and hematocrit measured by vetscan Hm5 n=6, ZT10. Insulin and glucagon measured by ELISA (Millipore EZRMI-13K, EZGLU-30K) n=6, ZT10.

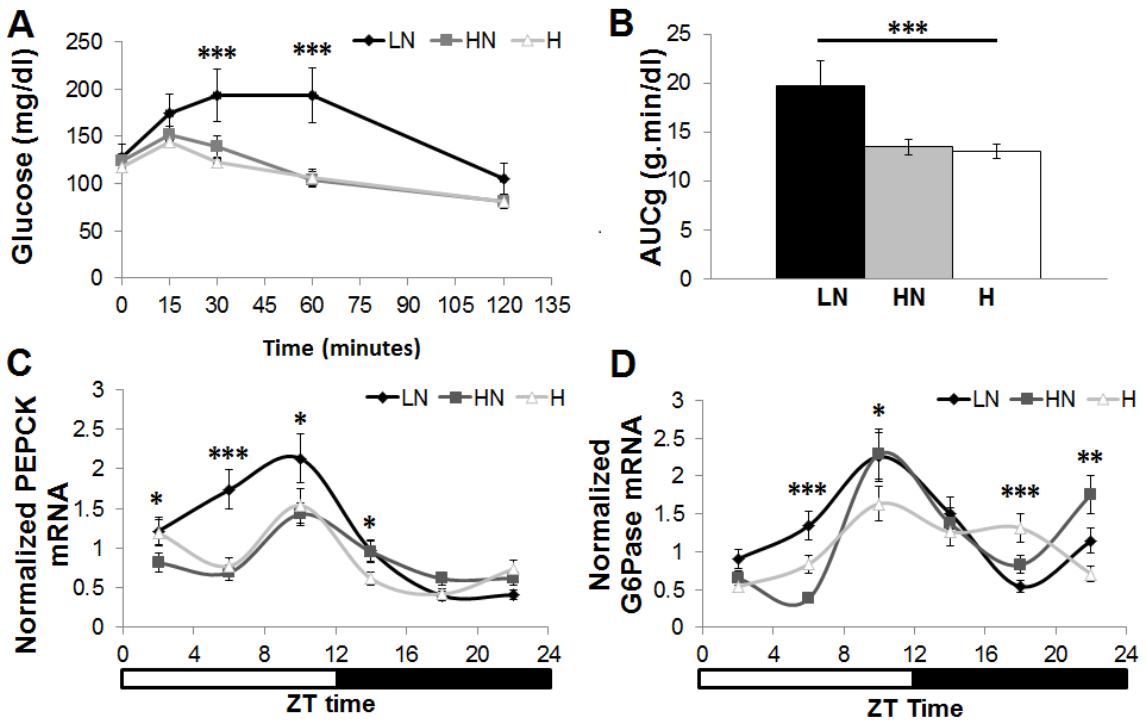

Figure 4.1 Dietary iron decreases parameters of glucose homeostasis and gluconeogenic transcription. A) *ad libitum* PTT at ZT12 and the B) AUCg (n=12-16) C) Liver PEPCK (n=6) and D) G6Pase mRNA as determined by RT-PCR normalized to cyclophilin and RPL13, which did not display circadian variation (n=6). *p<.05, **p<.01, and ***p<.001.

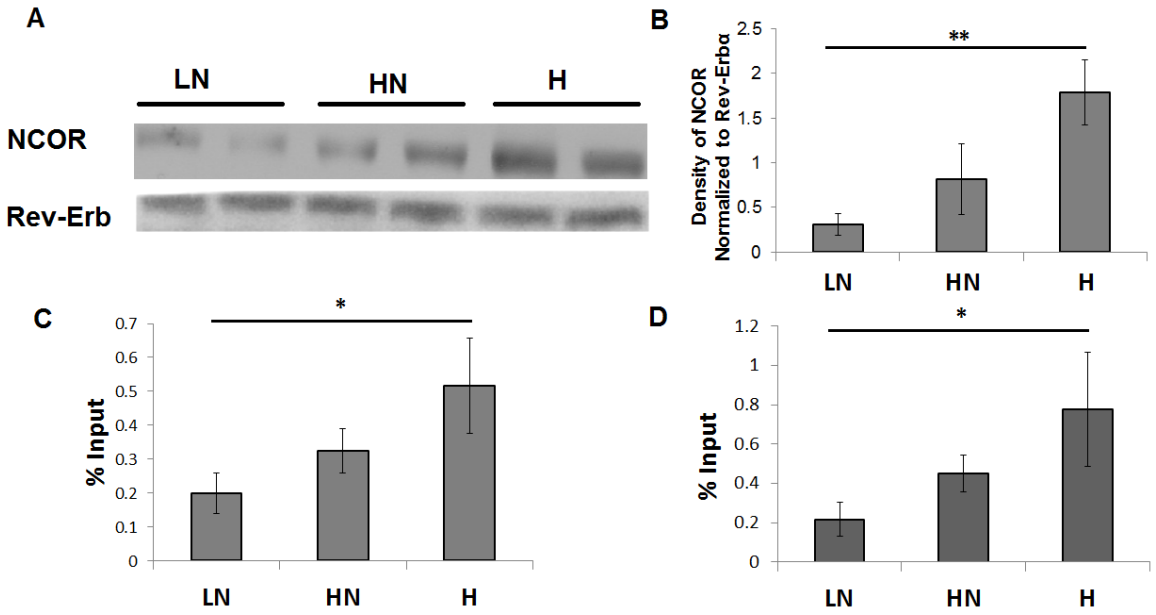

Figure 4.2 Dietary iron affects the formation of the Rev-Erbα repressor complex and its activity. A) Western blot of Rev-erbα IP extracts blotted for NCOR and Rev-Erbα at ZT14 and B) quantification of these blots (n=6). C) ChIP of NCOR to the PEPCK (n=4) and D) G6Pase promoter determined by RT-PCR normalized to input at ZT14 (n=4). *p<.05, **p<.01, and ***p<.001.

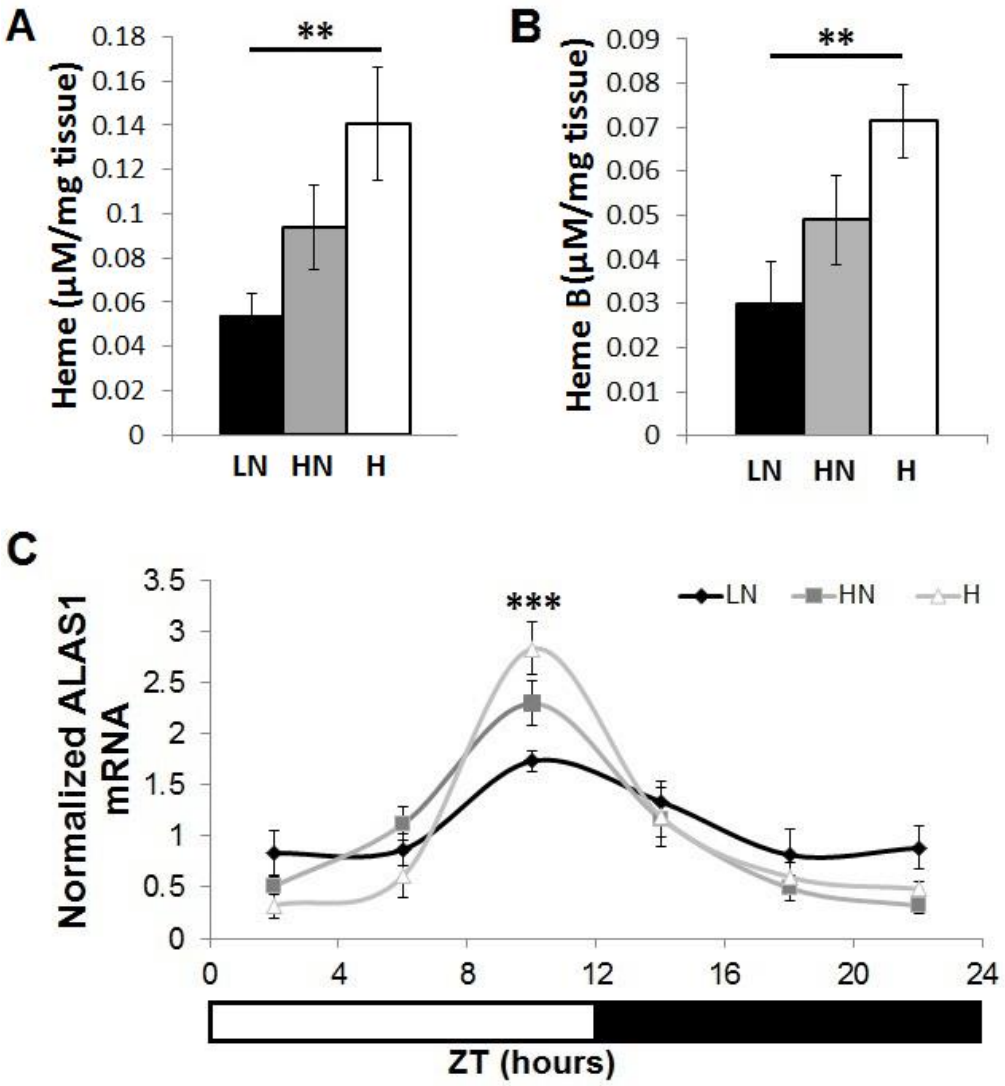

Figure 4.3 Hepatic heme synthesis and steady-state levels are altered with dietary iron. A) Total heme levels as measured by HPLC at) ZT12 (n=6). B) Heme b levels as measured by hemochromagen pyridine assay at ZT12 (n=12). C) ALAS1 transcripts determined by RT-PCR normalized to cyclophilin and RPL13 (n=6). *p<.05, **p<.01, and ***p<.001.

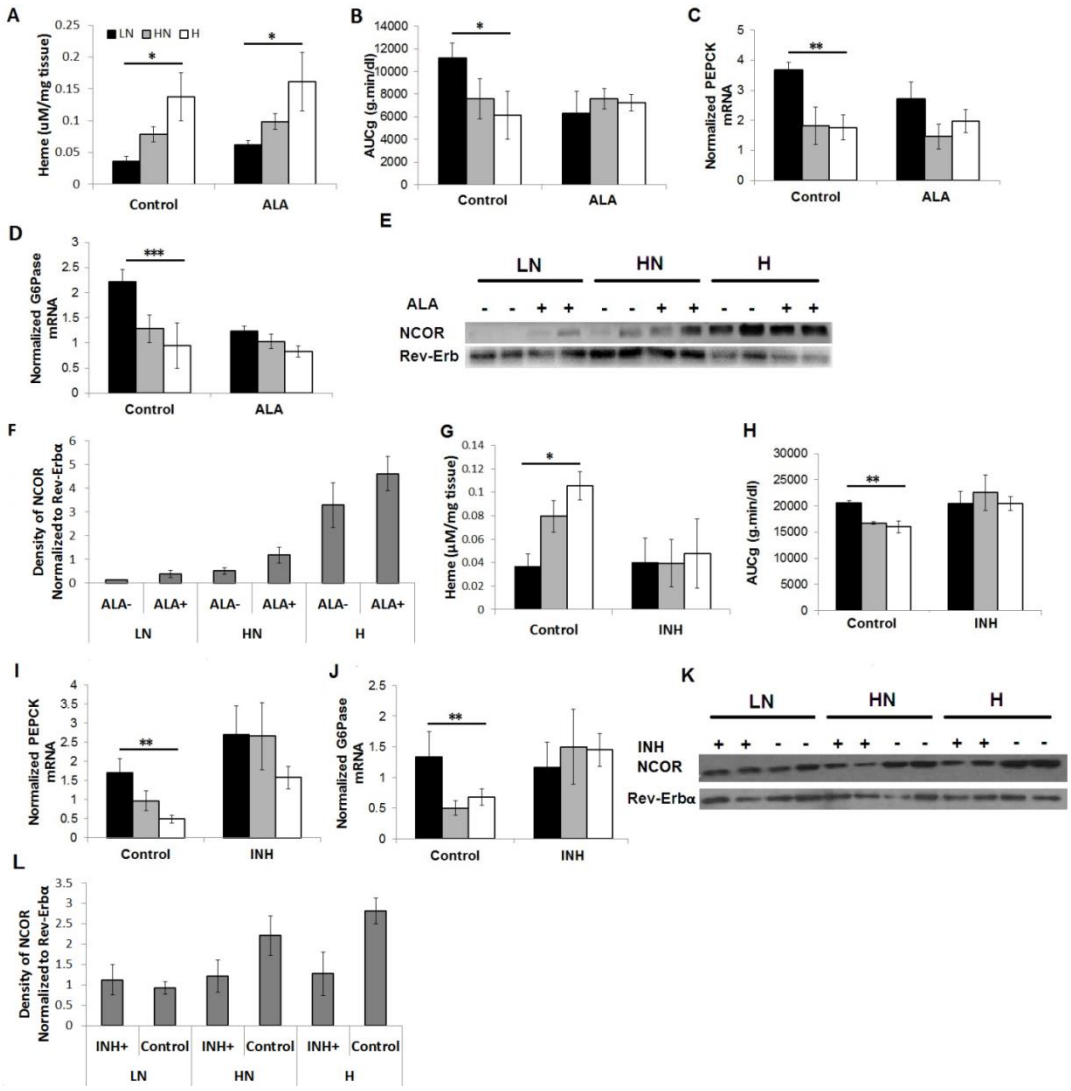

Figure 4.4 Drug induced increase or decrease of heme levels ablates variations in heme, Rev-Erbα/NCOR complex formation, and gluconeogenesis observed between the various diets. A) Heme levels as measured by HPLC with ALA treatment and control (n=6-12) B) AUCg from ZT12 PTT (n=6) C) PEPCK (n=9), and D) G6pase mRNA transcripts in ALA treated and control mice normalized to RPL13 and cyclophilin(n=9). E) Western blot of Rev-Erbα IP extracts blotted for NCOR and Rev-Erbα and F) quantification of the density of the NCOR blot normalized to the Rev-Erbα density. G) Heme levels as measured by HPLC with INH treated and control mice (n=3). H) AUCg for ZT12 PTT (n=5-8) I) PEPCK (n=5-8) and J) G6Pase transcript levels as measured by RT PCR normalized to RPL13 and cyclophilin in INH treated and control (n=5-8). K) Quantified density of NCOR bands normalized to Rev-Erbα density for L) Western blot for Rev-Erbα/NCOR coIP extracts blotted for Rev-Erbαand NCOR (n=3). *p<.05, **p<.01, and ***p<.001.

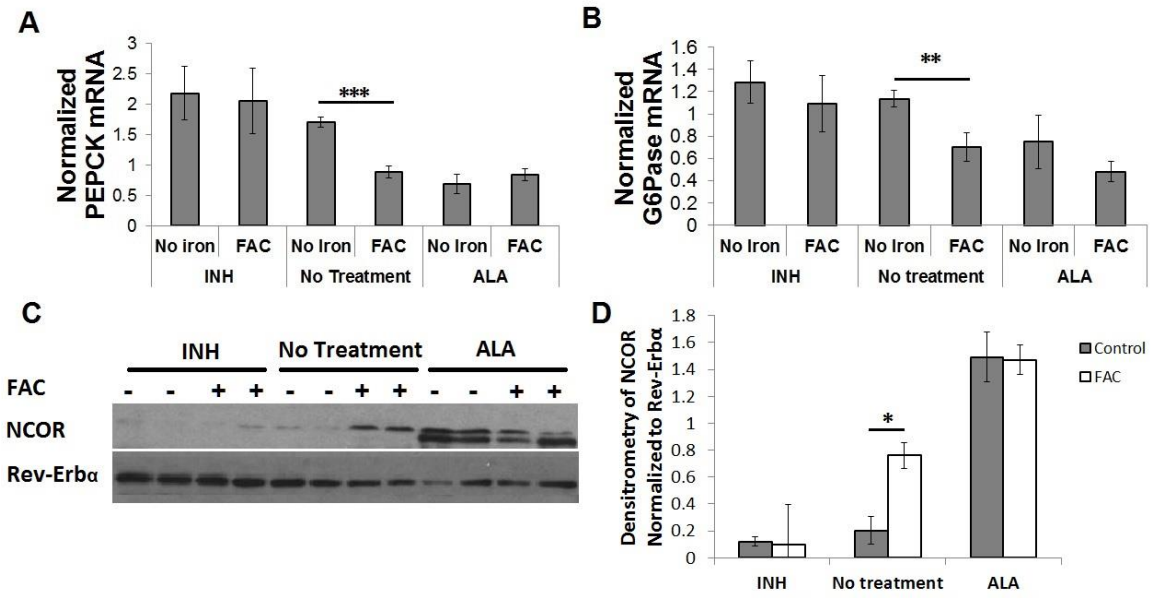

Figure 4.5 Treatment of HepG2 cells with FAC, ALA, or INH recapitulates mouse results. A) PEPCK (n=12-24) and B) G6Pase transcript levels as measured by RT PCR for control and FAC cells with no drug treatment, ALA, or INH treated (n=12-24). C) Western blot of Rev-Erbα IP cell extract blotted for NCOR and Rev-Erbα and D) quantification of the density of the NCOR band as normalized to Rev-Erbα (n=3). *p<.05, **p<.01, and ***p<.001.

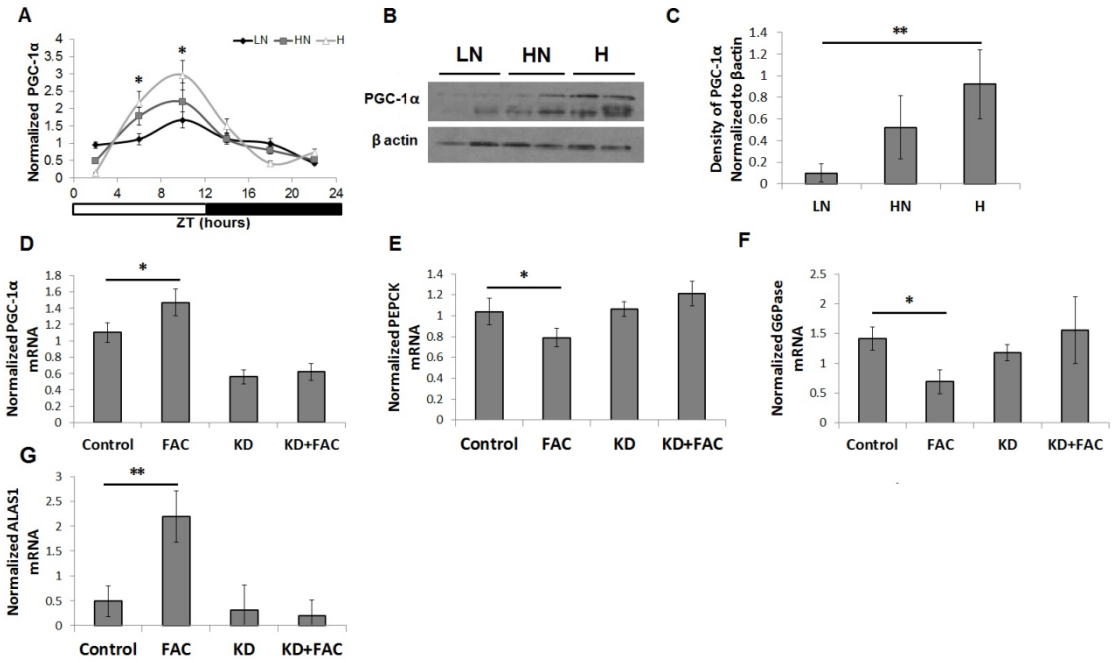

Figure 4.6 Increased dietary iron increases PGC-1α and knockdown of PGC-1α abrogates differences between iron treated and nontreated HepG2 cells. A) PGC-1α mRNA as measured by RT PCR (n=6). B) Western blot of liver extracts blotted for PGC-1α at ZT10 and C) Density of PGC-1α band normalized to β actin (n=6). D) Verification of PGC-1α KD by RT PCR (n=6) and E) PEPCK,(n=6) F) G6pase (n=6), and G) ALAS1transcript levels in PGC-1α KD normalized to Rpl13 (n=6). *p<.05, **p<.01, and ***p<.001.

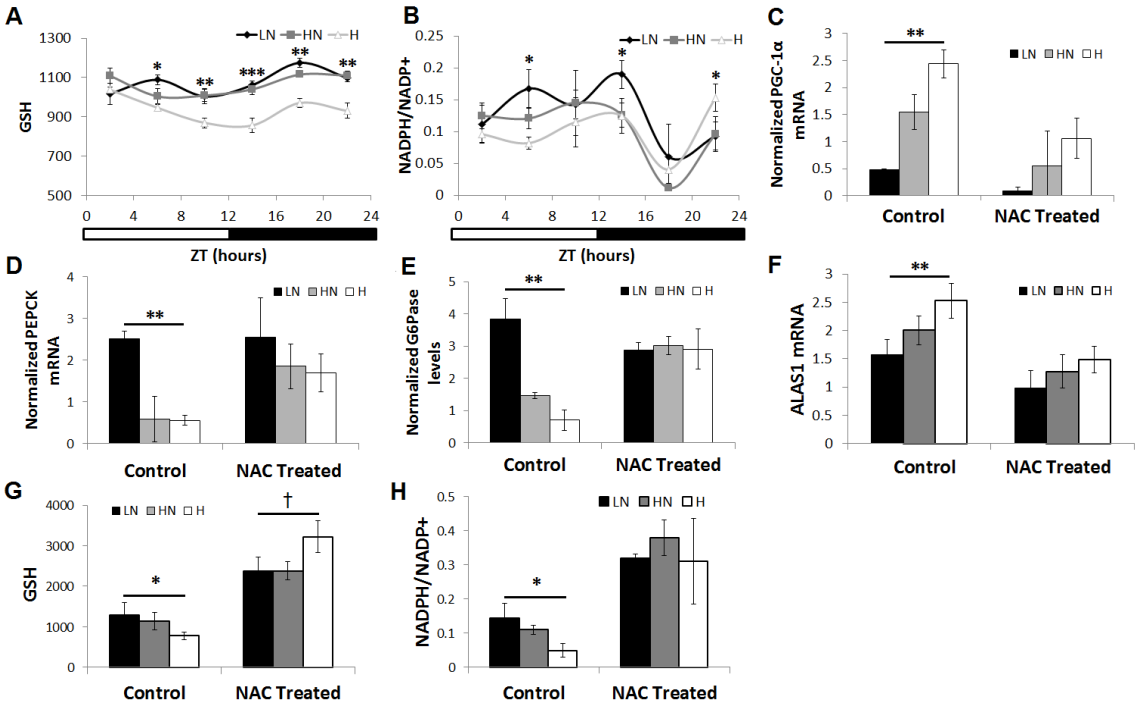

Figure 4.7 Dietary iron alters hepatocyte oxidant signaling and antioxidant treatment ablates differences in PGC-1α and gluconeogenic transcripts. A) GC MS/MS measurement of GSH (n=6) and B) NADPH/NADP+ in freeze clamped liver of mice on iron diets at various harvest times (n=6). C) Transcript levels of PGC-1α (n=3-6), D) PEPCK (n=3-6), E) G6Pase (n=3-6), and F) ALAS1 in NAC treated and control mice (n=3-6). G) GC MS/MS measurement of GSH (n=3-6) and H) NADPH/NADP+ in NAC treated or control mice at ZT12 (n=3-6). †p=.147, *p<.05, **p<.01, and ***p<.001.

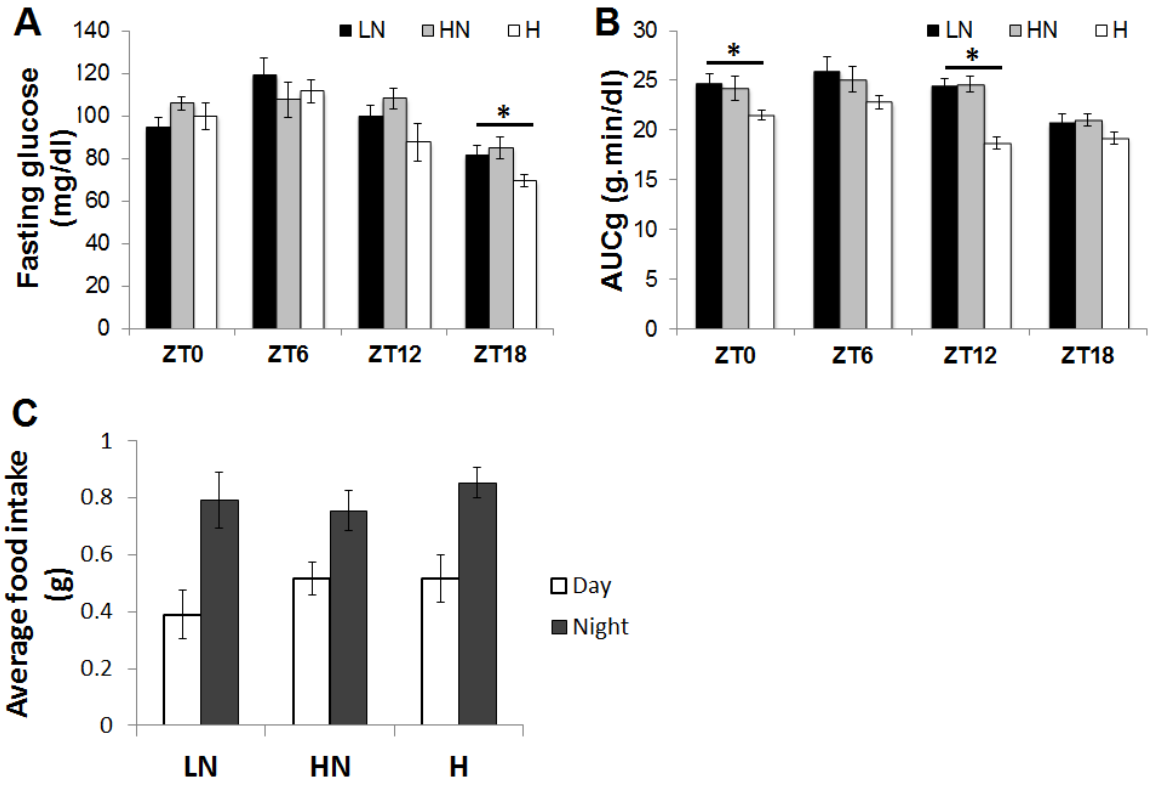

4.S.1 Parameters of circadian glucose and feeding in C57BL/6J male mice fed LN, HN, and H diets. A) Fasting glucose levels obtained after 6 hour fast throughout the dark and light phase (n=10-16, *p=.0428, LN vs H p=.1405, HN vs H p=.0449) B) Area under the glucose curve (AUCg) for GTTs performed at various time points after a 6 hour fast (n=10-16, p) C) Feeding behavior as measured by electronic scale in the Comprehensive Laboratory Animal Monitoring System (CLAMS; Columbus Instruments, Columbus, OH).

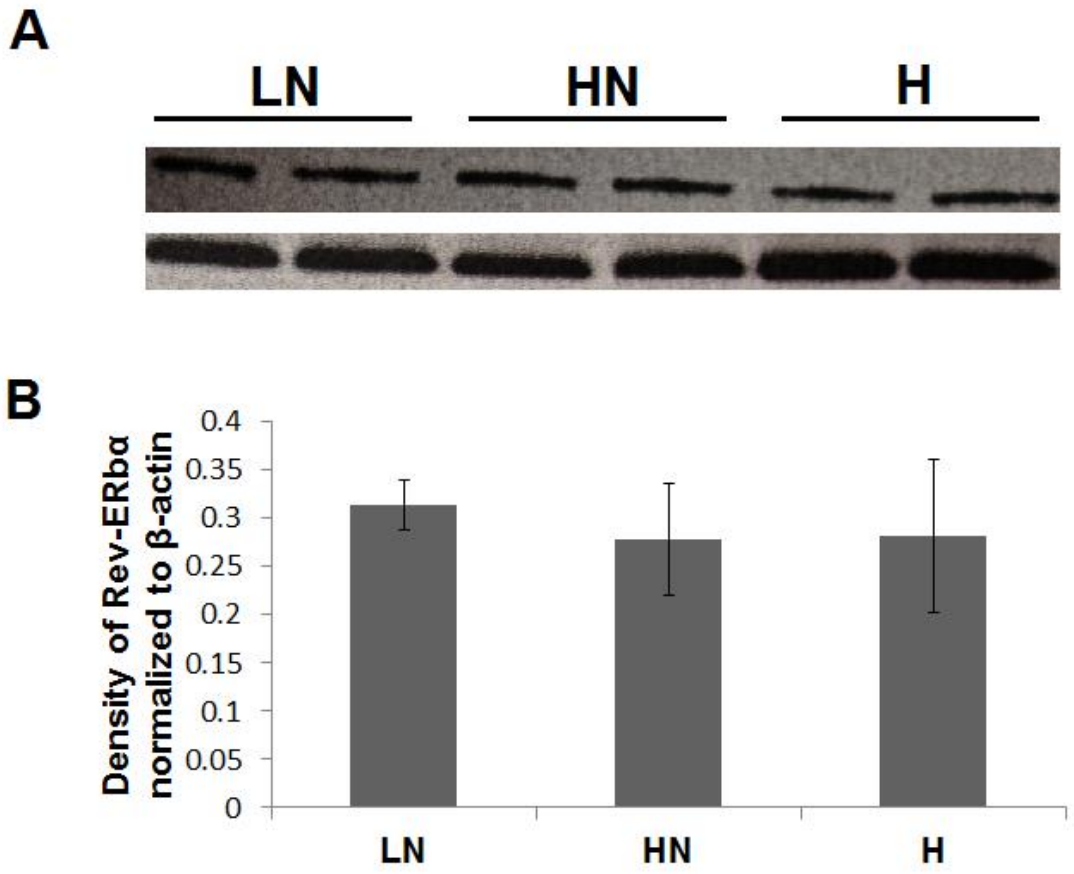

4.S.2 Rev-Erbα protein at ZT14 in the liver of C57BL/6J mice. A) Rev-Erb alpha blot B) quantification (n=4)

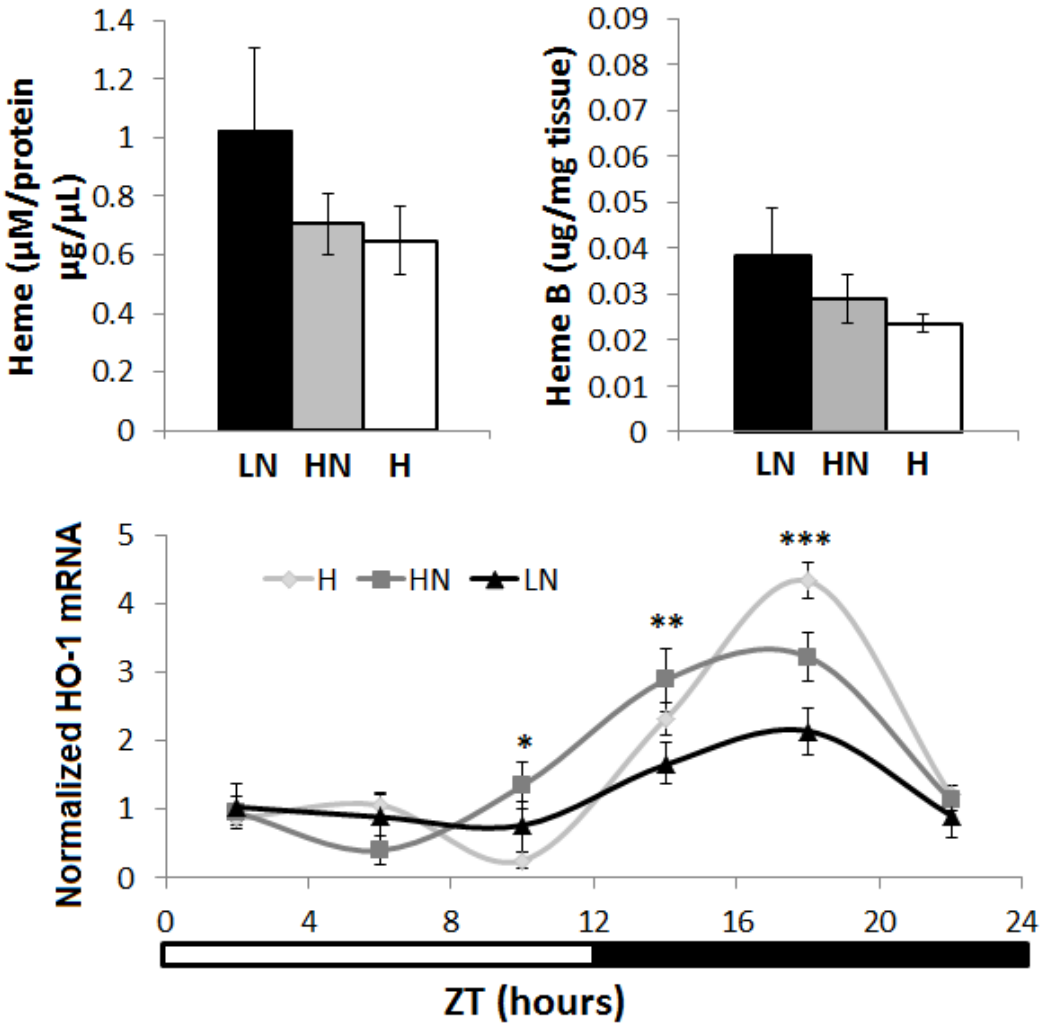

4.S.3 ZT0 heme and circadian HO-1 in livers of male C57BL/6J mice. 3A) ZT0 HPLC heme (p=.3236) B) ZT0 Hemochromogen pyridine heme b (p=.6361) C) HO-1 transcript levels as normalized by RPL13 and cyclophilin B (ZT10 p=.0289, LN vs HN p=.3219, LN vs H p=.2193, HN vs H p=.0137; ZT14 p=.0018, LN vs HN p=.00237, LN vs H p=.0021, HN vs H p=.537; ZT18 p<.0001, LN vs HN p=.0031, LN vs H p=.0002, HN vs H p=.0012)

CHAPTER 5

CONCLUSIONS

In the US alone, approximately 14% of the adult population has diabetes (both diagnosed and undiagnosed) and current models predict that this incidence will rise to 25 or 28% of the population developing diabetes by 2050 (Boyle *et al.*, 2010). Results from other projections in individuals younger than 20 are especially startling and suggest that diabetes incidence may double by the year 2050 (Imperatore *et al.*, 2012). With the continued rapid increase in this disease, it is important to explore the multifaceted causes associated with its rise. In this thesis, we have explored the impact of dietary iron on glucose homeostasis, specifically through its regulation of gluconeogenesis by increasing AMPK and Rev-Erbα activity. We showed that iron affects both of these pathways through either oxidative stress or oxidative signaling, and NAC treatment of mice abolished differences between the various iron diets.

In previous reports, we demonstrated that AMPK phosphorylation is increased in the skeletal muscle in hepcidin knockout mice (*Hfe*$^{-/-}$), a mouse model of the iron overload disorder hemochromatosis. The increase in AMPK activity seen in these mice correlates with increased removal of [1,2-$^{13}C_2$]D-glucose from the circulation, elevated insulin sensitivity as measured by AKT phosphorylation, and greater glucose uptake in

the skeletal muscle (Huang *et al.*, 2007). These differences may be due to the direct effects of iron on AMPK, or could result from the disease pathology of hemochromatosis.

In this thesis, we show increased AMPK phosphorylation in both skeletal muscle and liver with high dietary iron. In the liver, this increase in phosphorylated AMPK decreased hepatic gluconeogenesis by 13%, as shown by assessing the turnover of intraperitoneally injected [U-$^{13}C_6$]-D-glucose. We went on to show that iron increases AMPK activity through altering the acetylation of its regulatory kinase LKB1. Deacetylation of LKB1 has been shown to shift its cellular localization from the nucleus to the cytosol where it can phosphorylate AMPK. One of the major deacetylases of LKB1 is Sirt1 (Lan *et al.*,2008). We showed that treatment of cells with Sirtuin inhibitors nicotinamide or splitomicin abrogates the increased AMPK phosphorylation with iron treatment (Huang *et al.*, 2013). Sirt1 activity is known to respond to the oxidative state of the cell, and through NAC treatment of mice, we observed that the effects of iron on AMPK and AUCg of GTT were ameliorated. These results will likely impact other pathways, including circadian rhythms which are shown to regulate and be regulated by Sirt1. It will also be important to assess the effects of iron on other metabolic diseases including cancer, since we saw differences in both the acetylated and total levels of p53, a known tumor suppressor.

We also found that variations in the oxidative state of the cell created by altering dietary iron were able to affect the circadian rhythm of the liver by increasing heme levels to affect Rev-Erbα/NCOR complex formation. Redox cofactors such as GSH and NADPH cycle and vary in an iron dependent manner (Figure 4.7 A and B). These changes in redox signals alter PGC-1α transcription, as observed in peak transcription at

ZT10, which increase with dietary iron (Figure 4.6 A), and were ablated by treatment with the antioxidant NAC (Figure 4.7C). PGC-1α is known to regulate heme synthesis through transcriptional regulation of ALAS-1 (Handschin *et al.*, 2005). As iron increased, we observed a graded increase in peak transcripts of ALAS-1 and heme levels at ZT12 (Figure 4.3A-C). Heme is known to regulate the negative arm of the circadian regulon and is necessary for Rev-Erbα/NCOR complex formation, which inhibits the circadian factors Bmal1 and Clock as well as the gluconeogenic transcripts PEPCK and G6Pase (Yin *et al.*, 2007). We observed there was higher Rev-Erbα/NCOR complex formation in H-fed mice when compared to the HN- and LN- fed mice (Figure 4.2 A and B). The changes in Rev-Erbα/NCOR complex correlated to an expected decrease in gluconeogenesis (Figure 4.1 A-D). Differences between the iron diets of complex formation and gluconeogenesis were heme dependent and treatment with drugs that increase (ALA) or inhibit (INH) heme synthesis ablated observed differences (Figure 4.4).

PGC-1α is a transcriptional coactivator that is known to be involved in a number of diverse metabolic pathways, including mitochondrial biogenesis, adaptive thermogenesis, and metabolism of both glucose and lipids (Liang and Ward, 2006). Upregulation of PGC-1α in the liver in response to increased dietary iron is a novel finding, and given its broad activation of metabolic pathways, other tissue depots should be assessed for altered expression in response to iron. PGC-1α is also a known regulator of gluconeogenesis and is known to coactivate hepatic nuclear factor-4α (Hnf4α), glucocorticoid receptor (GR), and forkhead box1 (FOXO1) to increase transcription of PEPCK and G6Pase (Puigserver *et al.*, 2003; Rhee *et al.*, 2003). The contradictory

observation that PGC-1α increase in H-fed mice, while PEPCK and G6Pase transcripts are decreased could be due to multiple promoter inputs from both AMPK and Rev-Erbα/NCOR, or differences in PGC-1α binding partners. Iron has never been reported to affect Hnf4α or GR; however, in previous studies, we have shown decreased acetylation of FOXO-1 with iron treatment. Typically, deactylation is associated with activation, but much like FOXO-1 control of adiponectin, deacetylation can also increase FOXO-1 promoter coccupancy of the PPRE with PPARγ. This cooccupancy of FOXO-1 at the PPRE is inhibitory and may override the PGC-1α coactivation (Fan *et al.*, 2009; Gabrielsen *et al.*, 2012).

The results presented in this dissertation confirm that heme is limiting for Rev-Erbα/NCOR complex formation, although there is evidence that other factors are involved in the regulation of this complex, including the binding of NO, and the oxidation of thiol groups in the heme binding pocket (Cáceres *et al.,* 2011; Shimizu, 2012). Heme synthesis is highly regulated both at the level of anabolism and catabolism. ALAS-1 is transcriptionally inhibited by heme, and the enzyme that breaks down heme, heme oxygenase 1 (HO1), is transcriptionally upregulated by heme and by oxidative stress (Cable *et al.*, 2000). We observe heme levels are highest in the H-fed mice at ZT12, before the start of the active period, while they are lowest in the H-fed mice at ZT0 as the mice become inert. We also see that although ALAS-1 transcription is highest in H-fed mice at the peak at ZT10, H-fed mice have lower ALAS-1 transcript levels at other times, and increased HO-1 at ZT18. This temporal increase of heme synthesis directly before it is needed in pathways such as increased respiration, toxicity response, and energy metabolism may point to another example of circadian rhythms providing

orchestration of utilization and availability. It also suggests that upregulation of HO1 and downregulation of ALAS1 by heme, may not only be a mechanism to prevent the buildup of heme, which can be toxic in large quantities, but may also be a part of another regulatory loop that alters the circadian clock through regulation of heme to function in the daily rhythm of cellular metabolism.

Future directions

The decrease in gluconeogenesis that we observed in high iron diet is complicated by the understanding that iron in both pathologic and nonpathologic levels is associated with diabetes (Simcox and McClain, 2013). This may suggest that it may take multiple adverse conditions (i.e., genetic predisposition, obesity, dietary factors) to enter into a diabetic state. This multiple hit model is seen in diabetes associated with hemochromatosis. Patients with hemochromatosis actually have improved insulin sensitivity, and only begin to suffer from diabetes when their system is further stressed from weight gain, which leaves the insulin production insufficient for their mass (Cooksey *et al.*, 2004). Although the mice on high iron diet have lower gluconeogenesis, they have decreased adiponectin levels and may require a second stress such as obesity, or aberrant feeding patterns to develop diabetes (Gabrielsen *et al.*, 2012). Past studies performed in our laboratory have shown that restricting the food availability of mice to 8 hours from ZT3-ZT10 for 1 week shifted their liver clock and the mice had a fasting glucose greater than 160, while a fasting glucose greater than 125 is symptomatic of diabetes (data not shown). In the future, it may be of interest to repeat the restriction feeding studies in mice on various iron diets to ascertain if the observed abnormal glucose metabolism is worse in high iron fed mice.

The data presented herein show that dietary iron is able to regulate the core molecular clock by altering temporal heme availability to change Rev-Erbα and NCOR binding. We have also generated data that show a correlation between high dietary iron and increased transcript levels of other clock components, including Clock, Bmal1, Per2, and Rev-Erbα (Figure 5.1A-D). These results could indicate that iron is limiting for absolute peak transcription or could suggest that iron is important in temporally regulating liver clock transcripts. Distinguishing between these two possibilities is complicated because of the 4- hour time period between harvests, which make it difficult to ascertain if these peak values are indeed the true peak for each of the diets or if they are instead the highest observed peak. In the future, to answer this question, it will be important to utilize an *in vivo* monitoring system such as the mPer2^{Luciferase} mouse, a knockin model expressing a luciferase reporter behind the Per2 promoter. Another question that these results raise is whether iron is feeding into this regulatory loop through the Rev-Erbα/NCOR complex alone, or if it could function through other mechanisms, including AMPK, oxidant signaling, or hypoxia, which are all shown to be altered in dietary iron and affect circadian rhythm.

Another persisting question is the effects that dietary iron may have on body clocks other than the liver, including the central clock in the hypothalamus. At ZT10, we observed that the total iron levels increased with dietary iron in the liver (Table 4.1); however, in the hypothalamus, we observed decreased total iron stores with increased dietary iron (Figure 5.2 A). The SCN is known to regulate feeding behavior, activity, and body temperature. Through monitoring of body temperature with the VitaView Data Acquisition System of implanted wireless sensors (Respironics), we were able to monitor

circadian oscillations in body temperature. We observed that the L-fed mice varied from peak to trough by 1.44±0.04˚C while the HN group only varied by 1.26±.04˚C (Figure 5.2B). These differences could be due to either differences in heat capacity of the LN- fed mice (white or brown adipose depots) or due to differences in SCN regulation. In a recent publication, Chen *et al.* (2013) showed that iron was necessary to set the rhythm of the core molecular clock. Plants grown in iron deficient soil had lower peak heights in circadian factors, and when moved to a constant dark condition, the transcript peaks began to shift from the iron sufficient controls. To elucidate if dietary iron in mice functions to maintain circadian timing of the SCN similar to its function in Arabidopsis, we will keep the mice in constant dim light conditions while monitoring their body temperatures. After the light manipulation, we will also perform a cold tolerance test to assess if there are differences in thermogenesis between the diets.

Final summary

In summary, our results show that dietary iron is able to regulate gluconeogenesis through its input into two central metabolic pathways: AMPK and circadian rhythms. The modulation of these pathways by iron is through oxidative signaling, and suggests that moderate manipulation of dietary iron is able to change cellular metabolism.

References

Boyle J.P., Thompson T.J., Gregg E.W., Barker L.E., and Williamson D.F.(2010). Projection of the year 2050 burden of diabetes in the US adult population: dynamic modeling of incidence, mortality, and prediabetes prevalence. Population Health Metrics. 8(29) e1-12.

Cable E.E., Miller T.G., and Isom H.C. (2000). Regulation of heme metabolism in rat hepatocytes and hepatocyte cell lines: delta-aminolevulinic acid synthase and heme oxygenase are regulated by different hemedependent mechanisms. Arch. Biochem. Biophys. 384 (2): 280–295.

Cáceres L., Necakov A.S., Schwartz C., Kimber S., Roberts I.J., and Krause H.M. (2011). Nitric oxide coordinates metabolism, growth, and development via the nuclear receptor E75. Genes Dev. 25(14):1476-85.

Chen Y.Y., Wang Y., Shin L.J., Wu J.F., Shanmugam V., Tsednee M., Lo J.C., Chen C.C., Wu S.H., and Yeh K.D. (2013). Iron is involved in the maintenance of circadian period length in Arabidopsis. Plant Physiol. 161(3):1409-20.

Cooksey R.C., Jouihan H.A., Ajioka R.S., Hazel M.W., Jones D.L., Kushner J.P., and McClain D.A. (2004). Oxidative stress, beta-cell apoptosis, and decreased insulin secretory capacity in mouse models of hemochromatosis. Endocrinology. 145(11):5305-12.

Fan W., Imamura T., Sonoda N., Sears D.D., Patsouris D., Kim J.J., and Olefsky J.M. (2009). FOXO1 transrepresses peroxisome proliferator-activated receptor gamma transactivation, coordinating an insulin-induced feed-forward response in adipocytes. J Biol Chem. 284(18):12188–12197.

Gabrielsen J.S., Gao Y., Simcox J.A., Huang J., Thorup D., Jones D., Cooksey R.C., Gabrielsen D., Adams T.D., Hunt S.C., Hopkins P.N., Cefalu W.T., and McClain D.A. (2012). Adipocyte iron regulates adiponectin and insulin sensitivity. JCI. 122(10):3529-40.

Handschin C., Lin J., Rhee J., Peyer A.K., Chin S., Wu P.H., Meyer U.A., and Spiegelman B.M. (2005). Nutritional regulation of hepatic heme biosynthesis and porphyria through PGC-1alpha. Cell.122(4):505-15.

Huang J., Gabrielsen J.S., Cooksey R.C., Luo B., Boros L.G., Jones D.L., Jouihan H.A., Soesanto Y., Knecht L., Hazel M.W., Kushner J.P., and McClain D.A. (2007). Increased glucose disposal and AMP-dependent kinase signaling in a mouse model of hemochromatosis. JBC. 282(52)L37501-7.

Huang J., Simcox J., Mitchell T.C., Jones D., Cox J., Luo B., Cooksey R.C., Boros L.G., and McClain D.A. (2013). Iron regulates glucose homeostasis in liver and muscle via AMP-activated protein kinase in mice. FASEB J. 27(7):2845-54.

Imperatore G., Boyle J.P., Thompson T.J., Case D., Dabelea D., Hamman R.F., Lawrence J.M., Liese A.D., Liu L.L., Mayer-Davis E.J., Rodriguez B.L., and Standiford D. (2012). Projections of type 1 and type 2 diabetes burden in the US population aged <20 years through 2050: Dynamic modeling of incidence, mortality, and population growth. Diabetes Care. 35(12)2515-2520.

Lan F., Cacicedo J.M., Ruderman N., and Ido Y. (2008). Sirt1 modulation of the acetylation status, cytosolic localization and activity of LKB1: possible role in AMP-activated protein kinase activation. JBC. 283(41): 27628-27635.

Liang H., and Ward W.F. (2006). Pgc-1α: a key regulator of energy metabolism. Adv Physiol Educ. 30(4):145-151.

Puigserver P., Rhee J., Donovan J., Walkey C.J., Yoon J.C., Oriente F., Kitamura Y., Altomonte J., Dong H., Accili D., and Spiegelman B.M. (2003). Insulin-regulated hepatic gluconeogenesis through FOXO1-PGC-1alpha interaction. Nature. 423(6939):550-5.

Rhee J., Inoue Y., Yoon J.C., Puigserver P., Fan M., Gonzalez F.J., and Spiegelman B.M. (2003). Regulation of hepatic fasting response by PPARgamma coactivator-1alpha (PGC-1): requirement for hepatocyte nuclear factor 4 alpha in gluconeogenesis. Proc Natl Acad Sci USA. 100(7):4012-7.

Shimizu T.(2012).Binding of cysteine thiolate to the Fe(III) heme complex is critical for the function of heme sensor proteins. J Inorg Biochem. 108:171-7.

Simcox J.A. and McClain D.A. (2013). Iron and diabetes risk. Cell Metabolism.17(3):329-41.

Yin L., Wu N., Curtin J.C., Qatanani M., Szwergold N.R., Reid R.A., Waitt G.M., Parks D.J., Pearce K.H., Wisely G.B., and Lazar M.A. (2007). Rev-erbalpha, a heme sensor that coordinates metabolic and circadian pathways. Science. 318(5857):1786-9.

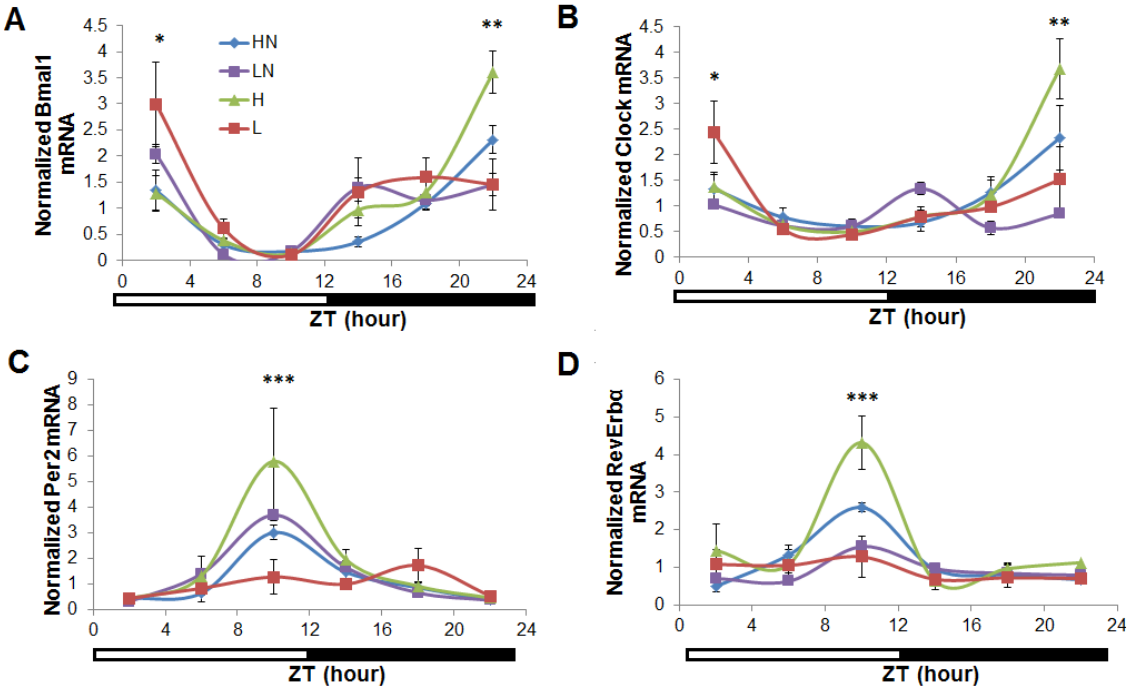

Figure 5.1 Transcripts of molecular clock components from the liver of C57BL/6J mice. A) Bmal1, B) Clock, C) Per2, and D)Rev-Erbα transcripts as measured by RT-PCR (n=6 per diet per timepoint, *p<.05, **p<.01, and ***p<.001 as measured by ANOVA, error bars represent SEM).

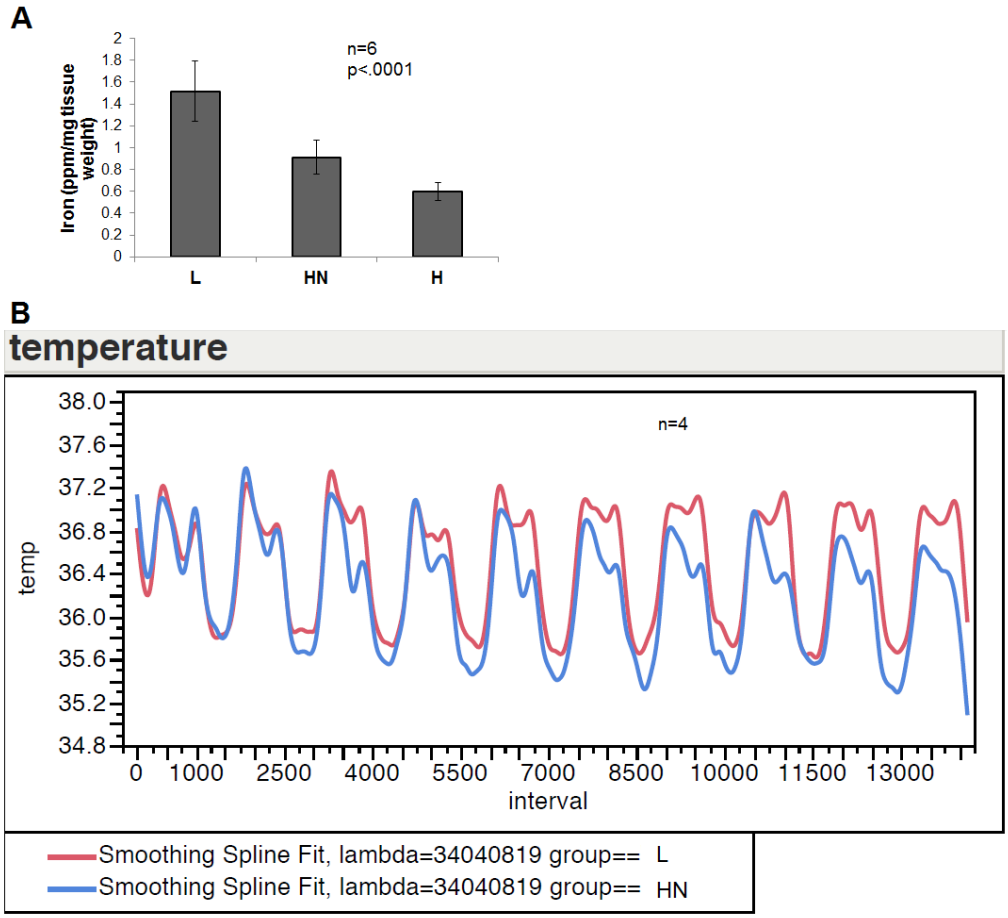

Figure 5.2 The effects of dietary iron on hypothalamic iron and body temperature. A) Total iron stores measured by ICP-OES, Optima 3100XL; PerkinElmer (p value calculated by ANOVA, L vs HN p=.0001, L vs H p<.0001, HN vs H p=.0346). B) Body temperature as measured by VitaView Data Acquisition System (Respironics) analyzed by jmp pro.